

UNIVERSITY OF EDUCATION, WINNEBA
COLLEGE OF TECHNOLOGY EDUCATION, KUMASI

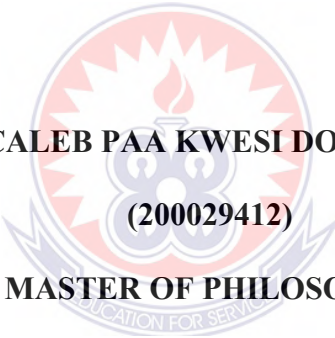
**OPTIMAL DESIGN OF GRID CONNECTED PV/WIND POWER
GENERATION FOR URBAN HEALTHCARE FACILITY USING HOMER
ENVIRONMENT**



NOVEMBER, 2022

UNIVERSITY OF EDUCATION, WINNEBA
COLLEGE OF TECHNOLOGY EDUCATION, KUMASI

**OPTIMAL DESIGN OF GRID-CONNECTED PV/WIND POWER
GENERATION FOR URBAN HEALTHCARE FACILITY USING HOMER
ENVIRONMENT**



CALEB PAA KWESI DONKOH
(200029412)
MASTER OF PHILOSOPHY

**A Thesis submitted to the Department of ELECTRICALS AND ELECTRONICS
TECHNOLOGY EDUCATION, UNIVERSITY OF EDUCATION Winneba,
School of Graduate Studies, in Partial Fulfilment of the Requirements for the
award of Master of Philosophy in Electrical and Electronics Engineering
Technology**

NOVEMBER, 2022

DECLARATION

Student Declaration

I, **CALEB PAA KWESI DONKOH**, declare that this dissertation, with the exception of quotations and references contained in the published works, which have all been identified and duly acknowledged, is entirely my own original work, and it has not been submitted, either in part or whole for another degree elsewhere.

SIGNATURE:.....

DATE:.....



Supervisor's Declaration

I hereby declare that the preparation and presentation of this work was supervised in accordance with the guidelines for supervision of dissertation as laid down by the University of Education, Winneba.

DR. Albert Kotawoke Awopone

SIGNATURE:.....

DATE:.....

DEDICATION

The study is dedicated to my son, Josiah Kobena Donkoh



ACKNOWLEDGEMENT

My biggest thanks goes to the Almighty God for his divine enablement and protection throughout my period of studies. Special Acknowledgment and thanks to my supervisor Dr. Albert Kotawoke Awopone for immerse guidance and supervision towards the success of this thesis. I also give thanks to my family for the support given me towards the successful completion of my course.



TABLE OF CONTENTS

DECLARATION	I
DEDICATION	II
ACKNOWLEDGEMENT	III
TABLE OF CONTENTS.....	IV
LIST OF FIGURES	IX
LIST OF TABLES	XI
NOMENCLATURE	XIII
ABSTRACT.....	XVII
CHAPTER ONE: INTRODUCTION.....	1
1.1. Background to the study	1
1.2. Statement of the problem.....	5
1.3. Objectives of study	7
1.4. Significance of the research.....	8
1.5. The Thesis structure.....	10
CHAPTER TWO: LITERATURE REVIEW.....	12
2.1. Microgrid	12
2.2. Grid connection architecture.....	12
2.3. Renewable PV penetration and incentives in Ghana	14
2.4.. Outlook for renewable wind energy in Ghana.....	18
2.5. Hybrid energy system components sizing approach.....	20
2.6. Software packages for simulating hybrid renewable architecture	23
2.7. Emperical verification of simulation with HOMER.....	24
2.7.1. Wind+PV+battery hybrid architecture.....	25
2.7.2. PV+diesel generator+battery hybrid architecture	28

2.7.3. Wind+PV+hydroelectric+battery hybrid architecture.....	29
2.7.4. Wind+diesel generator+battery hybrid architecture.....	29
2.7.5. PV+hydroelectric power+diesel generator+battery hybrid architecture	30
2.7.6. Wind+PV+fuel cell hybrid architecture	30
2.7.7. Wind+PV+diesel generator+battery hybrid architecture	30
2.7.8. Wind+PV+diesel generator+fuel cell+battery hybrid architecture	31
2.8. The energy storage system.....	32
2.9. Black Start Scheme	39
2.10. Point of Common Coupling (PCC) of Hybrid Systems.....	40
CHAPTER THREE: MATERIALS AND METHOD	42
3.1. Research methodology.....	42
3.2. HOMER Grid software as analytical framework.....	42
3.3. Simulation data used	45
3.3.1. Selected site specifications	45
3.3.2. Electric load assessment.....	47
3.3.3. Evaluation of meteorological data	51
3.3.3.1. Daily solar radiation and clearness index	51
3.3.3.2. Temperature conditions	52
3.3.3.3. Wind speed resources at selected location.....	53
3.3.4. Input data for Economic analysis.....	54
3.3.4.1. Interest rate.....	54
3.3.4.2. Levelized Cost of Energy.....	54
3.3.4.3. Total net present cost (TNPC)	55
3.3.4.4. Salvage value	56
3.3.4.5. Internal rate of return	56

3.3.4.6. Return on investment	56
3.3.4.7. Simple payback.....	56
3.3.4.8. Total annualised cost.....	57
3.3.5. Grid system input data	57
3.4. Hybrid power system components sizing approach.....	58
3.4.1. Solar photovoltaic array sizing	58
3.4.2. Wind turbine sizing.....	60
3.4.3. Sizing of battery bank as energy storage	61
3.4.4. The Power Converter sizing.....	63
3.5. Proposed system architecture.....	65
3.5. Proposed system architecture.....	65
3.5.1. Battery thermal condition monitoring and management	68
3.5.2. Load Management and Voltage regulation schemes	70
3.5.3. Black Start Scheme and allocation of Generation thresholds.....	72
3.5.3. Point of Common Coupling (PCC) for Grid-connected PV/Wind generation scheme using ETAP software	74
3.5.4.1. Input Data.....	74
CHAPTER FOUR: RESULTS AND DISCUSSION	77
4.1. Load Profile	77
4.2. Assessment of renewable energy resources.....	80
4.3. Base case Results	82
4.3. Optimisation results	89
4.3.1. Optimisation details	89
4.3.2. Case 1:Solar+wind+storage:LI ASM+Grid.....	89
4.3.2.1. Electricity generation and consumption.....	90

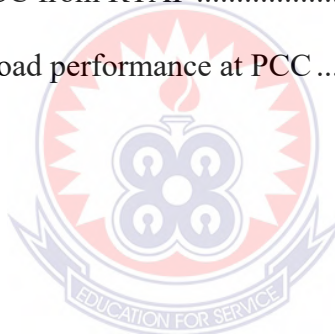
4.3.2.2. Economic evaluation.....	98
4.3.3. Case 2:Solar,wind and grid:.....	102
4.3.4. Case 3:Solar, battery storage and grid	104
4.3.5. Case 4:Solar and grid.....	107
4.3.1.6. Case 5:Wind, battery storage and grid.....	109
4.4 Results on Technical analysis at point of common couple for grid-connected PV/Wind generation scheme with Battery storage	111
4.4.1 PCC Branch characteristics.....	113
4.4.2 PCC Bus and power flow characteristics.....	114
4.4.4 Discharged voltage and Current to Hospital loads	115
4.5. Emissions Reduction and Monetary savings of Optimised case.....	117
4.5.1 Monetary Savings potential from Carbon price reforms	118
4.6. Rate of Depreciation of Optimal Case	119
CHAPTER FIVE: SUMMARY OF FINDINGS, CONCLUSION AND RECOMMENDATIONS.....	121
5.1. Summary of findings.....	121
5.1.1. Load profile.....	121
5.1.2. Economic analysis	122
5.1.3. Monetary savings of Carbon Emissions.....	124
5.1.4. Technical Impact of Point of Common couple on Optimised case	125
5.1.5 Rate of Depreciation of Optimised System	125
5.2. Conclusion	125
5.3. Recommendation	128
5.3.2. Suggestion for further studies	129

REFERENCES.....	131
APPENDICES	147
Appendix A: Sourced load profile of selected healthcare facility	147
Appendix B: Summary of cost and savings, Economic Metrics and Environmental impact of Optimized systems.....	153
Appendix C: HOMER Grid Electric load setup	154
Appendix D: ECG electricity bill for the month of September 2021	155
Appendix E: Case 2 system performance and Cash flow summary	156-157
Appendix F: Case 2 monthly bills (Predicted) and monthly emissions.....	158
Appendix G: Case 3 system performance and Cash flow summary.....	159-160
Appendix H: Case 3 monthly bills (Predicted) and monthly emissions	161
Appendix I: Case 4 system performance and Cash flow summary	162-163
Appendix J: Case 4 monthly bills (Predicted) and monthly emissions	164
Appendix K: Case 5 system performance and Cash flow summary.....	165-166
Appendix: L: Case 5 monthly bills (Predicted) and monthly emissions	167

LIST OF FIGURES

FIGURE	PAGE
Figure 1.1: Thesis structure.....	11
Figure 2.1: A microgrid architecture	13
Figure 2.2: Ghana’s solar energy installed capacity	16
Figure 2.3: Wind resource map of Ghana.....	19
Figure 3.1: Flow chart of methodology	44
Figure 3.2: Site map for KPC	45
Figure 3.3: KPC bed capacity	46
Figure 3.4: Time series load profile for KPC	50
Figure 3.5: Solar radiation and clearness index at selected site.....	52
Figure 3.6: Average monthly temperature data at selected site.....	52
Figure 3.7: Wind energy data (monthly average)	53
Figure 3.8: Proposed system architecture	65
Figure 3.9: HOMER Grid setup window.....	67
Figure 3.10. Capacity curve for deep-cycle battery model.....	69
Figure 3.11.Lifetime curve for deep-cycle battery model	70
Figure 3.9: ETAP Power line diagram for PCC Grid-connected Solar PV, Wind	76
Figure 4.1: Baseline and scaled load characteristics.....	77
Figure 4.2: Monthly load based on a 24-hour load profile	78
Figure 4.3: The day when highest load demand occurs.....	79
Figure 4.4: Wind turbine power curve.....	81
Figure 4.5: Grid system Results.....	84
Figure 4.6: Summary of monthly grid purchases.....	87

Figure 4.7: Optimized system architecture	89
Figure 4.8: Wind turbine electricity generation output.....	92
Figure 4.9: Solar PV electricity generation output	92
Figure 4.10: Energy purchased from grid	93
Figure 4.11: Energy sold to grid	93
Figure 4.12: Monthly electricity production of solar PV, turbine GT100 and Grid....	94
Figure 4.13: Summary monthly performance of the optimized system.....	96-97
Figure 4.14: Monthly utility bill savings	98
Figure 4.15: Economic and chronological cash flow.....	100
Figure 4.16: Schematic diagram of Case 2	102
Figure 4.17: Results of PCC from RTAP	112
Figure 4.18: Power and Load performance at PCC	115



LIST OF TABLES

TABLE	PAGE
Table 2.1: Available and reliable generation capacities	15
Table 3.1: Daily Load profile based on time series	49
Table 3.2: Average metrological data of the study area	53
Table 3.3. Economic Data entry	54
Table 3.4. Grid Input Data	58
Table 3.5. Capacity and the price of Jinko flat-panel Solar PV.....	59
Table 3.6. Properties of Solar PV Array	60
Table 3.7: Properties of Wind Turbine	61
Table 3.8: The capacity and the price of generic 1kWh Li-ion Battery	63
Table 3.9: Generic Battery storage properties	63
Table 3.10. Power Converter properties	64
Table 3.11: Components of Proposed Architecture.....	66
Table 3.12: ETAP Input data	75
Table 4.1: Monthly bills (Predicted).....	85
Table 4.2: Monthly Carbon dioxide Emissions	85
Table 4.3: Cast and Savings, Economics and Environmental Results for Base case ..	86
Table 4.4: Optimisation Results of the Proposed system	88
Table 4.5: Optimized system components cost and O&M	90
Table 4.6: Optimized system components	91
Table 4.7: Optimized monthly bills (predicted).....	99
Table 4.8: Monthly Carbon dioxide Emissions	99
Table 4.9: Case 1 in relation to Base case	101

Table 4.10: Case 2 Installation and Annual expenses.....	102
Table 4.11: Case 2 System components and electricity production	103
Table 4.12: Case 2 in relation to Base case	104
Table 4.13: Installation and Annual expenses	105
Table 4.14: Case 3 System components and electricity production	105
Table 4.15: Case 3 in relation to the Base case.....	106
Table 4.16: Case 4 Installation and Annual expenses.....	107
Table 4.17: Case 4 Component size and Annual electricity production.....	107
Table 4.18: Case 4 in relation to Base case	108
Table 4.19: Case 5 Installation and Annual expenses.....	109
Table 4.20: Case 5 Component size and Electricity production.....	110
Table 4.21: Case 5 in relation to the Base Case.....	111
Table 4.22: Results from ETAP PCC Branch characteristics	116
Table 4.23: Results from ETAP PCC Load performance	116
Table 4.24: Results from ETAP PCC Bus characteristics	116
Table 4.25: HOMER Cost summary and Rate of Depreciation (Optimised Case 1)	120

NOMENCLATURE

i	Index of each type of load,	
A_i	Number of hours,	
I_{th}	Device type used per day.	
P_i	Power rating of i th device type; number of device of i th type	
C_i	Number of particular loads	
$C_{ann,tot}$	Total annualised cost	[\$/year]
C_{cap}	Capital cost of the current system	[\$]
$C_{cap,ref}$	Capital cost of the reference system	[\$]
$C_{i,ref}$	Nominal annual cash flow for reference system	[\$]
C_i	Nominal annual cash flow for current system	[\$]
$C_{NPC,tot}$	Total net present cost	[\$]
CRF	Capital recovery factor	
C_{rep}	Component replacement cost	[\$]
$C_{rep,batt}$	Storage bank replacement cost	[\$]
$E_{prim,AC}$	AC primary load served	[kWh/year]
$E_{prim,DC}$	DC primary load served	[kWh/year]
$E_{grid,sales}$	Total grid sales	[kWh/year]
f	Yearly inflation rate	[%]
f_{PV}	Derating factor	[%]
i	Nominal interest rate	[%]
i_0	Rate at which you may acquire a loan	[%]
i'	Nominal interest	
IT	Solar irradiation	[kW/m ²]
I_s	Standard amount of radiation	[kW/m ²]

NOMENCLATURE

IRR	Internal rate of return	[%]
N	Lifetime of the system	[year]
N _{batt}	Storage bank number of batteries	
PWTG	Wind turbine power output	[kW]
PWTG,STP	Wind turbine power output at standard temperature and pressure [kW]	
RF	Renewable energy fraction	[%]
Q _{lifetime}	Single storage lifetime throughput	[kWh]
Q _{thrpt}	Storage throughput annually	[kWh/year]
R _{batt}	Life of storage bank	[year]
R _{batt,f}	Storage float life	[year]
R _{comp}	Component lifetime	[year]
ROI	Return on investment	[%]
R _{proj}	Project lifetime	[year]
R _{rem}	Component remaining life	[year]
U _{anem}	Wind speed at anemometer height	[m/s]
U _{hub}	Wind speed at the wind turbine hub height	[m]
YPV	Total installed capacity of the PV panel	[kW]
Z _{hub}	Wind turbine hub height	[m]
Z _{anem}	Anemometer height	[m]
α	Power-law exponent	
ρ	Actual air density	[kg/m ³]
ρ_0	Air density at standard temperature and pressure [1.225 kg/m ³]	
η_{rt}	Storage roundtrip efficiency	[%]

NOMENCLATURE

HPS	Hybrid Power System
DG	Distributed generation
KPC	Kasoa Polyclinic
MG	Microgrid
RES	Renewable Energy systems
COE	Cost of energy
NPC	Net present cost
DGR	Distributed generation resources
CSDG	Constant speed diesel generator
VSDG	Variable speed diesel generator
SOC	State-of-charge
FL	Fuzzy Logic
NREL	National Renewable Energy Laboratory
MS	Microsoft
DC	Direct current
AC	Alternating current
CO ₂	Carbon Dioxide
DOD	Depth of discharge
SOC	State of charge
GMA	Ghana Meteorological Agency
PRA	Power required from another source
PRN	Net power required
USA	United States of America
HOMER	Hybrid Optimization of Multiple Energy Resources.

NOMENCLATURE

HES	Hybrid energy system
SP	Solar Potential
ECG	Electricity Company of Ghana
TNPC	Total Net Present Cost
LCOE	Levelised Cost of Energy
PURC	Public Utilities Regulatory Commission
FIT	Feed-in Tariffs
GHGs	Greenhouse Gas Emissions
PV	Photovoltaic
DGR	Distributed Generation Resources
ENT	Nose and Throat
OPD	Out Patient Department
AC	Alternating Current
DC	Direct Current
RCH	Reproductive Child Health
CAPEX	Capital Expenditure
OPEX	Operational Expenditure
O&M	Operation and maintenance cost
S	Salvage value
NASA	National Aeronautics and Space Administration
GCRES	Grid-connected renewable energy system

ABSTRACT

Microgrid combines effective distributed generation schemes and interconnected loads in a specific location. In modern power distribution systems, microgrids can offer the opportunity to increase the amount of distribution generation and delivery of electricity when there are uncertainties with the national power grid. Hospitals are among the most energy intensive commercial buildings due to the significant air management requirements and high electrical load Equipment. Although hospitals have integrated additional on-site power generation to alleviate this situation, the problem of energy costs remains high. As a result, this study attempted to design optimal grid-connected solar PV, wind and battery storage system focusing on a typical urban healthcare facility in Ghana; Kasoa Polyclinic (KPC). To achieve the objectives of this study, the load profile data, methodological, economic data and components cost details are simulated using HOMER Grid software. HOMER Grid is the only demand rate reduction and optimization tool that considers generators as a peak shaving method. Study Results showed that the annual utility bill (base case) was US\$213,439.90 with a Total Net Present Cost (TNPC) of US\$7,004,608 and Levelised Cost of Energy (LCOE) at US\$0.2414 with 558.8tons/year of carbon dioxide emissions. The optimization (winning case) results also showed that the grid-connected hybrid system (solar/wind with battery storage) was more reliable and cost effective among the five cases compared to the base system. Thus, the reduced TNPC of the system at US\$3,098,562 and the LCOE of US\$0.093/kWh. Savings over the life of the project was US\$4,901,516 with reduced carbon emissions of 70.0 tons/year representing reduced emission cost of 2,100 Euros, translating to a monetary savings of 15,564 Euros (approximately US\$18,454/year). Therefore, this optimized model can be adopted to address technical, budgetary and environmental pressures.

CHAPTER ONE

INTRODUCTION

1.1. Background to the study

Distributed power systems, in the literature, can be conceptualized in diverse ways. One interpretation highlights the collaboration of small to medium-scale units that harness energy from a combination of renewable and non-renewable sources, and operate through a centralized power electronic control framework that coordinates all functional aspects (Uyterlined, Van Sambeek, & Cross, 2002). This networked assemblage of power-generating structures can either function as an autonomous source of power for targeted institutions such as hospitals, farms, residences, and small-scale industries, or can be linked to a larger grid network. Another application of such systems involves the provision of power in isolated regions through a hybrid energy framework, exploiting the rich energy sources available to enhance the quality of life for people in such remote areas (Nagaraj R., 2012).

If generation exceeds electricity demand, the excess electricity can be stored in local energy sources. Because of this, an independently distributed power system requires local energy storage sources that can be used later or injected into the grid through an intelligent process through the control supervision of advanced electronics and microprocessors. Typically, two or more sources in a hybrid power system with an advanced control system to ensure stability and reliability and their implementation is essential where long-distance transmission and distribution costs are high or where the availability of renewable energy sources is optimal (Ozerdem & Turkeli, 2005). For stability, two or more power sources

can be combined to balance each other's strengths and weaknesses. A combination of energy efficiency measures and the use of renewable energy will not only reduce electricity consumption and peak demand, thereby increasing power supply, but also reduce conventional power generation and greenhouse gas emissions from burning fossil fuels. Hybrid systems take advantage of the best properties of each energy source and can deliver grid-quality power. They can be developed as new integrated designs in small power distribution systems (mini-grids) and also retrofitted in diesel-based power systems. The interconnected system can be in different formations with different renewable energy sources.

Mini grids can be with wind and solar, or wind and fuel cell, or with solar, fuel cell and wind power (Iqbal M.T, 2003; McGowan, J.G. & Manwell, J.F 1999; Tarman, P. B., 1996)., Iqbal M.T, 2003[J]; Khan, M.J. & Iqbal, M.T 2005, Ntziachristos, L., Kouridis, C., Samaras, Z. & Pattas, K.,2005). These sources are environmentally friendly and use primary energy sources such as solar, wind and biogas, biomass etc. The sources can be divided into controlled sources and uncontrolled sources. Controlled sources mean output power can be easily regulated to target power; e.g. biogas. The power output from uncontrolled sources is unpredictable; e.g. solar and wind energy sources. In general, wind and solar energy sources do not meet the demand for needed energy when it is needed.

Therefore, special types of power plants should be built to avoid power shortages from uncontrolled sources (Yanning, Z., Longyun, K., Binggang, C., Chung-Neng, H. & Guohong, W., 2009). A microgrid combines effective distributed generation schemes and

interconnected loads in a specific location. A microgrid can be autonomously connected to or disconnected from the national grid, depending on physical or economic conditions. In modern power distribution systems, microgrids can provide an opportunity to increase the scale of decentralized power generation and delivery when there are uncertainties in the national power grid. Much research has been done on microgrid technology and operations, but there are fewer studies on demonstration programs and the development of commercial microgrids (Arefifar S.A., Mohamed, Y.A.R.I. & EL-Fouly, T.H.M., 2013). Electricity consumption and prices are increasing rapidly worldwide.

In order to meet these requirements, more powerful power plants need to be introduced or the structure of power generation needs to be changed with other approaches such as decentralized generation sources (DG). Among the DG sources, renewable energy sources have found more applications, mainly due to increasing concerns about environmental issues (Barbosa et al., 1998). Various renewable energy sources, wind power generation and photovoltaic systems have found more applications in distribution and household grids (Aichhorn A., Greenleaf M., Li H. & Zheng, J., 2012).

Furthermore, in light of the global pollution and energy crisis, decentralized power generation systems based on renewable energies such as PV and wind power generation are playing an increasingly important role in energy generation (Xu L., X Ruan, A., Mao, C. & Zhang, B., 2013). Combining suitable energy resources along with defining their ratings and operational strategies has been the focus of recent research. Various new techniques have been proposed in the literature that aim to improve the performance of

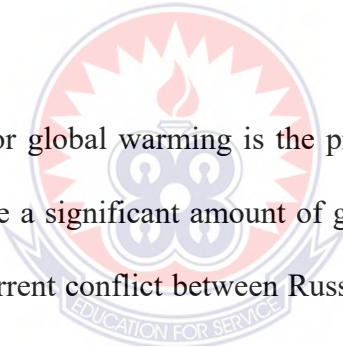
such systems through proper placement and planning, while minimizing distribution system costs and meeting system engineering constraints (Sedghi, M. & Ahmadian, A., 2016). However, most of these were designed for standalone systems in remote areas where it is either difficult or impossible to extend network service.

In addition, energy integration efforts have been widely used but such alternatives are distribution systems that will benefit both the grid and the customers (Edalati S., M. Ameri, M. Iranmanesh, H. Tarmahi, and M. Gholampour, 2016). As load demands are fluctuating with time, the variations in solar or wind energy generations do not always match frequently unable to meet the needs of customers sufficiently and reliably due to the volatility of renewable resources (Kazem H.A., T. Khatib, and K. Sopian, 2013). The microgrid system involving generation systems, storage units, and controllable loads can minimise the random nature of renewable energy sources (RES), resolve oversizing issues, and improve the reliability of the supply (Akinyele D., J. Belikov, and Y. Levron, 2018).

Therefore, it is predictable that electricity generation, transmission, and customers demand are met. Thus, there is a need to use a storage system or other components including a grid for providing an incessant power supply to the load (Suresh G., 2016). In one study, we look at the city of Bahir Dar in Ethiopia, which has unreliable power generation. Despite this, the country has a solar resource potential of between 5.16 kWh/m²/day and 6.69 kWh/m²/day with an average sunshine duration of 6.00 kWh/m²/day and wind speeds of 5.7 miles per hour (Argaw N., 2014).

1.2. Statement of the problem

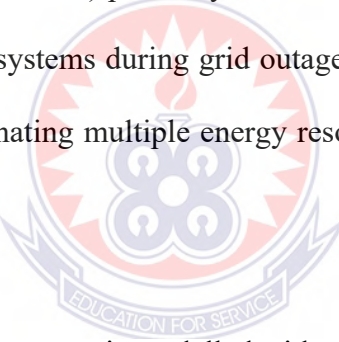
In Ghana, the frequent power outages or load shedding are primarily caused by the gaps in energy generation, technical faults, inadequate economic policies, and outdated power transmission equipment and conductors. This widespread issue of unstable electricity supply has been referred to as "Dumsor." Additionally, electricity tariffs are continuously rising. Furthermore, the depletion of finite fossil fuels such as coal, natural gas, and crude oil over time, along with the adverse effects of global warming associated with their use, pose significant challenges. Climate changes resulting from human activities that impact energy supply are increasingly affecting the world today (Norouzi N., Alipour, M., & Alidoost, F., 2021).

The logo of the University of Education, Winneba, is a circular emblem. It features a central sun-like symbol with rays, set against a background of a stylized building or structure. The text "UNIVERSITY OF EDUCATION" is written around the top inner edge of the circle, and "EDUCATION FOR SERVICE" is written around the bottom inner edge. The logo is semi-transparent and overlaid on the text.

One of the main reasons for global warming is the production of electricity from fossil fuels and these fuels release a significant amount of greenhouse gas emissions. This has been exacerbated by the current conflict between Russia and Ukraine. The price of fossil fuels has increased remarkably; therefore, this is the perfect time to step up implementation of renewable energy policies in countries that import fossil fuels. The introduction of renewable energy to replace fossil fuels and the fight against global warming has been successfully implemented in developed countries, from which developing countries can learn (Khan, H., I.; BiBi, R., 2022). Simply put, there is an ongoing problem of how to reduce electricity costs, sustain power generation, and protect the environment. However, the negative impact of power outages on healthcare is critical since healthcare facilities are essential to the safety, security and well-being of communities. The unpredictability of health crises requires hospitals to remain operational at all times, regardless of external

disruptions from power outages. Additionally, hospitals are among the most energy intensive commercial buildings due to significant air management requirements and equipment with high electrical loads. Although hospitals have integrated additional on-site power generation to alleviate this situation, the problem of energy costs and environmental issues remains. Most auxiliary generators on site are diesel generators but the exploitation of an optimal hybrid microgrid combining biogas, solar energy and even wind turbine generators is limited.

However, this study is aimed adding knowledge to prior research works by designing a hybrid renewable (Wind and Solar) power system for healthcare facilities to interconnect and support backup power systems during grid outages. Importantly, there is insufficient data on the value of coordinating multiple energy resources to achieve optimal technical and economic performance.



The proposed hybrid energy system is modelled with renewable energy sources from wind and solar, using a battery bank as an energy storage generator only for backup and to balance the system's peak power demand. This system can keep the constant power output under control. Battery bank energy storage is introduced to compensate wind and solar power generation systems; by using battery storage, we can supply constant current and the output power can be controlled. The network is introduced to provide the constant base load as an emergency measure. When this grid-connected hybrid renewable energy system produces more electricity than needed, the excess electricity is stored in batteries and we can use it for consecutive hours. Since the system is grid-tied, we can easily feed excess

electricity into the grid. The system becomes more economical by selecting the energy sources in ascending order of their energy production costs.

1.3. Objectives of the study

This study is set out to explore the to design an optimal Grid-connected renewable power generation focussing on a public commercial health care facility in Ghana known as Kasoa Polyclinic (KPC). The aim is to provide feasibility and reliability analysis of the proposed system in terms of technical features, cost effectiveness, renewable energy penetration and environmental friendliness with this scaled up model potentially adopted in other healthcare or public institutions.

The specific objectives are presented as follows:

- i. Conduct a load profiling to determine the estimated loads and time of operation for healthcare institution.
- ii. Conduct techno-economic comparative analysis of different grid-connected renewable energy generation systems in relation to the grid only architecture (Base case).
- iii. To model an optimal grid-connected renewable energy system using the HOMER Grid software environment.
- iv. Conduct comparative assessment of environmental impact for all optimized generation schemes in relation to the base case.

1.4. Significance of the research

The current state of electrical energy in Ghana faces various challenges, including production difficulties, sustainability concerns, limited access and high costs. The unstable power supply conditions have significant repercussions on the healthcare, industrial, and residential sectors, negatively affecting the reliability, stability, and quality of the power system. In a modern and financially developed society, energy plays a crucial role and the increasing energy demand strains the transmission and generation system, leading to frequent power outages.

The significance of research on grid-connected solar PV and wind power generation systems for hospitals is significant for various stakeholders, including:

- i. Hospitals: Research on grid-connected solar PV and wind power generation systems can provide hospitals with valuable insights and knowledge to help them optimize their energy systems, reduce costs, and enhance resilience and reliability. In Ghana, it has been observed that several healthcare facilities face challenges in meeting their high electricity costs despite their crucial services. These facilities remain connected to the national electrical power grid despite the difficulties hence causing financial loss to the gove. This study holds notable importance for public institutions, particularly hospitals, as it proposes a solution that could potentially alleviate their financial burden on the government.
- ii. Patients: In addition, the implementation of a grid-connected solar PV and wind power generation system can have a positive impact on the quality of care provided by hospitals. By reducing their dependence on the national power grid, hospitals

can guarantee the continuous operation of essential medical equipment and systems. This, in turn, enhances patient safety and improves the overall level of care delivered.

- iii. Healthcare providers: The use of clean energy sources such as solar and wind power can help healthcare providers improve their sustainability and reduce their environmental impact.
- iv. Governments: Research on grid-connected solar PV and wind power generation systems in hospitals can help governments understand the potential benefits and limitations of these systems, as well as inform policy decisions around renewable energy and energy efficiency.
- v. Utilities: The integration of renewable energy sources in hospitals can help utilities better understand how these systems can be integrated into the grid and improve grid reliability.
- vi. Researchers and academia: The study of grid-connected solar PV and wind power generation systems in hospitals can provide researchers and academics with valuable data and insights to further advance the field and inform future research and innovation.
- vii. Investors: Research on grid-connected solar PV and wind power generation systems in hospitals can help investors understand the potential benefits and risks of these systems, which can inform investment decisions in the renewable energy sector.

Overall, the significance of research on grid-connected solar PV and wind power generation systems for hospitals is significant for a wide range of stakeholders, including hospitals, patients, healthcare providers, governments, utilities, researchers, academia, and investors. This study to perform a comprehensive techno-economic analysis and optimization of on-site grid-connected solar PV and wind turbine systems using the HOMER grid environment. The proposed system that maximizes savings and reduces a site's electricity bill, significantly contributes to filling the research gap.

1.6. Thesis structure

This research study is centered on the optimization of design and feasibility analysis of renewable energy generation systems that are connected to the grid and are suitable for use in urban healthcare facilities. A depiction of the study framework and structure is illustrated in Figure 1.1. The study is organized into five chapters.

Chapter one of this research work contains the introductory part, which outlines the background and problem statement, the objectives and goals, the significance of the study, as well as the study's structure and framework, as shown in Figure 1.1.

The second chapter reviews previous empirical studies conducted in Ghana and other parts of the world. The studies examined various microgrid schemes, configurations and simulations, renewable energy generation, and the use of Homer Software in such analyses.

Chapter three of this study describes the materials and methods employed in the research. The chapter presents a detailed explanation of the criteria used for selecting power sources,

the simulation materials used, the energy audit conducted on the electrical equipment (load profile), and the assessment of energy resources available at the site. Additionally, the chapter covers economically prevailing data, as well as the use of HOMER and ETAP softwares in simulating the system.

Chapter four of this research study presents the detailed results and relevant discussions concerning the study, including the comparison of similar studies on economics, net present costs, levelized energy costs (using the HOMER cost analysis method), and the impact of emissions on the environment and the technical analysis using ETAP software. In chapter five, the final section of the study, a summary of the main findings, conclusion, and recommendations for further studies is provided.

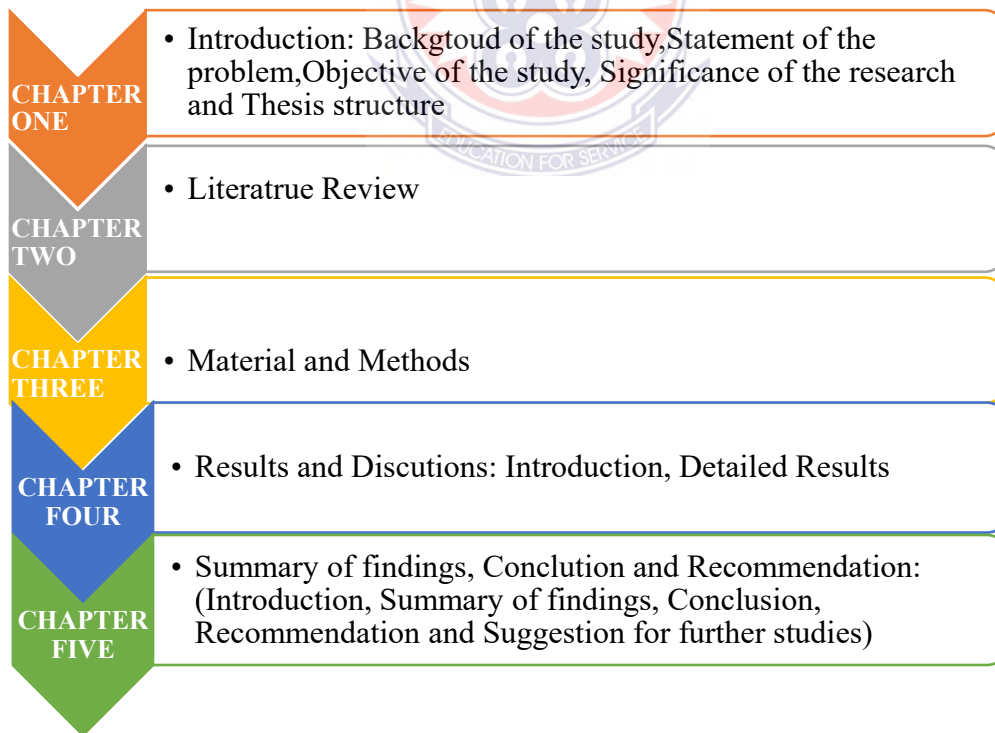


Figure 1.1 Thesis structure

CHAPTER TWO

LITERATURE REVIEW

This chapter provides a literature review on the impact of combining different energy generation sources with a focus on renewable energy sources on the existing national electricity grid. The chapter starts with microgrids, hybrid energy and previous studies using the simulation tool HOMER and other softwares used to simulate hybrid energy systems. The main highlight is on the different power generation configurations observations which serve as motivation for the study.

2.1. Microgrid (MG)

A microgrid is a small-scale, decentralized power system that is capable of operating either connected to or disconnected from a central grid. Microgrids typically consist of a combination of local generation sources, such as solar panels, wind turbines, or diesel generators, energy storage systems, and loads, such as homes, businesses, or critical infrastructure. (US Department of Energy. "Microgrid.", 2021).

According to the US Department of Energy, a microgrid is defined as "a group of interconnected loads and distributed energy resources within clearly defined electrical boundaries that acts as a single controllable entity with respect to the grid." Microgrids are designed to provide a reliable and resilient source of power to their users, even if the central grid experiences outages or disruptions (Liserre, M., & Wright, G, 2010).

Microgrids have become increasingly popular in recent years due to the growth of renewable energy sources and the need for more resilient and secure energy systems. They

offer several benefits over traditional central grid systems, including increased energy efficiency, reduced dependence on fossil fuels, and improved energy security.

(Lu, X., & Blaabjerg, F, 2020).

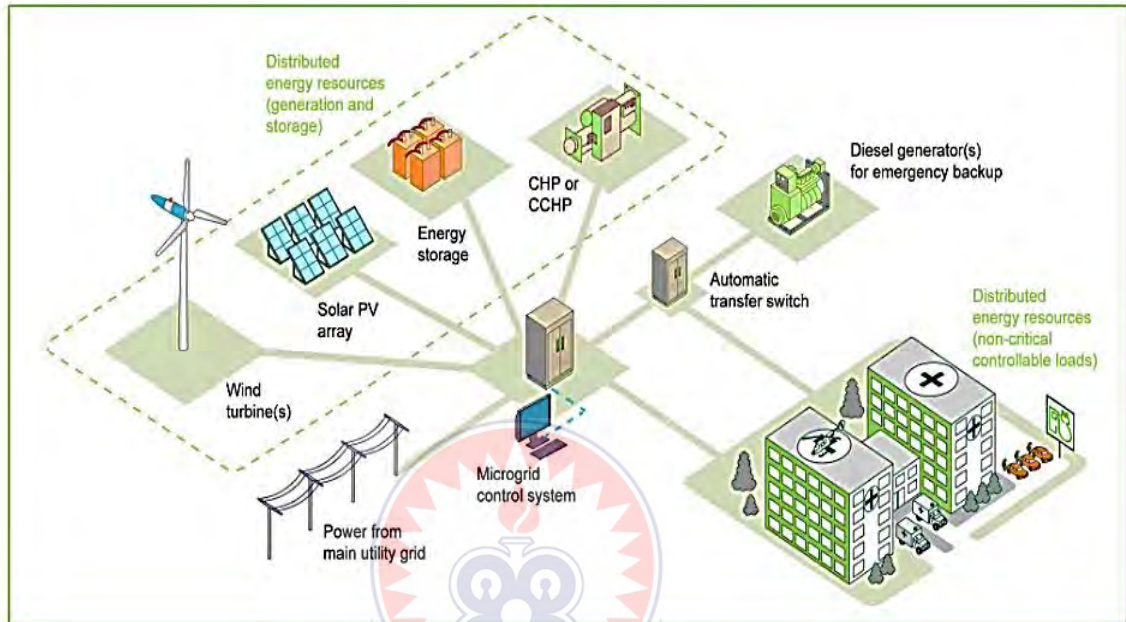


Figure 2.1: A microgrid architecture (Life is on Schneider Electric, 2019)

2.2. Grid connection architecture

One or more connection points to the overriding grid is a key component and must be well defined to balance energy production and demand within the microgrid using the overriding grid. Energy flows in the direction of the respective higher-level grid can be measured at these points in order to precisely measure the performance of the microgrid (Block C, Neumann D, Weinhardt C., 2008). There is a clear difference between a physical microgrid, which consists of an actual power distribution microgrid, and a virtual microgrid, which simply connects the microgrid participants via an information system. In contrast to a physical microgrid, virtual microgrids cannot be physically decoupled from

the higher-level network. Physical microgrids usually have a limited number of connection points to ensure efficient grid connection, but also to quickly decouple from the grid in the event of power failures.

For extended decoupling and island operation, microgrids require a high proportion of their own energy generation capacity and flexibility in order to ensure an appropriate level of security of supply and resilience. Flexibility can be provided in the form of demand or generation flexibility and storage capacity (Papaefthymiou G, Dragoon K., 2016). Because energy is a physical commodity and is transmitted in constrained networks, energy flow problems, e.g. Grid bottlenecks must be taken into account (Singh B., 2014).

2.3. Renewable PV penetration and incentives in Ghana

A physical microgrid can reduce the impact of grid problems by fully decoupling and controlling power supply within a community and builds on the existing distribution grid. The physical microgrid acts as a backup to avoid power outages. Due to the decoupling from the traditional grid, it can be operated in island mode. Then critical healthcare facilities such as clinic and. Hospitals receive energy at fixed prices. This explains the motivation behind this work to a large extent. Efforts to cover the load requirements and avoid financial losses are Ghana's further motivation for the study.

For the year 2020 alone, the forecast for the electrical load requirement is 3,115MW. This represents an increase of 311MW, or an 11% growth percentage, from the 2019 peak demand of 2,804MW that occurred on December 3, 2019. The projected energy

consumption including transmission grid losses for 2020 is 19,594GWh compared to the actual consumption of 17,887GWh in 2019, this corresponds to a projected growth of 9.5% an increase of 1,707GWh (Ghana Electricity Plan, 2020). Table 2.1 shows the installed capacity and reliable capacity of power generation facilities in Ghana in 2020.

Table 2.1: Available and reliable capacities (2020 electricity supply plan for Ghana)

Plants	Installed Capacity (MW)	Dependable Capacity (MW)	Fuel Type
Akosombo GS	1020	900	Hydro
Kpone GS	160	105	Hydro
TAPCO (T1)	330	300	LCO/Gas
TICO (T2)	340	320	LCO/Gas
TTIPP	110	100	LCO/Gas
TT2PP	80	70	Gas
KTPP	220	200	Gas/Diesel
VRA Solar Plant	2.5	0	Solar
TOTAL VRA	2263	1995	
Bui GS	404	360	Hydro
CENIT	110	100	LCO/Gas
AMERI	250	230	Gas
SAPP 161	200	180	Gas
SAPP 330	360	340	LCO/Gas
KAR Power	470	450	HFO
AKSA	370	350	HFO
BXC Solar	20	0	Solar
Meinergy Solar	20	0	Solar
Genser	60	60	Gas
CEN Power	360	340	LCO/Gas
Amandi	190	190	LCO/Gas
TOTAL IPP	2410	2240	
TOTAL (VRA, BUI & IPPs)	5077	4595	

There is the challenge of revenue losses caused by the inability or failure of public authorities to pay up their utility bills technical losses. At the national level, less attention is paid to the use of renewable energies, especially solar energy, in the grid system, which can significantly reduce the debt of the electricity sector on a large scale. Table 2.1 shows

that the national energy generation mix is only about 0.84% solar energy, there is little or no dependency. However, the total installed RE generation capacity in Ghana for 2020 is forecast to be 42.6MWp; this consists of 2.5MWp VRA Solar (Narong), 20.0 MWp BXC Solar (Winneba), and 20.0MWp Meinergy Solar (near Saltpond) and 0.1MWp Safi Sana. Total projected RES generation is 54.7GWh.

All these utility-scale solar PV systems are connected to the medium-voltage distribution system, the reliable capacity for solar energy through the national grid is practically zero (Ghana Electricity Plan, 2020). Figure 2.2 shows the percentage of installed solar power generation capacity for Ghana by different companies.

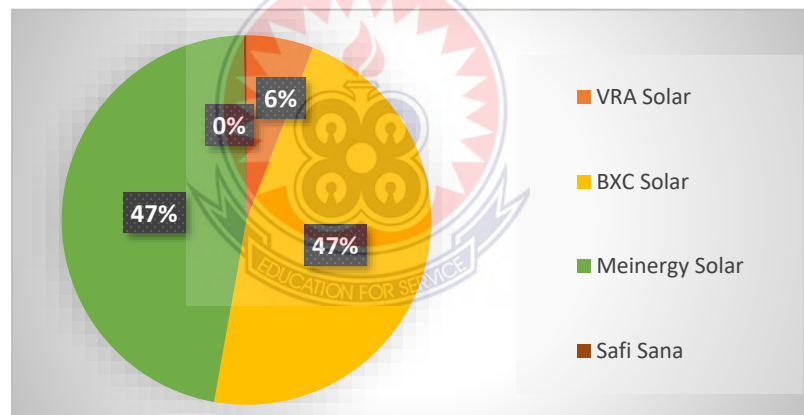


Figure 2.2: Ghana's solar energy installed capacity

The adoption and implementation of feed-in tariffs have a significant role in enhancing the implementation of technologies that use renewable energy resources (Vukman V. Bakić, Milada L. Pezo, Saša M. Stojković, 2016).

In Ghana, a techno-economic analysis proved the feasibility of using a grid-connected solar PV system to power air-conditioning systems during the day was conducted. The financial

analysis of the study revealed a potential savings of US\$1,600 compared to 100% grid power over a 10-year period. It also predicted potential 10-year savings of about US\$3,300 if the air conditioner ran solely on solar PV during the day, compared to electricity from the utility grid (Opoku R., Mensah-Darkwa, K. and Samed Muntaka, A., 2018). Parity for a 4.05 Wp solar PV system and compared the levelised cost of electricity of the system to the retail electricity price. It was found that commercial electricity consumers with installation costs of 3,567/kW and electricity production costs of 0.28/kWh need investment subsidies or subsidies of up to 22.9% in order to achieve parity. Non-residential occupiers above 600 kWh were competitive with solar PV. According to another study, private electricity consumers need investment support or subsidies between 40.6% and 92.5% to achieve parity with grid electricity (Quansah, D., Adaramola, M. and Anto, E., 2017).

Feed-in tariffs (FIT) are fixed electricity prices approved by regulators for the renewable electricity fed into the grid. Tariffs for FITs are developed together with the levelised cost of electricity (LCOE) for the RE technology used and are usually guaranteed for the economic lifetime of the project typically 15 to 25 years (Feed-in tariffs, 2020). FIT policies have been introduced in developed countries that contribute RES (e.g., solar PV, wind, small hydro, biomass, waste, geothermal, and tidal power) to their energy mix. African countries lag behind in implementing FIT and net metering policies due to network infrastructure and pricing challenges (Organization for Economic Co-operation and Development 2020). Like most African countries, Ghana has developed and enacted RE laws and policies to encourage RE with FITs guaranteed for 10 years. The Public Utilities

and Regulatory Commission (PURC) is mandated by law to develop a FIT pricing system. Grid infrastructure and pricing challenges for both renewable energy producers and grid operators have hampered the implementation of the directives and necessitated a review (PURC website, 2012).

The predominant resource used in FIT and Net Metering applications in Ghana is solar PV as it brings benefits to the local economy and electricity system. Promote and implement resilience. In Amman, Jordan, study on the impact of incentive tariffs on the introduction of grid-tied PV installation for a household. Grid-tied systems with an appropriate incentive tariff proved to be competitive in terms of COE and payback period (El-tous Y., 2012). A study of the potential energy cost savings and effectiveness of a grid-tied system using the South African FIT program for a residential building showed energy cost savings of 69.4% and a payback period of 19 years. The study also showed that the grid-tied system was cost-effective and eliminated the need for backup power.

2.4. Outlook for Renewable wind energy in Ghana

Wind energy is one of the fastest growing renewable energy sources in the world today (Islam MT, Shahir S, Uddin TI, 2014). However, Ghana is not yet able to harness this important renewable resource for grid power generation, although the country has sufficient potential., The average wind speed, measured about 10 km off the coast of Ghana, is about 5.5 meters per second (m/s) at a height of 50 m (Akuffo F.O., 2007). This makes the region suitable for wind turbines, especially with the development of low speed wind turbines. Wind resource data from National Aeronautics and Space Administration

(NASA) meteorology data for selected locations is presented in the next chapter. A wind resource map of Ghana developed by the National Renewable Energy Laboratory (NREL) shows the enormous potential of the country's wind resources as shown Figure 2.3 and that there are very good wind conditions of 7.8m/s to 9.9m/s along the eastern border with

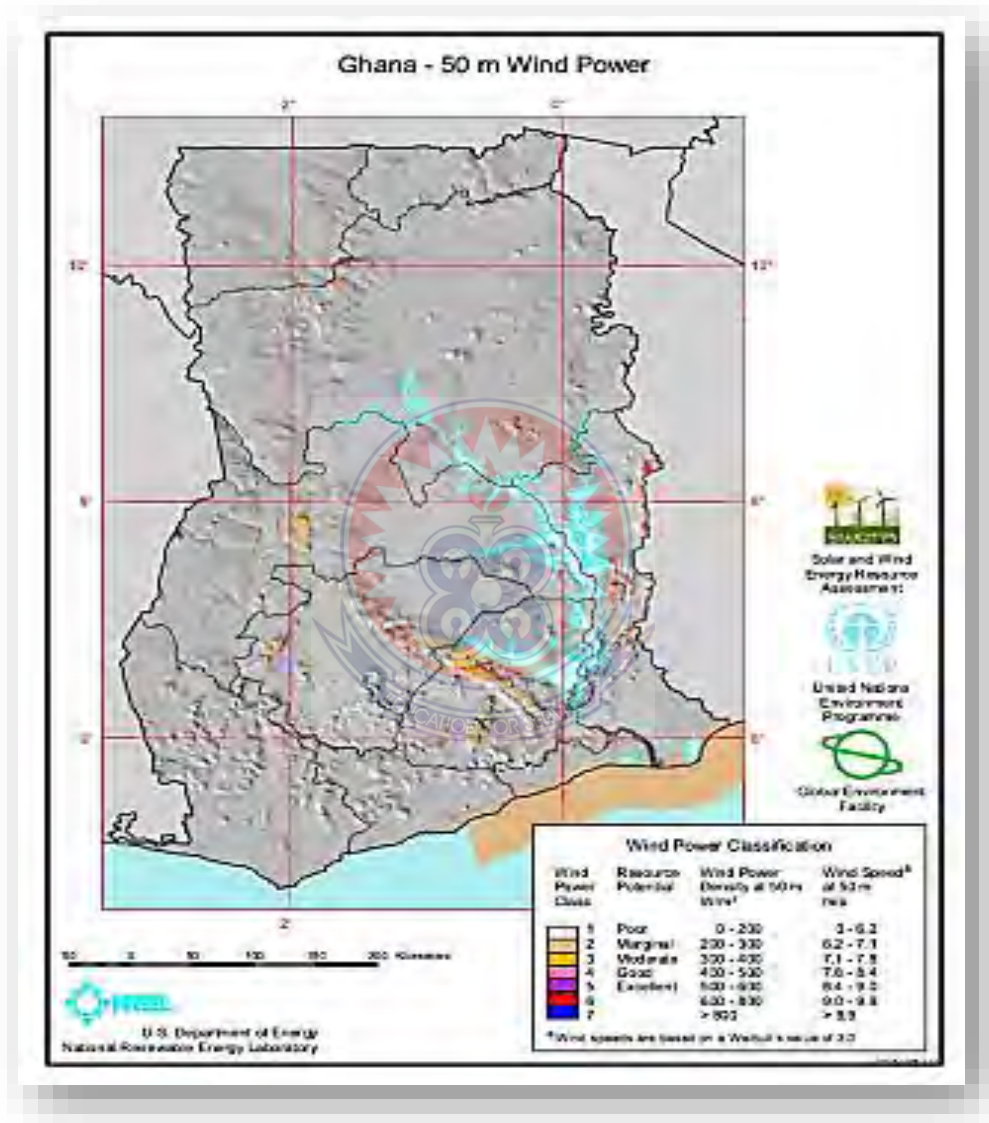


Figure 2.3: Wind resource map of Ghana (Wind research maps, 2004)

Togo. This has the potential to generate wind power density of 600W/m²-800W/m² over an area of around 300km²-400km².

A key reason for energy suppliers' reluctance to develop renewable energy sources in developing countries like Ghana has always been the cost factor. In comparison, however, wind power projects are less capital intensive and their energy costs are relatively lower than most renewable energies (Gyamfi S, Modjinou M, Djordjevic S., 2015).

Research conducted in Ghana suggests that the use of renewable energy technologies (RET) could increase to 30% by 2030, and this target can be achieved by using appropriate mechanisms to harness the country's abundant renewable potential (Awopone K. A., Ahmed F Zobaa, Walter Banuenumah, 2017).

2.5. Hybrid energy system components sizing approach

The rapidly improving green technologies enable renewable energy producers to use renewable sources with high efficiency. Although the advanced technologies of renewable energy generators and power conversion units are able to improve the level of energy harvesting, the energy available to consumers is determined by the energy flow path in a system configuration, which refers to the arrangement of components in a hybrid energy system.

For the discussion in this section, systems consisting of a diesel generator, a PV generator, a wind turbine and a battery are considered. There are a number of approaches to connecting the system components. In general, these connections are roughly classified as

series and parallel configurations, but are only applicable to the DC bus system, hence it is also called DC-coupled system (Khanniche S., 2006).

In a series configuration, the inverter and battery bank must be sized to meet peak load demand. The current from the PV generator and diesel generator must flow through the battery bank before the load demand is provided. Because of this, the battery bank is frequently cycled, which can result in shorter battery life. In addition, the recycling of energy from PV and diesel generators also leads to low overall system efficiency (Dehbonei H., Nayar, C. V. & Chang, L., 2003).

The parallel configuration is suitable for DC, AC or mixed bus system designs. This has been illustrated in two alternative parallel hybrid power system configurations. One of the advantages of parallel connection over series connection is that the energy sources are switched in such a way that the generators can meet the load demand separately. When the generators run in parallel with the renewable energy generator, the power can be supplied directly to the loads without going through the battery. Only the excess energy generated is stored for peak shaving purposes to supply the loads that exceed the capacities of the combined sources, e.g. during peak loads that usually occur in the evenings.

In terms of controllability, the parallel configuration is flexible, and an advanced system-level control strategy can be implemented to allocate and control the dispatchable components (Wichert B., 2000). Since the parallel configuration enables the implementation of a specific control strategy, this study deals with the AC-coupled parallel

hybrid power system, which has to be operated together with the renewable energy generator to ensure a reliable power supply. However, there are some disadvantages associated with using CSDG. Traditionally, a CSDG is sized to meet peak demand, which is short-lived in day-to-day operations (Nayar C. V., 2010). As the name suggests, the CSDG runs at a constant speed and must be operated from a minimum power of around 40% to 50% of the rated power of the CSDG.

In addition, the rigid operating regime of a CSDG also reduces the flexibility of system-level control. Research studies in (Pena, R., Cardenas, R., Proboste, J., Clare, J. & Asher, G., 2008) have proposed and discussed variable speed engine operation to overcome the problems of CSDGs. Rather than forcing the diesel generator to operate at over 40% of rated power at rated speed, the variable speed engine operating range allows the system to extract more power for efficient system operation. A variable speed diesel generator set (VSDG) has a wider operating range and can be operated at optimum speed for different power outputs, resulting in higher generator operation efficiency (Regen Power Pty. Ltd, 2010).

In a variable speed generator, the engine is run at a relatively low speed for low power requirements and vice versa. Running the diesel generator at variable speed can also help optimize the use of renewable energy in a system. Also, a VSDG exhibits better fuel efficiency compared to the CSDG because the CSDG is not operated at the optimal speed to follow the load request for minimal fuel consumption.

2.6. Software packages for simulating hybrid energy systems

A number of software packages have been developed to facilitate the design of a hybrid energy system. These simulation tools enable long-term performance analysis to help system designers and analysts decide on the optimal hybrid off-grid power system solution for a specific site or application. Some of these simulation tools are available online (courtesy of the programmers and their institutions) and are free to download. One of these software packages is HOMER. HOMER is an acronym for Hybrid Optimization of Multiple Energy Resources. HOMER is software application developed by the NREL in the United States. This software application is used to provide options for off-grid and standalone and distributed generation applications.

Homer software is the preferred application for the study because it combines engineering and economics into a powerful model that allows users to quickly and efficiently identify the most cost-effective options and also simulates real-world performance and offers a choice of optimized design. In addition, HOMER takes into account geographically specific criteria and risks such as fuel price changes, load growth, accelerated battery aging and changing weather patterns.

Another simulation tool is RET Screen, developed by Natural Resources Canada with input from Canadian government, industry and academics. Components are modelled in Microsoft (MS) Excel format and therefore require the MS Excel simulation platform. The software can be used to evaluate the performance of various power systems ranging from residential to industrial applications. HYBRID2 was developed by the University of

Massachusetts and NRET AT. The simulation models are programmed with MS Visual Basic. This software can simulate overall system performance and economics for various system configurations.

2.7. Empirical verification of simulation with HOMER

MG optimization models help to evaluate designs of both off-grid and grid-tied power systems for different applications. When configuring the system, many decisions should be taken into account: the large number of technology options and fluctuations in technology costs and the availability of energy resources complicate these decisions. Development of a hybrid energy system model identifying the economic configuration of PV and wind with diesel generation, (Jimenez A., 2018) used HOMER software as a useful in evaluating design problems in the planning and early decision-making stages of rural electrification projects owing to its flexibility. It evaluates a range of Equipment options across different limitations and sensitivities to optimize small power systems.

HOMER's optimization and sensitivity analysis algorithms facilitate the assessment of several possible system configurations. Simulation modelling in Homer is provided with inputs describing technology options, component costs, and resource availability. These inputs are used by HOMER to simulate system configurations (or mixtures of components) and generate results that can be viewed as a list of viable configurations sorted by current net cost. It also displays simulation results, compares configurations and evaluates them on an economic and technical basis. Sensitivity analysis can be utilized to identify the factors that have the greatest effect on the design and operation of a power system. HOMER Pro

is applied to design and find optimized hybrid power system configurations in terms of stability, low cost, size and number of components before installation (Matinn, M. A., Deb, A. & Nasir, A., 2013; Murthy S. S., Mishra S., Mallesham G. & Sekhar P. C., 2010). An investigation through a simulation study of a hybrid power system, economic combination of PV, Diesel generator, Converter and Battery storage was done. The simulated results using HOMER gave the comparative economic analysis with each configuration and evaluate the best configuration (Vania, N. & Kharea, V., 2013).

Thus, HOMER is useful in performing an energy balance configuration for each hour to choose whether a configuration is viable or not. For the same possible combination, the total cost of ownership over the lifetime of the project in a given area before installation is estimated (Nurunnabi M. & Roy N. K., 2015).

2.7.1. Wind+PV+battery hybrid architecture

A successful study of the performance of photovoltaic systems under different circumstances and climatic conditions with the aim to optimize the size and inclination of the PV generator in the system was carried out. Under four climate zones, tropical, subtropical, hot, dry and warm, the PV system performance was studied and an optimized state was achieved with HOMER software. Finally, it was concluded that a PV system can effectively lower electricity bills and reduce carbon emissions (Liu G., M. Rasul, M. Amanullah, and M. Khan, 2012).

An efficient power system of sustainable and reliable renewable energy has been developed in Khartoum to meet domestic power needs and total life cycle costs. For this purpose, the

basic data of solar radiation, wind speed and other input information were collected and then a hybrid optimization simulation model was developed. The simulation was used to identify the most technically reliable renewable system that meets household needs (Elhassan Z. A., M. F. Zain, K. Sopian, and A. Abass, 2012).

Other research to investigate the possibility of providing electricity to a remote area in Ethiopia that is disconnected from the main power grid. A hybrid system consisting of solar modules and a wind generator is used to generate electricity. The HOMER software has been used effectively to study the optimal sizing and operation strategy of hybrid renewable energy systems. This hybrid energy includes wind energy and solar energy. In addition, the emission to the atmosphere is zero considering this design and also the use of a diesel generator can be minimized by maximizing the use of renewable energy (Raza, N. A., Othman, M. M. & Musirin, I., 2010).

In a study, different combinations of generation systems are tried in order to obtain the optimal configuration. An effective development of a hybrid system, based in particular on photovoltaics and wind energy, using a computer program for design and dimensioning, to meet the load requirements of a single-family house in Palestine according to their requirements. Wind and sun measurements serve as input. The hybrid system minimizes electricity generation costs throughout the life of the project. It turns out that the use of hybrid energy as the main energy source for every place proves to be advantageous both in the economic area and in the conservation of natural resources and for optimization purposes, HOMER software is used (Karim D.A., and I. Mahmoud et al., 2012).

In another study, HOMER software was used to investigate the possibility and feasibility of using a self-contained solar/micro hydro system for low-cost power generation that can meet the power needs of a typical remote and isolated rural area. Targeted optimization was carried out here in order to improve the technical design and the economic efficiency of the hybrid system (Kusakana K., J. Munda, and A. Jimoh, 2009).

A development in a combination of PV output power and battery power as a backup source to meet the load requirements with a variable speed generator both a traditional constant speed generator and novel variable speed generators. In order to improve the reliability of this system, a constant speed generator based on fossil fuels is used, as the renewable energy generation technology is strongly influenced by climatic conditions (Lim et al., 2010). A study based on HOMER software to develop a system to meet the daily load requirements of Gkceada, Turkey's largest island, with renewable power generation technology. Here the hybrid system consists of solar modules, wind turbines and batteries for emergency power supply. Component values are determined by simulations. Energy costs are also taken into account so that they can be minimised (Demiroren A and U. Yilmaz, 2010).

HOMER software was used to study the feasibility and reliability of a zero energy house in Newfoundland. The input data was year-round recorded wind speed information, solar data, and electricity usage information in a typical R-2000 home in Newfoundland. The optimized performance of the overall system is analysed and worked out in detail (Iqbal, 2003). A related study uses renewable energy technology to meet the load needs of a large

hotel in a subtropical coastal area of Queensland, Australia. HOMER software was used for optimization purposes. After successive experiments and analysis, it was concluded that wind energy is more viable and reliable than PV panels and also more economical as a renewable technology in large-scale operation (Dalton G., D. Lockington, and T. Baldock, 2008).

2.7.2. PV+diesel generator+battery hybrid architecture

HOMER software has been used effectively to design an optimization model that can Analyse all small power technologies individually and also hybrid systems to determine the most cost effective solution to power needs. The minimum discounted total costs were formulated with the use of renewable raw materials and the daily and monthly load profile (Lilienthal P., 2004). A draft of a PV energy plant for seawater desalination in Kuala Perlis. The design consists of site selection, load selection, system sizing and cost efficiency. Together with the test setup for a desalination plant, this design is also being verified for feasibility and reliability (Baharudin N., T. Mansur, R. Ali, Y. Yatim, & A. Wahab, 2007).

Another study presents the use of HOMER software to design and model a residential power system for a specific residential family in Boulder, Colorado. Here, a PV grid is used to generate electricity with a battery bank for emergency power supply. Cost efficiency is taken into account in this study (Johnson N., P. Lilienthal, & T. Schoechele, 2011). A projected solar irradiance and load requirements in the supervisory control to develop an On-Grid hybrid energy system. Here, models for forecasting and predicting solar resources and load demand are developed and these models are used to control a

variable speed off-grid PV diesel generator hybrid energy system (Lim P., and C. Nayar, 2012).

2.7.3. Wind+PV+hydroelectric+battery hybrid architecture

A study was conducted in Ethiopia to determine the reliability and feasibility of a hybrid hydroelectric-solar-wind generator system. The load requirements for lighting, radio, television, electric bakers, water pumps and our mills are tested. Elementary schools and health posts are also supplied. They developed a system that generates electricity at a cost of less than US\$0.16 per kWh (Bekele G., and B. Palm, 2007).

2.7.4. Wind+diesel generator+battery hybrid architecture

As wind energy sometimes does not provide the required power to cope with the meteorological fluctuations of the area under consideration, in a study, a backup diesel generator was included in a study of a diesel plant in a village in north-eastern Saudi Arabia. HOMER is used to model and design the system. Various wind speed data were collected for simulation purposes. During the simulation program, fuel prices are kept within certain limits and the effectiveness of the system is discussed (Rehman S., I. Amin, F. Ahmad, S. Shaahid, and A. M. Shehri, 2007)

Another study on the usefulness of a wind home system using HOMER software was conducted in a coastal region of Bangladesh. Here there is an opportunity to use wind power as a renewable energy technology, as the wind potential in this region is more or less large. With a wind speed variation between 4m/s, it was concluded that, taking into

account environmental influences, power consumption and long-distance accessibility, a wind home system is applicable in most coastal regions (Khadem S.K., 2007).

2.7.5. PV+hydroelectric power+diesel generator+battery hybrid architecture

Design of a hybrid system of solar energy, hydroelectric power and diesel generator. The aim was to evaluate power generation during the peak hours of solar radiation. The optimization models consist of two variants, one with PV modules, diesel generators and micro hydroelectric power plants and one with PV modules and hydroelectric power plants (Alexandre B., de Souza Paulo Hroeff, and K. Arno, 2012).

2.7.6. Wind+PV+fuel cell hybrid architecture

A study on the feasibility and reliability of a hybrid system with HOMER. The system consisted of solar and wind energy as well as hydrogen as a storage unit to cover the electricity demand as an island system. The input data used were technology options, component costs and fall back performance, with the end results being viable system configurations based on current net costs (Türkay B.E., & A. Y. Telli, 2011).

2.7.7. Wind+PV+diesel generator+battery hybrid architecture

A hybrid model design to improve power supply in telecom operator facilities since there are problems using only diesel generators, renewable energy sources such as solar photovoltaic, wind turbine generators or both are used. Using renewable technologies has proven to be more economical than a single storage system (Bajpai P., N. Prakshan, & N. Kishore, 2009).

In the remote hilly rural area of India using a hybrid power generation system, HOMER software was successfully used to conduct a study. The final design was the one with the lowest emissions of environmental pollutants such as carbon dioxide, carbon monoxide, hydrocarbon, particulate matter, sulphur dioxide and nitrous oxide. This design consisted of five wind turbines (10kW), a PV panel (9kW), 30 batteries (6V, 6.94kWh each) and a diesel generator (65kW). Current net construction costs were US\$1,270,921 with capital costs of US\$148,133 and energy costs of US\$0.296/kWh (Rajoriya A., & E. Fernandez, 2010).

2.7.8. Wind+PV+diesel generator+fuel cell+battery hybrid architecture

An effective use of HOMER software to present a study for optimization and comparison between renewable technology and conventional power generation techniques for a telecommunication site in Mulligan, Labrador, in Canada. Renewable technologies reduce pollution while reducing the overall cost of generating electricity. The result was a cost-effective solution that reduced diesel generator run time, which in turn reduced emissions (Badawe M. E., T. Iqbal, and G. K. Mann, 2012). HOMER simulation tool was used for planning, modelling and cost simulation of self-sufficient solar and biomass energy in Sarawak. The main goal of this setup was to develop an optimized, reliable, functional and autonomous system to cover the electricity needs of the area under consideration and thus also ensure economic viability (Barsoum N., W. Y. Yiin, T. K. Ling, and W. Goh, 2008).

On the islands of the Indian Sundarbans, the simulation tool HOMER was used to investigate how remote villages could be supplied with renewable energy technology.

Around 20 islands with more than 100,000 households in 131 villages in India need electricity as a basic requirement for their daily life. Since the wind potential in this region is very low, biomass and solar panels are used as renewable technologies (Mitra I., and S. G. Chaudhuri, 2016).

In all of these previous studies, there is the need for more research in the area of grid-connected renewable energy generation sources to provide constant power to critical facilities. While HOMER Pro is excellent for analysing off-grid systems, HOMER Grid is designed for on-grid or behind-the-meter systems, it can also monitor off-grid systems in the event of a prolonged grid outage, an extreme case, model weather event. Therefore, to achieve the main objective of this work, HOMER Grid software is used for the feasibility studies of grid-connected renewable power generation for urban healthcare facilities:

2.8. The energy storage system.

Much of the hybrid energy systems described in the literature consisted of large energy storage elements to store excess renewable energy and meet peak load demand. Research studies discussing various configurations and modes of operation of hybrid energy systems can be found in (Muljadi, E. & Bialasiewicz J. T., 2003). However, the initial cost of the systems, including the massive energy storage elements, is usually prohibitive and inconvenient, especially for small and medium-sized applications in remote areas. For example, the initial cost of a hybrid power system with a large battery bank may include costs for the battery case, ancillary components, shipping, and installation. The investment

costs for such a system would increase with the penetration of renewable energies due to the massive battery storage required.

In addition, the battery bank is the most sensitive component in a system where its state of charge must be controlled and monitored to prevent overcharging or over discharging.

Another issue will be the lifespan of batteries, as these elements typically have a short lifespan due to frequent charging cycles and need to be replaced every five to ten years. In addition, the used batteries must be recycled or disposed of in accordance with current safety regulations. Unfortunately, most developing countries lack recycling facilities and proper battery disposal regulations. In some applications, diesel generators are designed to charge the battery when the state of charge is low (Darbyshire J., 2010).

The battery charging process is normally based on set point control, which only ends when the battery bank is fully charged. This strategy is very likely to result in energy loss, which means that the excess renewable energy may not be stored in the battery bank as it was charged by the diesel generator the day before. Consequently, this will result in the excess renewable energy ending up in landfill. Also, during the power cycle process, charge and discharge losses may occur due to the inefficiency of the charger and battery. For applications with special requirements, e.g. B. telecom towers, however, there may be times when battery storage is mandatory for a reliable power supply. In such an application, system operation can be optimized by selecting an appropriate battery bank size.

Among the numerous configurations of hybrid power supply systems, the combination of a renewable energy generator and a diesel generator without complex control proves to be

more robust and viable for remote applications compared to high-penetration renewable energy systems that require large size energy storage elements and complex system control. For these reasons, several researchers have proposed hybrid energy systems without energy storage elements. In a study on the feasibility of a system without storage elements by retrofitting renewable energy generators into existing diesel-based systems was presented (Ruther, R., Schmid, A. L., Beyer, H. G., Montenegro, A. A. & Oliveira, H. F., 2003) An experimental study reported showed the possibility of practical implementation of hybrid propulsion systems without energy storage elements (Yamegueu, D., Azoumah, Y., Py, X. & Zongo N., 2011).

While system configuration is known as one of the factors affecting system operation, an appropriate power management strategy that determines overall system performance is another aspect that deserves the same attention. A significant number of research studies on different dynamic control strategies have been discussed. Setiawan introduced the voltage-controlled voltage-source inverter and current-controlled current-source inverter and demonstrated the component operability for an AC-coupled mini-grid hybrid system using PSIM simulation software (Setiawan A.A., 2009). Darbyshire proposed frequency shift control for decentralized renewable energy distribution systems, one of which he successfully implemented at the Eco Beach Project, Broome, Australia (Darbyshire J., 2010).

A study was conducted on the performance of a standalone inverter operating in grid-tied mode for a hybrid PV wind system (Dali, M., Belhadj, J. & Roboam, X., 2010). Grid-tied

inverter control techniques and system operation have been discussed (Jih-Sheng L., 2007). Further examples of the use of power conditioning units for dynamic strategies can be found in (Agbossou, K., Kelouwani, S., Anouar, A. & Kolhe, M., 2004). Other than the standard dispatch strategies, intelligent-based power management also has a major position in the area of hybrid power system research. Dufo- López et al., used a genetic algorithm for the optimisation of stand-alone renewable systems with hydrogen storage due to the low computational requirements (Dufo-López R., Bernal-Agustín J. L. & Contreras, J., 2007).

In more sophisticated schemes, operation of the diesel generator and batteries are scheduled in accordance with renewable resources and load demand forecasts to improve overall system efficiency. Wichert proposed the algorithm of 3-hour allocation of photovoltaic resources and load demand forecasts for planning and controlling a PV diesel battery system and a laboratory setup was built to demonstrate the proposed method (Wichert, 2000). Panikar et al., proposed a neuro-fuzzy controller for a wind-diesel-battery hybrid system (Panickar P. S., Rahman, S. & Islam, S., 2001). Mitchess et al., presented the idea of a predictive controller implementation to minimize the energy wastage caused by fully charging the battery from a standby power plant instead of charging it with renewable energy (Mitchess, K., Nagrial, M. & Rizk, J., 2006).

Despite the enormous concerted efforts that have been made in researching the design and operation of hybrid propulsion systems, all the previously mentioned publications have only focused on systems using a conventional diesel generator, while not many

performance studies have been completed for a hybrid propulsion system using a grid-tied renewable power generation system. However, few research studies on advanced power management for a hybrid power system using a VSDG have been reported and this represents a knowledge gap required for grid-connected power generation from renewable sources, which could offer both financial and environmental benefits. Therefore, this work proposes a predictive energy management concept for the configuration of grid-connected renewable energy systems.

A studied case of a remote residential area in Malaysia and the use of HOMER to analyse the economics of a hybrid system. The study uses 40 households with a peak demand of 2 kW. The peak demand is 80 KW, the analysis takes into account the basic demand of around 30 KW. While such high rural demand may be typical of Malaysian conditions, this is certainly not the case for others. The study also does not consider the use of electricity to be productive (Lau K. Y., M. F. M. Yousof, S. N. M. Arshad, M. Anwari, & A. H. M. Yatim., 2010). As we found from the above literature, the studies mainly focused on the supply of electric power for household purposes only, and did not consider the demand for institutional purposes, irrigation applications, municipal and commercial activities for socio-economic development, and the studies did not focus on the performance reliability and quality of the power supply. The current study addresses several limitations that were present in previous research, including inadequacies in modeling and estimating overall load profiles.

The main objective of another study was to model micro-grid systems from a combination of renewable energy sources such as solar photovoltaic and wind with storage battery

operating in a grid-connected mode in the city of Bahir Dar, Ethiopia. There is a need to use a storage system or a grid system to provide uninterrupted power to the load. The system is designed to reliably meet the city's customer load needs with good power quality, which cannot be met with conventional system generation alone. Residential, institutional, commercial, agricultural and small industrial loads are estimated with an average electricity demand of 15,467 KWh per day. Optimum sizing of the microgrid system components is done using HOMER Pro software. The simulation results showed that the PV-wind-based grid-tied microgrid system with a storage battery is sustainable, technically economically feasible and environmentally friendly in meeting the load requirements in terms of the optimal sizing of PV module and wind turbine (Meziegebu Getinet Yenalem, Livingstone, M.H. Ngoo, Dereje Shiferaw, & Peterson Hinga, 2020).

A recent study aimed to conduct a techno-economic performance and optimization analysis of grid-connected PV systems, wind turbines and battery packs for Syiah Kuala University, located at the tip of the island of Sumatra in the tsunami-affected region. HOMER simulation software was used to analyse and optimize the renewable energy needs of the institution. The methodology began with site specification, average electrical load demand, daily radiation, clearness index, daily site temperature, and system architecture. The results showed that the energy storage was initially included in the simulation, but later removed to save money and optimize the share of renewable energy. Based on the optimization results, two types of energy sources were selected for the system, solar PV and wind turbine, contributing 62% and 20%, respectively.

In addition to the share of renewable energy, another reason for system selection is the cost of energy (CoE), which has fallen from US\$0.060/kWh to US\$0.0446/kWh. In summary, the study found that by connecting solar PV and wind turbines to the local grid, this renewable energy system can contribute up to 82% of the electricity needed. However, the obstacle to the implementation of renewable energy in Indonesia is the cheap price of electricity, mainly generated with cheap coal, which is abundant in the country (Riayatsyah T. M. I, T. A. Geumpana, I. M. Rizwanul Fattah, Samsul Rizal & T. M. Indra Mahlia et al., 2022). A method for economic assessment and calculation of greenhouse gas emissions (GHGs) from a grid connected renewable energy system (GCRES). An investigation is carried out in large-scale operation of 67MWh/day GCRES. A comparison is made between a GCRES and a standard grid operation, focusing on environmental and economic impacts. Emissions and the share of renewable energy production in total energy consumption are calculated as the most important environmental indicators.

The costs including NPC (Net Present Cost), COE (Cost of Energy) and payback period are calculated as economic key figures. Using the hourly mean global insolation, temperature and wind speed data relative to the In Salah and Aurar sites characterized by an arid and hot climate according to the Koppene Geiger climate classification, a long-term continuous implementation of hybrid renewable energy systems using the HOMER Software to simulate. As a result, a GCRES is observed to reduce 30% and 35% of greenhouse gas emissions and 81% and 76% of COE during the operational phase for In Salah and Adrar, respectively. Investing in GCRES should only be considered if there are

plans to produce parts of the equipment locally, resulting in a significant reduction in costs and consequently emissions (Djohra Saheb Koussa, 2016).

A feasibility analysis of a grid-tied PV/wind option for a rural health centre using HOMER Evaluation to determine the most appropriate renewable energy systems for the clinic. Wind speed and solar irradiance from NASA's Surface Meteorology and Solar Energy website, along with hourly load data for the clinic, are used to perform simulations, optimization, and sensitivity analysis for the RES.

The RES feasibility study shows that the optimal grid-tied PV/battery system is the most economically viable option for the health centre. The system consists of the grid, 2kW PV modules, two 6FM200D batteries and a 1kW converter. The total net cost (NPC) for this system is US\$8,901 with an initial capital cost of US\$2,800 and a levelised cost of electricity (COE) per kWh of US\$0.096. This system will save 542.753kg (0.5427tons) of carbon dioxide per year. The result of this research shows that 43% of the electricity generated comes from renewable sources, which means that the clinic will continue to be powered even if the power grid is interrupted for an extended period of time (Rilwan Usman, Adamu Gidado, 2017).

2.9. Black start Scheme

According to the International Council on Large Electric Systems (CIGRE), a black start is "the process of restoring the power system to normal operation following a total or nearly total blackout, without relying on external power supplies". The goal of a black start is to

quickly restore power to critical loads, such as hospitals, water treatment plants, and emergency services, and then gradually restore power to the rest of the system (International Council on Large Electric Systems, 2016).

A well-designed black start scheme is crucial for ensuring the reliability and resilience of the power system in the event of a blackout. Black start schemes vary depending on the size and complexity of the system, but they generally involve the use of backup generation and battery storage systems, as well as specialized equipment and procedures to safely restart the system (Huang, X., & Sauer, P. W. (2015).

2.10. Point of Common Coupling (PCC) of hybrid systems

In the context of grid-connected renewable systems, the Point of Common Coupling (PCC) refers to the point in the electrical system where a distributed generator, such as a wind turbine or a solar photovoltaic array, is connected to the utility grid. The PCC is an important location for monitoring and controlling the flow of power between the distributed generator and the utility grid, and for ensuring that the system remains stable and reliable. According to a study, "The PCC can be defined as the point of connection between the distributed generator and the grid, where the power injection and extraction occurs, and where the power quality and stability must be maintained." (Shalchi and Guerrero, 2011). Similarly, a study defines the PCC as "the point of interconnection between the distributed generator and the power grid, where the voltage and frequency of the distributed generator are synchronized with those of the grid, and where the power quality and stability are ensured." (Khalesi and Mohamed, 2016). In the context of grid-

connected renewable systems, the PCC is often monitored and controlled using advanced power electronics devices, such as voltage source inverters, which are capable of regulating the voltage and frequency of the system, and of controlling the flow of power between the distributed generator and the grid.

In a study, a technical analysis was carried out for a grid-connected photovoltaic/wind generation scheme which consisted of a thorough investigation into the electrical and technical aspects of the system, which included an assessment of power quality, harmonics, voltage fluctuations, and voltage unbalance (Giraja S. C., Amresh K. Singh, Sanjay Agrawal, & N.K. Sharma, 2017)

In another research; “Design, Simulation and Stability Analysis of Wind-PV-Diesel Hybrid Power System Using ETAP”, a review of the hybrid power system is presented and detailed analysis of steady state and transient stability is performed by using ETAP software to model the hybrid wind-solar electric power system. (Md Saleh Ebn Sharif, Md Monower Zahid Khan, Md Moniruzzaman & Anamika Bose, 2017).

CHAPTER THREE

MATERIALS AND METHOD

This chapter first highlights the modelling method used; HOMER Grid simulation tool and assumed analytical framework, selected site, load profile selected site meteorological assessment data, system component costs and input economic data.

3.1. Research methodology

In order to properly examine the operational behaviour of all possible scenarios, the evaluation of renewable energy projects often requires the application of relevant criteria to on-site site data. The Homer grid analytical framework was used in this study (Halabi, L.M.; Mekhilef, S.; Olatomiwa, L.; Hazelton, 2017). Again, the detailed technical analysis on the characteristics of point of common coupling of grid-connected renewable systems employed Electrical Transient and Analysis Programme (ETAP) and Load management and voltage regulation schemes adopted for this study.

3.2. HOMER Grid software as analytical framework

The Hybrid Optimization Multiple Energy Resources Grid (HOMER Grid 641.8.9 Evolution Edition) was used for this study; developed in the USA by the National Renewable Laboratory in 2018, this latest version of HOMER software provides a more efficient way to model hybrid energy systems and analyse solutions to reduce electricity costs for a grid-tied system.

The techno-economic analysis of the simulation of renewable energies for off-grid systems has been widely published in the past (Halabi et al., 2017) and (Bahramara et al., 2016). However, very few feasibility studies have been conducted on optimal grid-connected electric renewable hybrid systems using the HOMER grid as a simulation tool (Riayatsyah et al., 2022). The data collected from the selected location were examined using these criteria. Each criterion was addressed and studied to characterize the overall system design, with a focus on the selection of renewable energy components. It is a powerful tool that integrates technical and economic data into a single model, enabling complicated calculations to quickly assess self-consumption value, load charge reduction and energy arbitrage. Users can analyse multiple components and design outcomes, find cost-competitive points for alternative technologies, explore strategies to reduce project risk, and identify the best cost-effective design. It also replicates real-world performance to help system designers and optimizers make better decisions.

In this study, a comprehensive assessment of the commercial utilization of KPCs and the available resources found is given as input before running the simulation with the software. In addition, the spectrum of components with different limitations, sensitivities and Life Cycle Costs (LCC), which includes initial capital, replacement, maintenance and operating costs, are fed into the HOMER. Then HOMER runs the necessary simulation to meet the required load requirement. Figure 3.1 illustrates the HOMER analysis framework. The system adjusts the size of the components when the demand is not met by the given situation, and then displays the optimal component size with its maximum energy production.

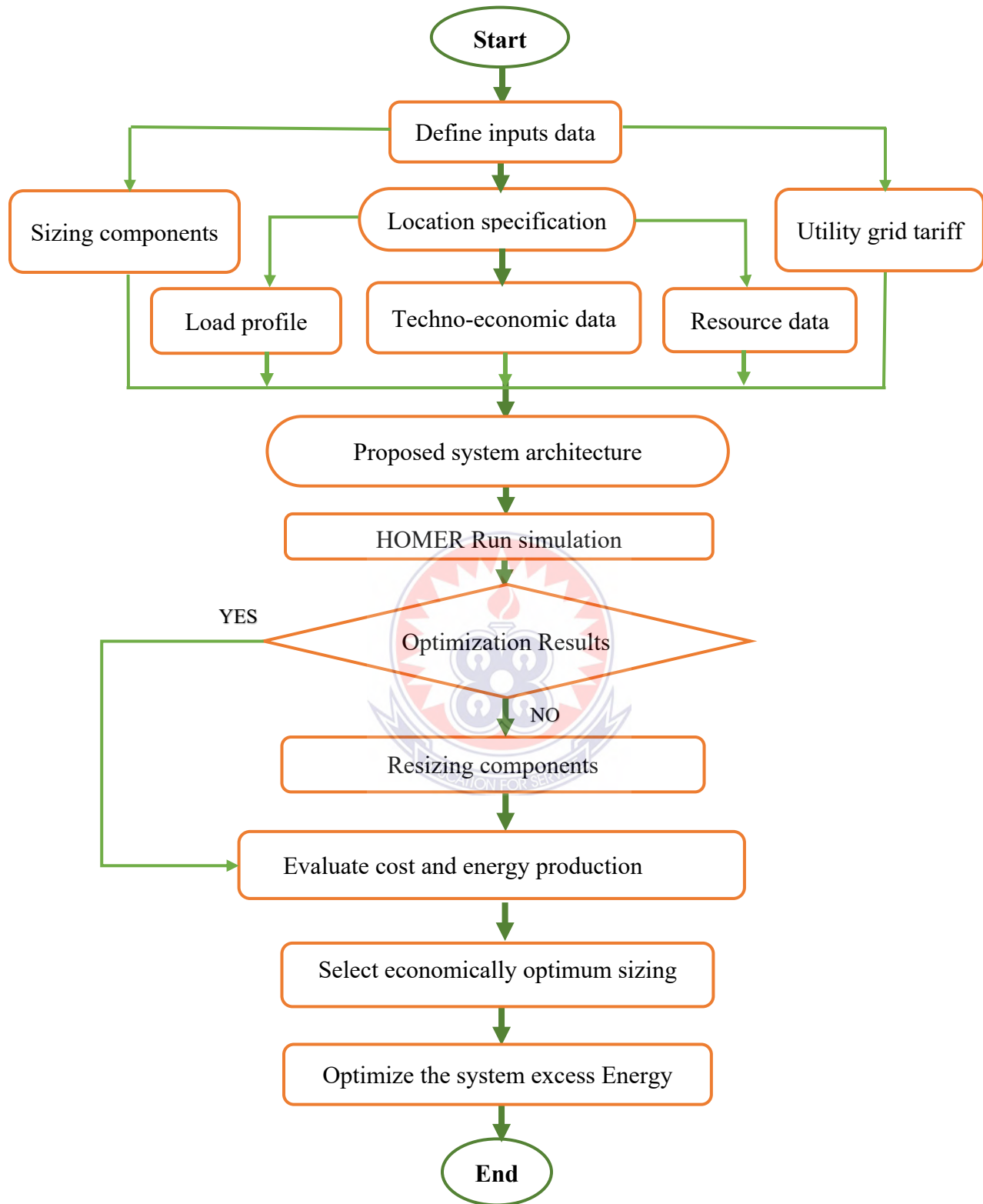


Figure 3.1: Flow chart of methodology

3.3. Simulation data used

3.3.1. Selected site specification

There are many favourable locations for distributed energy generation throughout the Ghanaian territory. Since choosing a specific site is not an easy task, interest focuses on the model of a grid-connected renewable power generation system for a municipal health facility called Kasoa Polytechnic (KPC) in the Kasoa sub-municipality of Awutu Senya East Municipality of the Central Region of Ghana.



Figure 3.2: Site map for KPC

KPC as a public health institution was established in 1995 as a health post and expanded into a health centre in the early 2000s. In 2013, the facility was expanded into a polyclinic and has been operated as such ever since. Kasoa sub-parish is one of the five (5) sub-parishes in Awutu Senya East Parish. The sub-municipality consists of 15 parishes with Kasoa as the capital. The sub-municipality is bordered by North Kasoa and Opeikuma sub-

municipalities to the north, Gomoa East (Nyanyarno) District to the south, Odupongkpehe Sub-municipality to the east, and Gomoa East (Budumburam) Municipality to the west.

The main clinical services that KPC currently provides to these communities are: 24-hour Medicare, 24-hour emergency, records, inpatient services, diagnostic services - laboratory, ultrasound, electrocardiogram service, drug and pharmacy, eye care, ear, Nose and Throat (ENT), Dental Services and Psychiatry/Community Mental Health. Operating out of one building in the early 2000s, the facility clinical (OPD) had two rooms, each with two beds, which served as emergency departments. The maternity ward and ANC also worked in the same room with partitions that had six beds for women in labour and a single bed in the maternity ward. However, during the upgrade to a polyclinic in 2013, a 10-bed male and female ward was established, as well as a 14-bed maternity ward and a 2-bed workstation. The polyclinic with its limited space now has male, female, maternity and emergency wards with a bed capacity of 34 as follows in Figure 3.3.

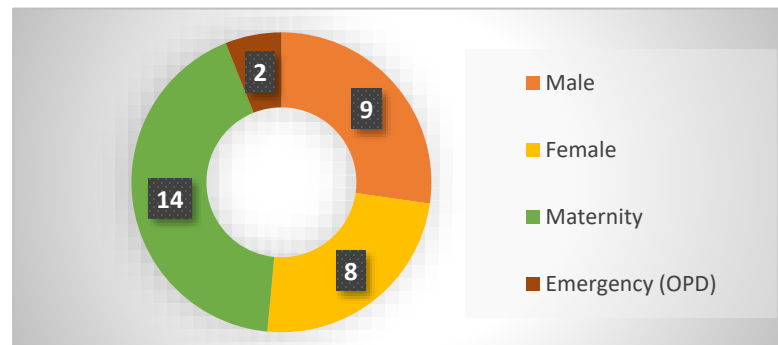


Figure 3.3: KPC bed capacity.

The facility operates under eighteen departments/units listed as follows: Ambulance, Medical Records/Health Information, Pharmacy, Laboratory, Prenatal, Maternity, General

Ward, Otorhinolaryngology, Ophthalmology, Psychiatry, Dentistry, Scan/ECG, X-ray, RCH, Disease Control, General Administration, Accounting, and Procurement/Business.

Kasoa Polytechnic is connected to the national grid with its own transformer and standby diesel generator set. However, the simple tariff payments are not regular because the institute billing has not taken place. The power consumption and the available institute bill are used to predict the system load demand based on the electrical load of the commercial HOMER grid (Riyatsyah et al., 2022). However, to achieve the objective of this work, the load profile of all departments at KPC in the facility was obtained, calculating the average load demand.

3.3.2. Electric load assessment

In the city of Kasoa, the demand for electricity is very high for both private households and businesses due to rapid population growth resulting in proportional growth in high energy consumption of appliances. In this work, KPC was considered as a commercial government power facility considering almost all available loads installed at KPC. Common loads such as light bulbs, fans, air conditioners, refrigerators, televisions, irons, computers power rating taken with their times of operation. Others included the laboratory and diagnostic equipment; dental chair, electrophoresis tank, microscope electrolyte analyser, blood roller, irradiation machine, haematology analyser. In this study, the load profile data was estimated considering the existing available load and its rated average consumption during specific times with the 24-hour day period. The estimated load consumption for all

electrical equipment considered for KPC is given in Appendix A. The total energy requirement per day (ED) can be calculated using the Eq. (3.1) (Mezigebe Getinet Yenalem, Livingstone, M.H. Ngoo, Dereje Shiferaw, & Peterson Hinga, 2020).

$$ED = \frac{\sum_{i=1}^N A_i P_i Q_i \times C_i}{1000} (KWh) \quad (3.1)$$

Table 3.1 presents the time-series data and energy consumption based on the gathered information from various departments of the health institution. The calculated average daily energy demand was 70.089 kWh, 87.865 kWh, 90.910 kWh, and 12.350 kWh for the load assessment in Administration block (A), Medical stores (B), Pharmacy (C), and Reproductive and Child Health (RCH) (D), respectively.

Additionally, the energy demand for other loads was determined to be 168.976 kWh, 70.148 kWh, 88.488 kWh, 37.472 kWh, 16.728 kWh, 42.596 kWh, 226.104 kWh, 584.25 kWh, 584.25 kWh, and 65 kWh for the Out Patient Department (E), Emergency ward (F), Records (G), Men's ward (H), Women's ward (I), Eye and Antenatal unit (J), Laboratory (K), Scan & Dental unit (L), and Maternity ward (M), respectively. The total energy consumption was estimated to be 1,284.822 kWh per day, with a maximum demand of 163.868 kWh at a derating factor of 0.73.

Table 3.1: Daily Load Profile based on time series

A..	B.	C.	D.	E.	F.	G.	H.	I.	J.	K.	L.	M.	TIME	HOURLY COMSUMPTION
0.4	3.234	1.167	0	2.02	0.488	0.1	0.39	0.39	0.3	7.757	0.2	2.104	0	18.55
0.4	3.234	1.167	0	4.62	2.558	0.1	0.39	0.39	0.3	7.757	0.2	2.104	1	23.22
0.4	3.234	1.167	0	4.62	2.558	0.1	0.39	0.39	0.3	7.757	0.2	2.104	2	23.22
0.4	3.234	1.167	0	4.62	2.558	0.1	0.39	0.39	0.3	7.757	0.2	2.104	3	23.22
0.4	3.234	1.167	0	4.62	2.558	0.1	0.39	0.39	0.3	7.757	0.2	2.104	4	23.22
0.4	3.234	1.167	0	4.62	2.558	0.1	0.39	0.39	0.3	7.757	0.2	2.104	5	23.22
0.4	3.234	1.167	0	4.62	2.558	0.1	0.39	0.39	0.3	7.757	0.2	2.104	6	23.22
0.4	3.234	1.167	0	4.62	2.558	0.1	0.39	0.39	0.3	7.597	0.2	2.104	7	23.06
0.4	3.234	1.167	0	4.62	2.558	0.1	0.39	0.39	0.3	7.597	0.2	2.104	8	23.06
7.569	4.667	7.061	1.922	10.152	4.17	7.721	3.694	0.966	4.607	11.565	38.895	5.326	9	108.315
8.298	4.667	7.061	1.922	10.152	4.17	7.721	3.694	0.966	4.607	11.565	38.895	5.326	10	109.044
8.298	4.667	7.061	1.922	10.152	4.17	7.721	3.694	0.966	4.607	11.565	38.895	3.326	11	107.044
8.298	4.667	7.061	1.922	10.152	4.17	7.721	3.694	0.966	4.607	11.565	38.895	3.326	12	107.044
7.749	4.667	7.061	1.922	10.152	4.17	7.721	3.694	0.966	4.607	11.565	38.295	3.326	13	105.895
7.599	4.667	7.061	1.922	10.152	4.17	7.721	3.694	0.966	4.607	11.565	38.295	3.326	14	105.745
7.499	4.667	7.061	0.803	10.152	4.17	7.721	3.694	0.966	4.607	11.565	35.295	3.326	15	101.526
7.499	3.452	7.061	0.015	10.152	4.17	7.401	3.694	0.966	4.607	11.217	31.09	3.251	16	94.575
1.28	3.234	7.061	0	10.152	2.558	6.232	0.71	0.966	0.66	11.217	2.7	3.251	17	50.021
0.4	3.234	6.911	0	10.152	2.558	6.232	0.71	0.966	0.44	8.737	0.2	3.251	18	43.791
0.4	3.234	2.195	0	10.152	2.558	5.632	0.71	0.966	0.44	8.897	0.2	3.251	19	38.635
0.4	3.234	2.195	0	10.152	2.558	5.632	0.71	0.966	0.44	8.897	0.2	3.251	20	38.635
0.4	3.234	2.195	0	3.076	2.558	1.156	0.59	0.646	0.38	8.897	0.2	2.132	21	25.464
0.4	3.234	2.195	0	3.076	2.558	1.156	0.59	0.59	0.38	8.897	0.2	2.132	22	25.408
0.4	3.234	1.167	0	2.02	0.488	0.1	0.39	0.39	0.3	8.897	0.2	2.104	23	19.69
70.089	87.865	90.910	12.350	168.976	70.148	88.488	37.472	16.728	42.596	226.104	304.255	68.841		1284.822kWh

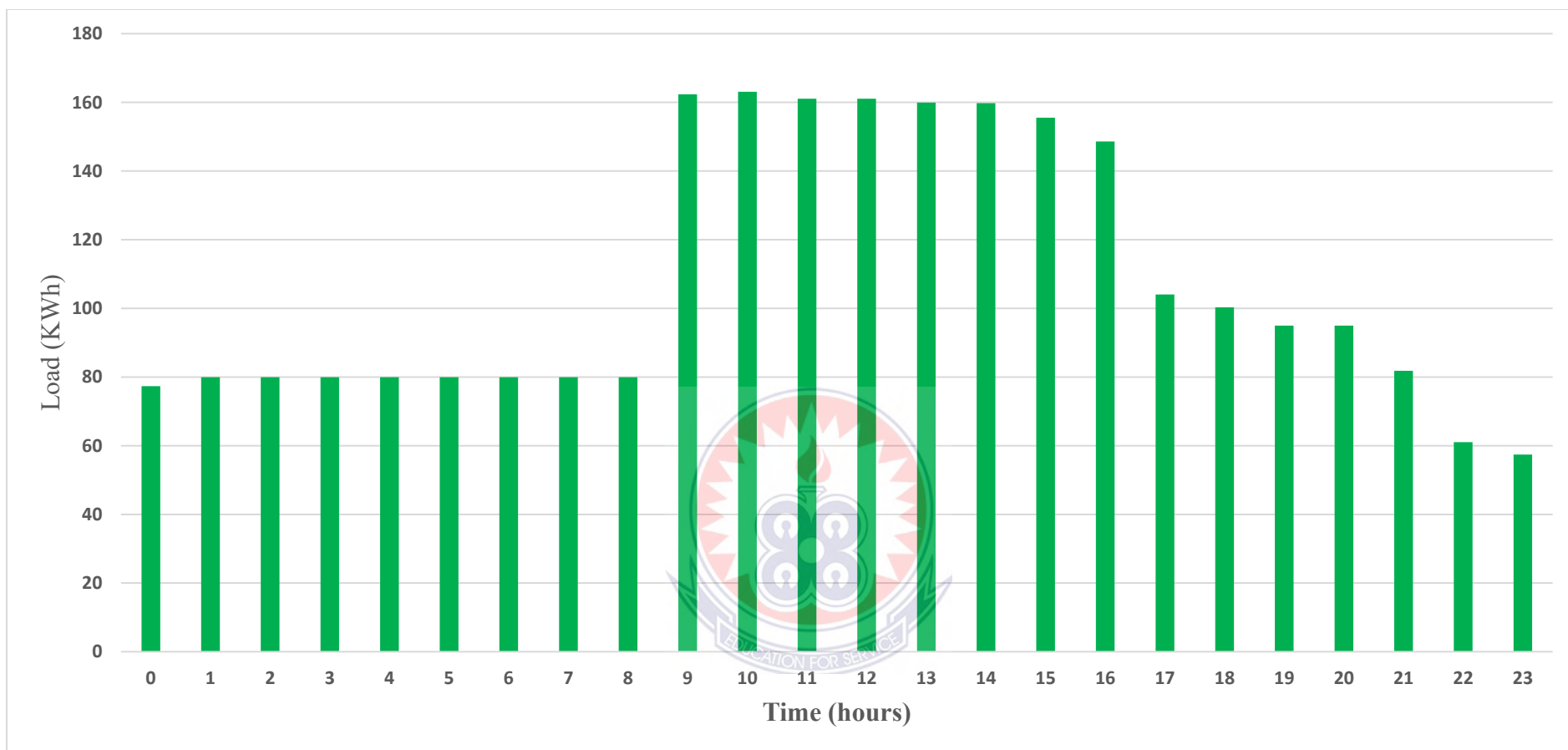


Figure 3.4: Time series load profile for KPC

3.3.3. Evaluation of meteorological data

In this study, the main meteorological assessments for wind speed, temperature conditions, and solar energy radiation resources used as metrological input data and are described as follows:

3.3.3.1. Daily solar radiation and clearness index

The daily Radiation and Clearness Index statistics are indicators of atmospheric clearness. The portion of the sun's energy penetrates the atmosphere and reaches the earth's surface. It is a one-dimensional number between 0 and 1, calculated by dividing the surface radiation by the extra-terrestrial radiation. The Clearness Index has a high value in clear and sunny weather and a low value in cloudy weather solar irradiance of KPC at a location of 5°32.0 N latitude and 0° 25.6 W longitude was taken from NASA Meteorological and Solar Energy Wave website.

Table 3.2 shows high insolation of 5,410 kWh/m²/day occurs in March, followed by the months of February, April, January, December and November, while the low insolation occurs in June, August, September, July, October and the lowest of 4,970 kWh/m²/day in May. The Clearness Index peak of 0.555 occurs in January, followed by December, February, November, March and 0.515 for the month of April. Figure 3.5 shows the solar radiation and brightness index for the entire year under consideration.

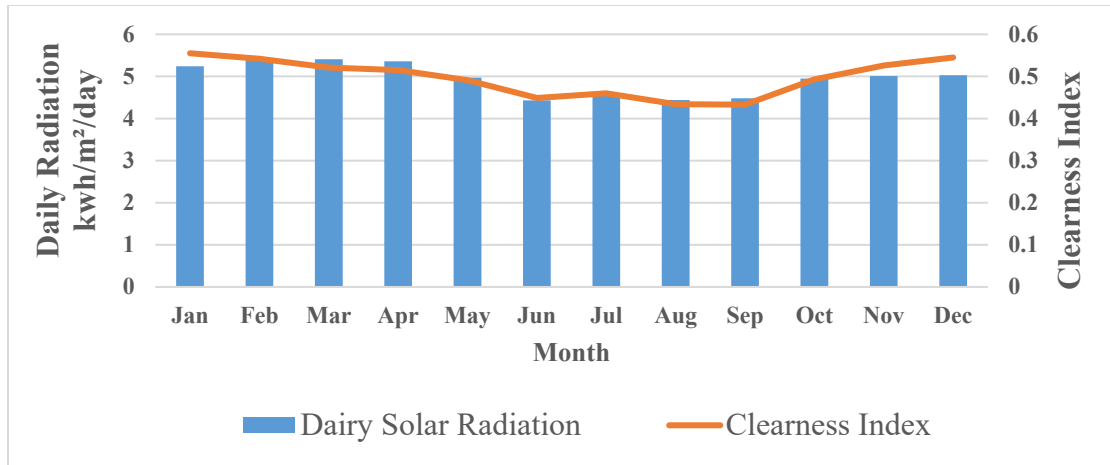


Figure 3.5: Solar radiation and clearness index at selected site

3.3.3.2. Temperature conditions

Monthly mean temperature is obtained from NASA surface meteorology. The daily temperature of the selected locations is shown in Figure 3.6.

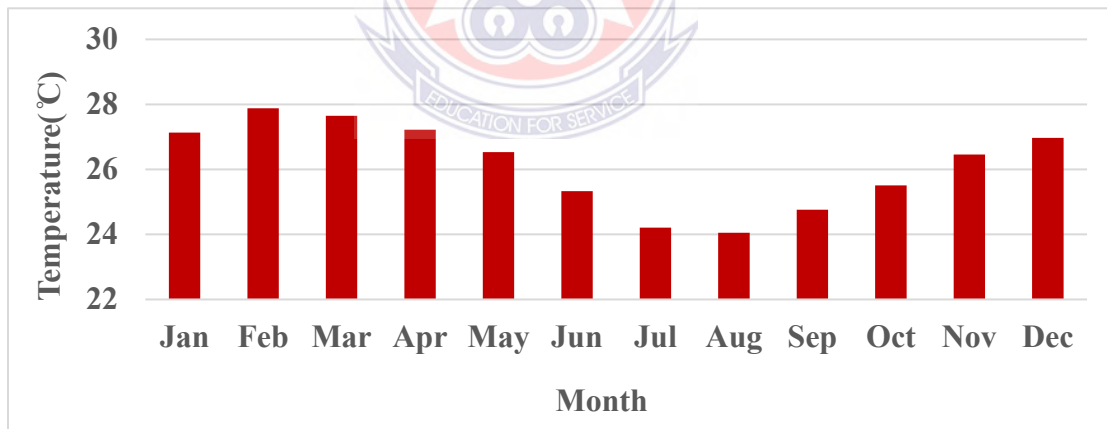


Figure 3.6 Average monthly temperature data at the selected site

The average annual temperature of selected site is 26.14 °C. Table 3.2 shows the monthly average temperature with the highest temperature record of 27.88 °C in February and minimum of 24.05 °C record in the month of August.

3.3.3.3. Wind speed resources at selected site

Based on the geographic location of the major city of Kasoa, the average monthly wind data was taken from a ten-year average from the NASA database website with Table 3.2 shows the selected site's average annual wind speed of 3.78 m/s at an anemometer height of 50 m. Also, Figure 3.7 shows the monthly average wind speed from January to December; the least record of 3.12 m/s in December and the highest record of 4.90 m/s in the month of August.

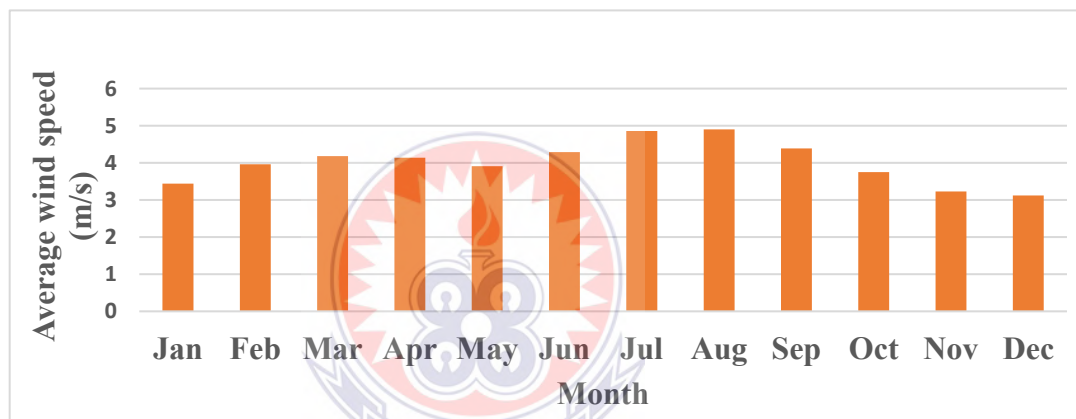


Figure 3.7: Wind energy data (monthly average)

Table 3.2: Average metrological data of the study area (NASA, 2022)

Month	Daily Temperature (°C)	Wind Speed (m/s)	Clearness Index	Solar Daily Radiation (kwh/m ² /day)
January	27.130	3.440	0.555	5.240
February	27.880	3.960	0.542	5.400
March	27.650	4.180	0.521	5.410
April	27.220	4.140	0.515	5.360
May	26.530	3.910	0.491	4.970
June	25.330	4.290	0.449	4.430
July	24.210	4.860	0.460	4.580
August	24.050	4.900	0.434	4.440
September	24.760	4.390	0.433	4.480
October	25.510	3.750	0.493	4.950
November	26.460	3.230	0.526	5.010
December	26.970	3.120	0.545	5.030

3.3.4. Input data for Economic analysis

For the purposes of this study, some economic data were required to calculate the techno-economic analysis of the proposed technical system. This data includes the local Ghanaian currency rate, the nominal discount rate, the expected inflation rate and the project lifetime. The economic parameters under the simulation, the year's inflation was taken as 29.8% with a discount rate of 14.5% and the exchange rate of US\$ 1 (GhC5.95peswes) equivalent as presented in Table 3.3.

Table 3.3: Economic Data Entry (Bank of Ghana, 2021)

Description	Value	Unit
Currency	US\$ 1	GhC5.95peswes
National discount rate	14.14	%
Inflation rate	16.46	%
Project lifetime	25	Year

3.3.4.1. Interest Rate

The annual real interest rate, sometimes referred as the real interest rate or simple interest rate, is one of HOMER's inputs and is the discount rate used to convert one-time costs to Annualised expenses (HOMER Grid, 2021). The following equation relates the annual real interest rate to the nominal interest rate and the interest rate i is given by the Eq. (3.2)

$$i = \frac{i' - f}{1 + f} \quad (3.2)$$

3.3.4.2. Levelised Cost of Energy (LCoE)

The average cost/kWh of useable electrical energy generated by the system is defined by HOMER as the LCoE. HOMER divides the yearly cost of generating electricity (total annualised cost minus cost of feeding the load) by the total useable electric energy output

and the CoE is calculated using Eq. (3.3)

$$CoE = \frac{Cann, tot}{Eprim, AC + Eprim, DC + Egrid, sales} \quad (3.3)$$

The total annualised cost is the sum of each system component's annualised costs plus the other annualised costs. It is a significant number as HOMER utilises it to compute both the levelised and total net present costs of energy.

3.3.4.3. Total Net Present Cost (TNPC)

The total net present cost (TNPC) of a system is equal to the present value of all expenses incurred during the lifetime of the system minus the present value of all income earned during the lifetime of the system. Costs include capital expenditures, replacement costs operation and maintenance costs, fuel costs, environmental penalties and the cost of purchasing electricity from the grid. Residual value and network sales are two sources of income.

Total NPC is calculated by adding the total discounted cash flows in each year of the project life cycle using Eq. (3.4)

$$CNPC = \frac{Cann, tot}{CRF(i, Rproj)} \quad (3.4)$$

In this study, the lifetime of the system is 25 years and the capital recovery factor is a ratio that is used to assess an annual present value (a series of Equal annual cash flows). The capital recovery factor is presented in Eq. (3.5).

$$CRF(i, N) = \frac{i(1+i)^N}{(1+i)^N - 1} \quad (3.5)$$

3.3.4.4. Salvage value (S)

The worth of a power system component that is still usable at the end of the project's lifespan is referred to as the salvage value. HOMER uses this equation to figure out how much each component is worth at the conclusion of the project's life cycle and is calculated using Eq. (3.6).

$$S = C_{rep} \frac{R_{rem}}{R_{comp}} \quad (3.6)$$

3.3.4.5. Internal Rate of Return

The internal rate of return (IRR) is the discount rate at which the reference case and the optimized system have the same net present cost.

HOMER calculates the IRR by dividing the present value of the difference between the two cash flow sequences by the discount rate.

3.3.4.6. Return on Investment

The annual cost savings compared to the original expenditure is known as the return on investment (ROI). The ROI is calculated by dividing the difference in capital cost by the average annual difference in nominal cash flows during the project's lifespan and the return on investment is calculated by using Eq. (3.7).

$$ROI = \frac{\sum_{i=0}^{R_{proj}} C_{i,ref} - C_i}{R_{proj} (C_{cap} - C_{cap,ref})} \quad (3.7)$$

3.3.4.7. Simple Payback

The number of years it takes for the cumulative cash flow of the difference between the

optimized and reference case systems to transition from negative to positive is known as simple payback. The payback period is the time it takes to recover the investment cost difference between the optimized and reference case systems.

3.3.4.8. Total Annualised cost

The total annualised cost of a component is the cost that would result in the same net present cost as the component's actual cash flow sequence if distributed evenly throughout the project's lifespan. The annualised cost is calculated by multiplying the net present cost by the capital recovery factor, as shown in the following Eq. (3.8).

$$C_{ann, tot} = CRF(i, R_{proj}) \times CNPC, tot \quad (3.8)$$

3.3.5. Grid system input data

In this study, the grid system is used as a backup power element or excess power absorber. The main grid feeds in electricity when electricity from renewable energy sources such as solar PV and wind is insufficient to meet energy demand, and the grid consumes electricity when excess electricity is generated in a net metering arrangement. One study estimated the selling price of electricity from the grid at US\$0.04/kWh and the resale price of electricity from the microgrid at US\$0.05/kWh (Türkay et al., 2011).

In another study in Ghana, the simple network tariff option net metering with a network electricity price of US\$ 0.2/kWh was chosen. The net price of the grid surplus was assumed to be 0.1/kWh, which was below the minimum PURC tariff. The rate for excess electricity from the grid was lower to compensate for transmission company transmission losses and

operation and maintenance (O&M) costs (Mubarick Issahaku, Adam Sandow Saani & Khadija Sarquah, 2021). Electricity tariff scheme for customers in Ghana depends on monthly consumption and classification. For non-household or commercial customers, the first 300 kWh costs GhC 0.798/kWh. From 300 kWh to 600 kWh the tariff is GhC 0.849; any purchase over 600 kWh in the same month increases to GhC 1.340/kWh (PURC Ghana, 2021).

In this study, based on the time-series load consumption in Table 3.1. HOMER Grid calculates the total monthly energy consumption from the August peak of 80,073.558 kWh. Taking into account the peak consumption and the reduced tariff range (0-600 kWh) for commercial users, the reduced range accounted for only 0.075% of the total consumption in August.

The basic grid tariff selected for net metering, the grid electricity price of US\$ 0.23/kWh, is adopted on the basis of the highest consumption class and the Ghanaian cedi equivalent. The excess grid price was assumed to be US\$0.1/kWh, which was below the PURC minimum tariff to compensate for transmission company transmission losses and O&M costs.

Table 3.4. Grid input data (PURC Ghana, 2021)

Description		Unit
Tariff (Imported)	US\$ 0.23/kWh	GhC1.34.peswes/kWh
Sold (Exported to Grid)	US\$ 0.1/kWh	GhC0.60peswes/kWh
Fixed Charge (Service charge/month)	US\$ 2.09/month	GhC12.43peswes/month
Demand Rate (US\$ 0.23- US\$ 0.1	US\$ 0.13/kWh	GhC0.77peswes/kWh

3.4. Hybrid power system components sizing approach

3.4.1. Solar photovoltaic array sizing

In a photovoltaic system, a discount factor, which is a scaling factor, is applied to the power of the PV array and a 90% discount factor is added for the component to account for the losses and the losses due to the pollution of the PV module (Demiroren et al., 2010).

The energy output of the PV generator is determined using the Eq. (3.9)

$$P_{pv} = f_{pv} \times Y_{pv} \times \left(\frac{IT}{I_s}\right) \quad (3.9)$$

In this study, Jinko monocrystalline connected in series were considered. The cost of Turnkey solar PV from a local Ghanaian installer is Gh¢11,580.00 per kW (US\$1,946.22 per kW) (Wilkins Engineering Ltd, Accra Ghana). It is manufactured considering efficiency, lifespan, initial capital costs, and operation and maintenance costs as 13%, 25 years, US\$1,946.22 and US\$0 respectively with reduction factor of 85% for each module for the different effects of temperature and dust.

Table 3.5: Capacity and the price of Jinko flat-panel solar PV.

Capacity(kW)	Capital Cost (US\$)	Replacement Cost(US\$)	O&M Cost (US\$)/Year
5	13,092.45	13,092.45	0
10	130924.50	130924.50	0
1000	13092450.00	13092450.00	0
2000	26184900.00	26184900.00	0

Solar PV price will decrease as installed capacity increases; for this project the price will drop to 93%, 66% and 54% for 10kW, 1000kW and 2000kW respectively. The solar PV price and properties used are shown in Table 3.4 and Table 3.6 respectively.

Table 3.6: Properties of Solar PV Array

Parameter	Specifications
Name	Jinko Solar 310 JKM310PP-72B
Abbreviation	Jin310
Panel Type	Flat Plate
Rated Power Capacity	0.31kW
Temperature Coefficient	-0.432
Operating Temperature	46.1°C
Efficiency	13%
Manufacturer	Jinko Solar
Open Circuit Voltage VOC	45.90V
Rated Current	8.96A

3.4.2. Wind turbine sizing

HOMER models a wind turbine as a device that converts wind kinetic energy into AC or DC electricity via a power curve (a graph of power output against wind speed at hub height). HOMER Grid estimates the wind turbine's electricity production every hour in a four-step procedure.

First, the wind resource data to determine the average wind speed for the hour at the anemometer height. Second, it uses either the logarithmic or power laws to calculate the correlation of wind speed at the turbine's hub height.

The third step is to do with the turbine's power curve, which is used to calculate the turbine's power output based on traditional air density assumptions for a particular wind speed. The fourth step is the air density ratio, which is the ratio of actual to standard air density multiplied by the total power output. To extrapolate wind speed data in HOMER, use the power-law in Eq. (3.10).

$$U_{hub} = U_{anem} \left(\frac{Z_{hub}}{Z_{anem}} \right) \quad (3.10)$$

Applying density correction, power curves generally describe wind turbine performance under conventional temperature and pressure conditions. HOMER adjusts to real-world circumstances by multiplying the air density ratio by the power value estimated by the power curve with the air density at standard temperature and pressure (1.225 kg/m³), using Eq. (3.11)

$$P_{WTG} = \left(\frac{\rho}{\rho_0} \right) \times P_{WTG, STP} \quad (3.11)$$

Wind Turbine For this paper, Eco cycle EOX M-21 [100kW] horizontal axis wind turbine, the hub height of 34m, and a lifetime of about 25 years, the initial capital cost of US\$210,000, Replacement cost is US\$210,000 and operation and maintenance costs of US\$3,500 is considered. The amount of electricity produced by the wind turbine is highly dependent on wind speed availability and variations (Energy P., 2021).

Table 3.7: Properties of Wind Turbine

Parameter	Specifications
Name	Eocle EOXM 21[100kW]
Abbreviation	EOXM21
Capacity	100.00
Nominal Capacity	100kW
Cut-in wind speed	2.75m/s
Cut-out speed	20m/s
Manufacturer	Eocle

3.4.3. Sizing of battery bank as energy storage

A group of one or more separate batteries is called a battery bank. A single battery is modelled by HOMER as a device capable of holding a specified amount of direct current

with a fixed energy efficiency, subject to limitations on how quickly it can be charged or discharged and how much energy it can pass through before it needs to be replaced.

HOMER implies that battery properties remain constant over time and are unaffected by environmental influences such as temperature. HOMER predicted battery bank life simply by monitoring the amount of energy passing through it, since lifetime throughput in this situation is independent of cycle depth; for this study, the lifetime of the battery bank was assumed to be 4 years using HOMER grid. The lifetime of the battery banks in years is calculated by HOMER using Eq. (3.12).

$$R_{batt} = \text{MIN} \left(\frac{N_{batt} \times Q_{lifetime}}{Q_{thrpt}}, R_{batt, f} \right) \quad (3.12)$$

The expense of cycling energy through the storage bank is known as the battery wear cost. Suppose the storage characteristics show that throughput is a constraint on storage life. In this case, HOMER estimates that the storage bank will need to be replaced when its total throughput equals its lifetime throughput. As a result, the storage bank approaches its necessary replacement with each kWh of throughput. HOMER uses the following calculation to compute the cost of storage wear as expressed using Eq. (3.13).

$$bw = \frac{C_{rep, batt}}{N_{batt} \times Q_{lifetime} \times \sqrt{\eta_{rt}}} \quad (3.13)$$

Batteries are used in the grid as a backup and to maintain a constant voltage during peak loads or power failures. In this study, a lead-acid battery manufactured by Generic with a capacity of 1.2 kWh and a maximum capacity of 276 Ah, an initial cost of US\$300 per kWh, an O&M cost of US\$0/kwh, and a lifespan of 25 years considered are price considerations for generic 1kWh Li-Ion is shown in Table 3.8.

Table 3.8: The capacity and the price of generic 1kWh Li-ion. Battery

Capacity(kW)	Capital Cost (US\$)	Replacement Cost(US\$)	O&M (US\$)/Year)
5	1,500	1,500	0
10	3,000	3,000	0
1000	300,000	300,000	0
2000	600,000	600,000	0

Table 3.9: Generic Battery Storage properties

Parameter	Specifications
Name	Generic 1kWh Li-Ion [ASM]
Abbreviation	LI ASM
Capacity	1kWh
Nominal Capacity	1.02kW
Maximum Capacity	276Ah
Capacity Ratio	1
Other round-trip losses	8%
Fixed bulk temperature	20°C

3.4.4 The Power Converter sizing

A converter is a device that converts electrical energy from direct current to alternating current in the reverse process and from alternating current to direct current in the rectification phase (Zhang, X., & Liu, X., 2015). HOMER can model both solid state and rotary transducers where the inverter capacity, or the maximum amount of AC power that the device can produce by converting DC power is denoted by the converter size. The rectifier power is defined as a percentage of the inverter power, the maximum direct current power that the device can produce by rectifying alternating current.

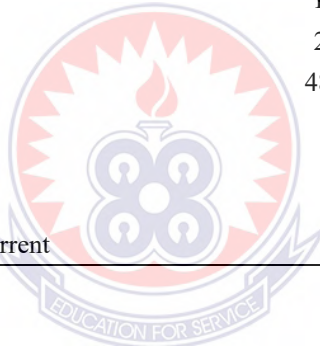
As a result, rectifier capacitance is not a unique selection variable. HOMER implies that the inverter and rectifier capabilities are continuous and that the device can handle the load for as long as needed. The inverter can run in parallel with another AC power source; a

generator or the power grid. The converter's inversion and rectification efficiencies are the ultimate physical attributes of the converter, which HOMER expects to remain constant.

In a research, the economic characteristics of the converters are the capital costs, the operation and maintenance costs and the replacement costs in US dollars per year and the projected life of the converters in years are US\$ 700, US\$ 550 and US\$ 0 per year (Burkart R.M. and J. W. Kolar, 2017).

Table 3.10: Power Converter properties

Parameter	Specifications
Name	Younicos Y.converter250
Abbreviation	Youn250
Capacity	250kWh
AC output Capacity	480V_AC
Maximum Capacity	276Ah
Peak Efficiency	97
Frequency	97%
Max. Battery DC Current	350A



3.5. Proposed System architecture

The system architecture was originally developed to simulate the renewable energy system. In this case, the system architecture consists of power sources from grid, PV, wind turbine, lithium battery, inverter and load as shown schematically in Figure 3.8.

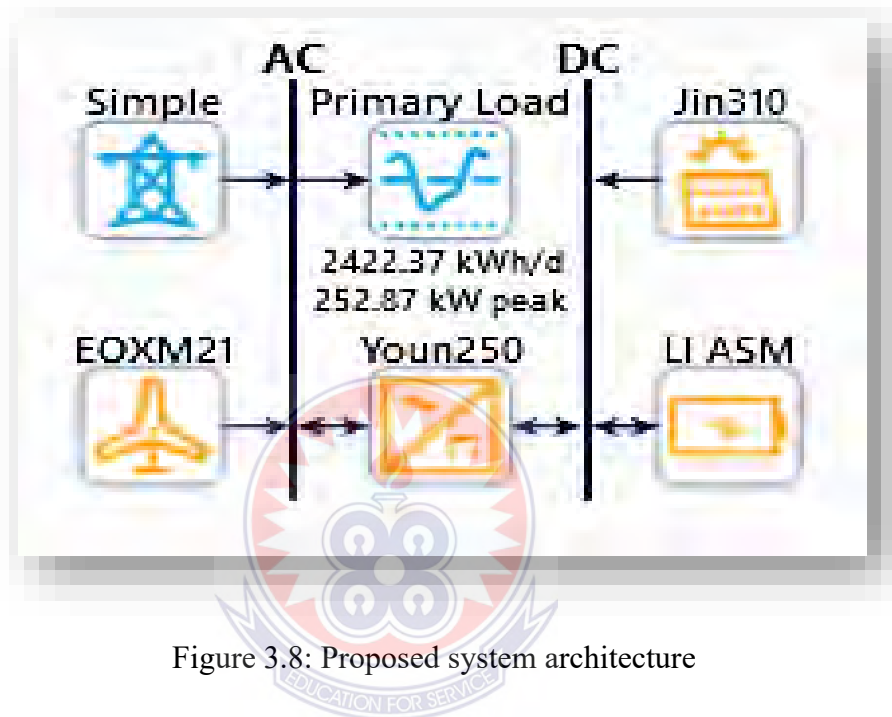


Figure 3.8: Proposed system architecture

The detailed information of the proposed system is tabulated in Table 3.10 with the proposed renewable energy system sizing and component lifespan for solar PV, wind turbines and battery storage clearly outlined. HOMER pro software developed by the NREL in the USA is a microgrid optimization tool for technical and financial assessments. It is designed to model both grid-tied and isolated microgrids using conventional energy sources to power loads (Boqtob O., H. El Moussaoui, H. El Markhi, & T. Lamhamdi, 2019).

In order to obtain accurate and optimized component sizes, HOMER requires input information such as solar irradiance, wind speed, load data, memory, and microgrid component details with their corresponding costs, and the Homer grid is used. HOMER Grid is a tool that can help a site owner identify different options to reduce a site's electricity bill. It compares the costs and savings of installing different combinations of batteries, solar panels and generators. HOMER Grid uses powerful optimization to find the system that maximizes your savings.

Table 3.11: Components of Proposed Architecture

Input Component	Name	Capital Cost (US\$)	Replacement Cost (US\$)	O&M Cost (US\$)	Lifetime
Solar PV	1kW Flat-plate PV	2,618.49/kW	2,618.49/kW	0/year	25 year
Storage	1kWh Lead Acid	300/kW	300/kW	0/year	10 year
Wind Turbine	GT [10kW]	210,000	210,000	3,500/year	25 year
Converter	System Converter	700/kW	550/kW	100/kW	15 year
Utility Grid	Simple Tariff	0.23kWh			

The HOMER Grid provides design Setup window where components are selected as inputs and their estimated installation costs, operational and maintenance costs, replacement costs, interest and energy costs as shown in Figure 3.9. are simulated for system performance under different situations. Detailed results are discussed in the next chapter of this work.

The screenshot displays the HOMER Grid software interface. At the top, the title bar reads "HOMER Grid [WITH BAT.hgrid]* x64 1.9.0 (Evaluation Edition)". Below the title bar are buttons for "Design" and "Results", and a "Library" icon. The main window is titled "Setup" and shows a map of West Africa with a red pin indicating the location "GHW8+CRR, Kasoa New Market Rd, Kasoa, Ghana (5°32.8'N, 0°26.0'W)". A sidebar on the left lists various components: Setup, Electric Load, Utility, Components (PV, Storage, Converter, Generator, Wind Turbin), Outages, Programs, Resources, CHP, and EV Charging. A search bar at the bottom of the map area contains the text "KASOA POLYCLINIC, GHANA WEST AFRICA". To the right of the map is a schematic diagram showing the system configuration: AC GRID, Primary Load (2422.37 kWh/d, 321.42 kW peak), DC Jin310, EOXM21, Youn250, and LI ASM. Below the map is a table of project parameters:

Parameter	Value	Unit
Name:	URBAN HEALTHCARE FACILITY USING HOMER ENVIRONMENT	
Author:	CALEB PAA KWESI DONKOH	
Description:	A Thesis submitted to the Department of ELECTRICALS AND ELECTRONICS TECHNOLOGY EDUCATION, UNIVERSITY OF EDUCATION, School of Research and Graduate Studies, in Partial Fulfillment of the Requirements for the award of Master of Philosophy in Electrical and Electronics Engineering Technology.	
Discount rate (%)	14.14	(%)
Inflation rate (%)	16.46	(%)
Project lifetime (years)	25.00	(years)

At the bottom of the window, there is a section for "Suggested Changes:".

Figure 3.9: HOMER Grid setup window

3.5.1 Battery thermal condition monitoring and management

The battery bank is a group of batteries and the HOMER model views a single battery as a device that stores a fixed amount of DC electricity with constant energy efficiency. It has limitations on charging/discharging speed, depth of discharge, and energy cycling before replacement. HOMER assumes that the battery properties remain unchanged and unaffected by external factors.

In HOMER Grid, the crucial physical characteristics of the battery are defined by its nominal voltage, capacity curve, lifetime curve, minimum state of charge, and round-trip efficiency. The capacity curve depicts the battery's discharge capacity, represented in ampere-hours, relative to the discharge current, expressed in amperes. This curve is established by measuring the ampere-hours that can be discharged at a constant current from a fully charged battery. The capacity curve typically exhibits a decreasing trend with increasing discharge current. The lifetime curve displays the battery's ability to withstand a specified number of discharge-charge cycles as a function of cycle depth. This number of cycles is observed to decrease with increasing cycle depth. The minimum state of charge represents the limit below which the battery should not be discharged to prevent permanent damage, and HOMER enforces this limit in its system simulations. The round-trip efficiency indicates the percentage of energy that can be drawn out of the battery relative to the energy stored within it.

To calculate the battery's maximum allowable rate of charge or discharge, HOMER uses the kinetic battery mode (Manwell J. F and J. G. McGowan, 1993), which models the

battery as a two-tank system rather than a single-tank system has two effects. First, it means the battery cannot be fully charged or discharged all at once; a complete charge requires an infinite amount of time at a charge current that asymptotically approaches zero. Second, it means that the battery's ability to charge and discharge depends not only on its current state of charge, but also on its recent charge and discharge history.

A battery rapidly charged to 80% state of charge will be capable of a higher discharge rate than the same battery rapidly discharged to 80%, since it will have a higher level in its available tank. HOMER tracks the levels in the two tanks each hour, and models both these effects.

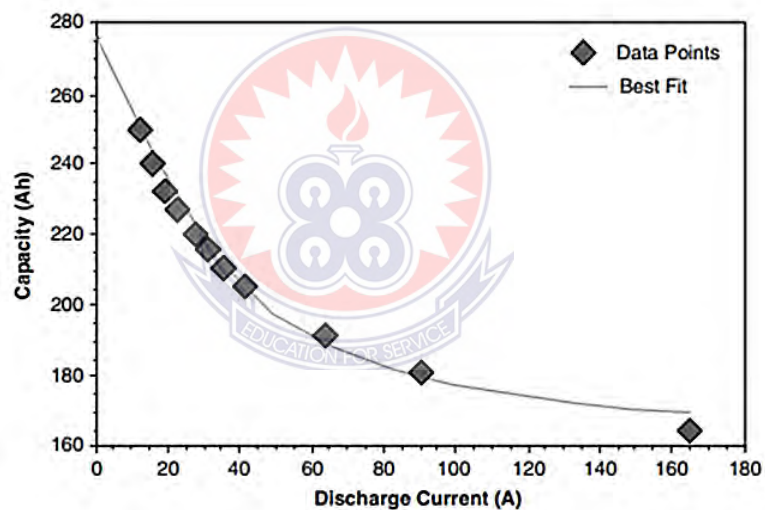


Figure 3.10 Capacity curve for deep-cycle battery model US-250 from U.S. Battery Manufacturing Company (www.usbattery.com).

Figure 3.10 shows a lifetime curve typical of a deep-cycle lead–acid battery. The number of cycles to failure (shown in the graph as the lighter-coloured points) drops sharply with the product of the number of cycles, the depth of discharge, the nominal voltage of the battery, and the aforementioned maximum capacity of the battery. The lifetime throughput

curve, shown in Figure 3.11 as black dots, typically shows a much weaker dependence on the cycle depth. HOMER makes the simplifying assumption that the lifetime throughput is independent of the depth of discharge.

The value that HOMER suggests for this lifetime throughput is the average of the points from the lifetime curve above the minimum state of charge, but the user can modify this value to be more or less conservative.

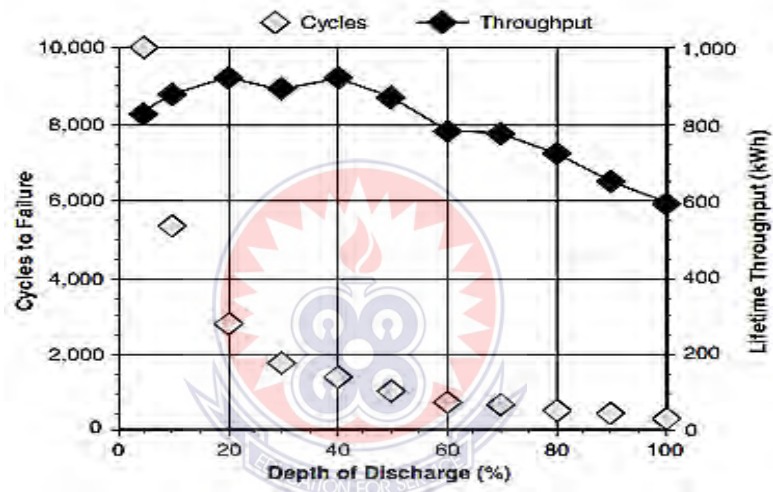


Figure 3.11. Lifetime curve for deep-cycle battery model US-250 from U.S. Battery Manufacturing Company (www.usbattery.com).

3.5.2 Load Management and Voltage regulation schemes

Load management and voltage regulation schemes can be integrated into a grid-connected renewable energy system by using smart inverters or controllers, AVRs, tap-changing transformers, SVRs, battery storage systems, and energy management systems. These techniques can help to optimize the use of renewable energy resources and improve system efficiency:

- i. Load analysis: The total load is 111.274 kW, and the peak demand occurs between 9 a.m. and 3 p.m. daily hence, the use of load balancing to distribute the load across the day and load shedding or demand response techniques to reduce the peak demand during the peak period.
- ii. Renewable energy analysis: The solar and wind power generation in kWh per year constitutes the total renewable energy production with key individual percentage of contribution noted. We can use the battery storage system to store excess energy during times of high supply and release it during times of low supply to provide voltage regulation services and maintain stable voltage levels in the system.
- iii. Battery storage system sizing: Based on the load and renewable energy analysis, we can size the battery storage system to provide the required backup power and voltage regulation services. Assuming a capacity utilization factor of 70%, we can calculate the required battery storage capacity as follows:

$$\text{Annual load demand} = 111.274 \text{ kW} \times 24 \text{ hours} \times 365 \text{ days} = 974,731 \text{ kWh} \quad (3.14)$$

$$\text{Annual renewable energy generation} = \text{kWh (solar)} + \text{kWh (wind)} = \text{kWh} \quad (3.15)$$

$$\text{Annual excess renewable energy} = \text{Annual renewable energy generation (kWh)} - \text{Annual load demand (kWh)} \quad (3.16)$$

$$\text{Required battery storage capacity} = (\text{Annual excess renewable energy kWh}) / (365 \text{ days} \times 24 \text{ hours} \times 0.7) \quad (3.17)$$

- iv. Load management and voltage regulation strategies: We can use load balancing, load shedding, and demand response techniques to manage the load, and use the battery storage system to provide voltage regulation services. During the peak period, excess renewable energy can be used to charge the battery storage system, and the stored energy can be used to power the load during the off-peak period. During times of low renewable energy supply or high demand, the battery storage system can be discharged to provide backup power and voltage regulation services.
- v. Implementation and validation: The load management and voltage regulation scheme can be implemented using smart inverters or controllers, automatic voltage regulators (AVRs), static voltage regulators (SVRs), and the battery storage system. An energy management system (EMS) can be used to monitor the system performance and adjust the strategies based on real-time data. The system should be tested and validated to ensure its effectiveness in providing stable voltage levels, optimized use of renewable energy resources, and improved system efficiency.

3.5.3. Black Start Scheme and allocation of Generation thresholds

In this study, the KPC hospital recorded an aggregate electrical demand of 1284.822 kWh in a 24-hour period. The critical load demands were determined to be 68.841 kWh for the maternity ward, 226.104 kWh for the laboratory, and 168.976 kWh for the OPD (as presented in Table 3.1).

The allocation of generation for the black start scheme, expressed as a percentage, is presented as follows:

- i. The auxiliary grid supply for the hospital will be utilized in conjunction with the primary supply derived from renewable energy sources (such as solar photovoltaic and wind energy) to meet the needs of the critical loads. The study outlines the priority order for supplying critical loads in a specific facility. The critical loads consist of the Maternity ward, Laboratory, and OPD, with energy requirements of 68.841 kWh (5.35% of the total load), 226.104 kWh (17.63% of the total load), and 168.976 kWh (13.07% of the total load), respectively. Additionally, the Emergency Ward requires 70.148 kWh of energy, which represents 0.57% of the total load per day. In the event of a power interruption, it is crucial to ensure continuous power supply to the critical loads, while non-critical loads may receive power in the case of a black start. The Solar PV and Wind power systems would be used to supplement the Grid supply and help reduce its load. The grid would serve as a background support, ready to provide additional power if needed.
- ii. A battery storage system would be used to store excess energy generated by the Solar PV and Wind systems, which can be used during times when the generator is under high load or the Solar PV and Wind systems are not generating enough power.
- iii. For the Black start scheme, once the critical loads have been fully restored, the remaining load (680.664 kWh, which is 52.89% of the total load), can be gradually added back to the system.

This black start scheme would prioritize the restoration of the most essential loads and ensure a reliable and continuous supply of power to the hospital during a blackout. The combination of the Grid, Solar PV and Wind power systems, battery storage, and the grid would provide a robust and resilient power system for the hospital.

3.5.4. Point of Common Coupling (PCC) for Grid-connected PV/Wind generation scheme using ETAP software

This section describes the methodology to implement the Hybrid Wind-Solar System and Grid by employing ETAP software. The Solar PV, Wind and Battery storage Hybrid power system was tested on a simple network to determine technical effects on the Grid based on previous research using the ETAP software (Md Saleh et.al., 2017).

3.5.4.1. Input Data

The study case ID is "LF," which suggests that the analysis was performed for a load flow study. Load flow analysis is used to determine the steady-state operating conditions of a power system, including the voltage, current, and power flow through the system components. The data revision is "Base Configuration Normal," which indicates that the analysis was performed using the base configuration of the power system without any modifications.

The loading category and generation category are both "Design," which means that the analysis was performed using the designed loading and generation conditions.

The diversity factor for the loading is "Normal," which means that the loads were assumed to be evenly distributed over time and a total load profile of Kasoa health care facility of 1284.822kWh (Table 3.1) or 111.274kW is taken as test network. This total load is grouped into two; Critical load (39.671kW) and other loads (71.603kW). The critical loads are Administration block, Maternity ward, Laboratory, OPD and Emergency ward (Table 3.12). The other loads is the sum of the load in the Medical stores, Pharmacy, RCH, Records Department, Male ward, Female ward, Eye and Antenatal clinic, Scan and dental unit. (Appendix A).

The Grid (ECG) main line of 11kVA with installed Hospital transformer capacity of 100kVA and 120mm Aluminium service cable represents the current power line system.

Table 3.12 presents the input load data for ETAP simulation environment.

Table 3.12: ETAP Input data

		Energy	Load
		kWh	kW
A.	Critical Loads		
	Administration Block	70.089	8.298
	Maternity ward	68.841	5.326
	Laboratory	226.104	11.725
	OPD	168.976	10.152
	Emergency Ward	70.148	4.17
B.	Other Loads	680.664	71.603
Total estimated load profile		1284.822	111.274

The power system has four buses: Solar Bus, ECG Bus, Wind Bus, and PCC Bus (Grid-connected Solar, Wind power generation bus). The nominal voltage for Solar Bus and ECG is 0.415 kV, while the nominal voltage for ECG Bus is 11 kV, as Shown in the power line diagram in the ETAP simulation window (Figure 3.12).

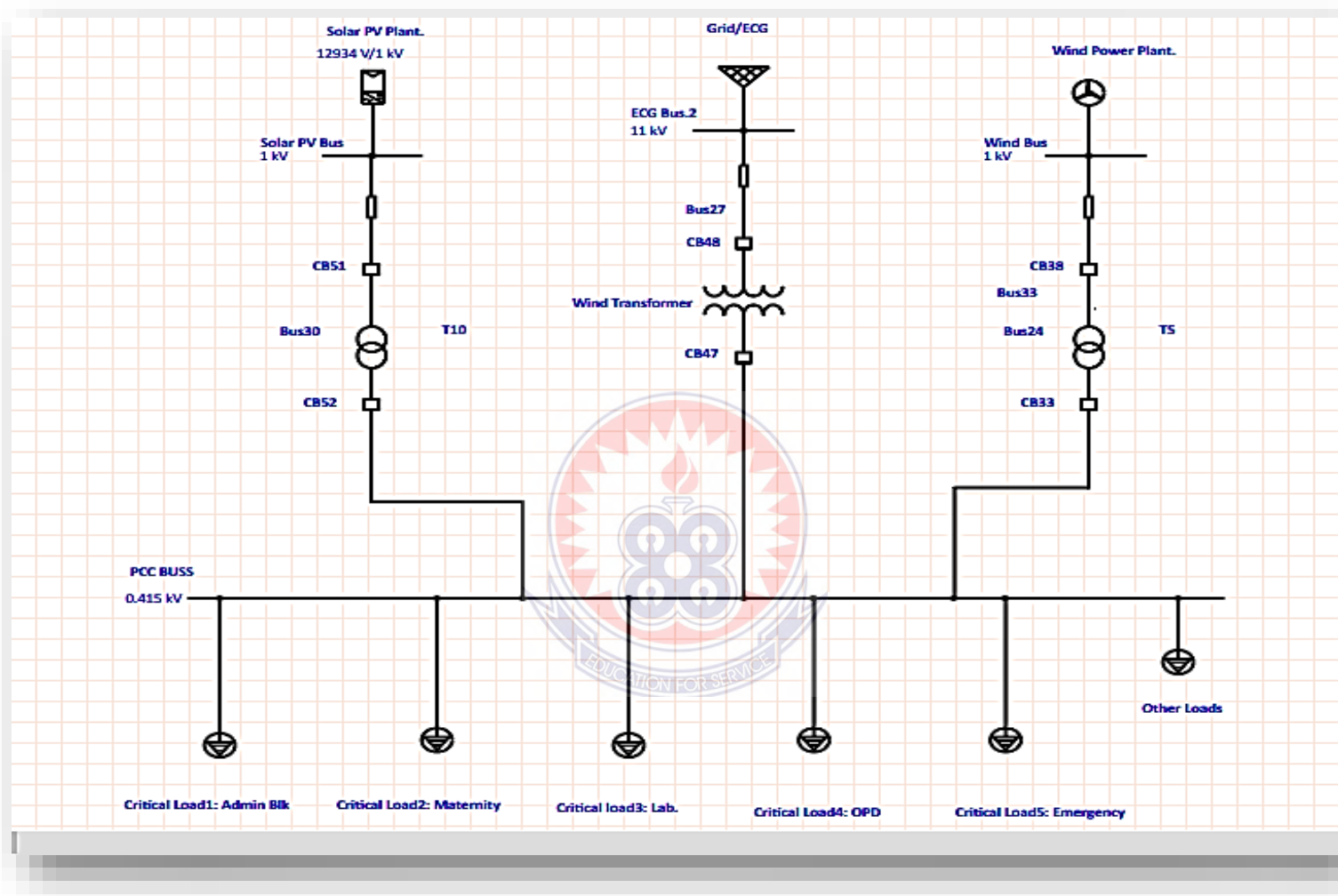


Figure 3.12. ETAP Power Line Diagram for PCC Grid-connected Solar PV, Wind and Battery storage

CHAPTER FOUR

RESULTS AND DISCUSSION

This study aims to design an optimized grid-connected PV/wind model for a city health facility using the Homer Grid simulation tool. This chapter presents the results of the study; the load profile and base case are discussed first, followed by the optimization results which are compared with the base case as well as the carbon dioxide emission reduction potential on the environment.

4.1. Load Profile

A simulation using the hourly time series input data (Table 3.1) revealed that the seasonal baseline and scaled data characteristics are shown in Figure 4.1 for seasonal loads (January to December).

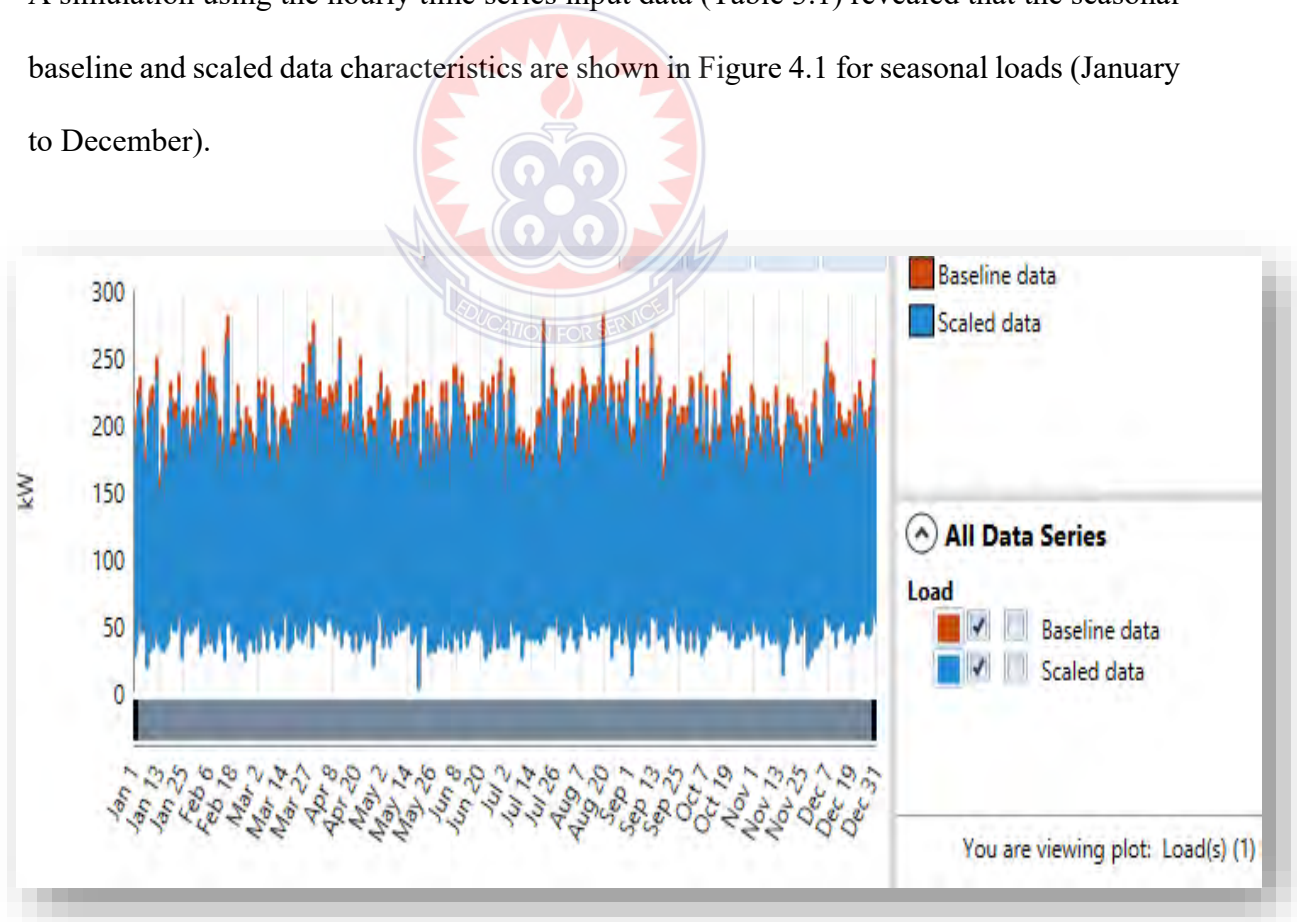


Figure 4.1: Baseline and scaled load data characteristics

The results of the study showed that the scaled data, represented in red, was twice the baseline data, represented in blue. The scaling of the data did not alter the statistical characteristics of the base data, but rather, it changed the analytical values of the base data. The HOMER tool simulation used the scaled data of 2,422.37 kWh/day and a scaled peak load of 321.42 kW, as shown in Appendix C, based on the raw load-time series from the selected site. The highest load demand was observed in the month of August, while the lowest demand occurred in November, with a value of 230.03 kW throughout the year of study and the monthly load profile of the system was also analysed as shown in Figure 4.2.

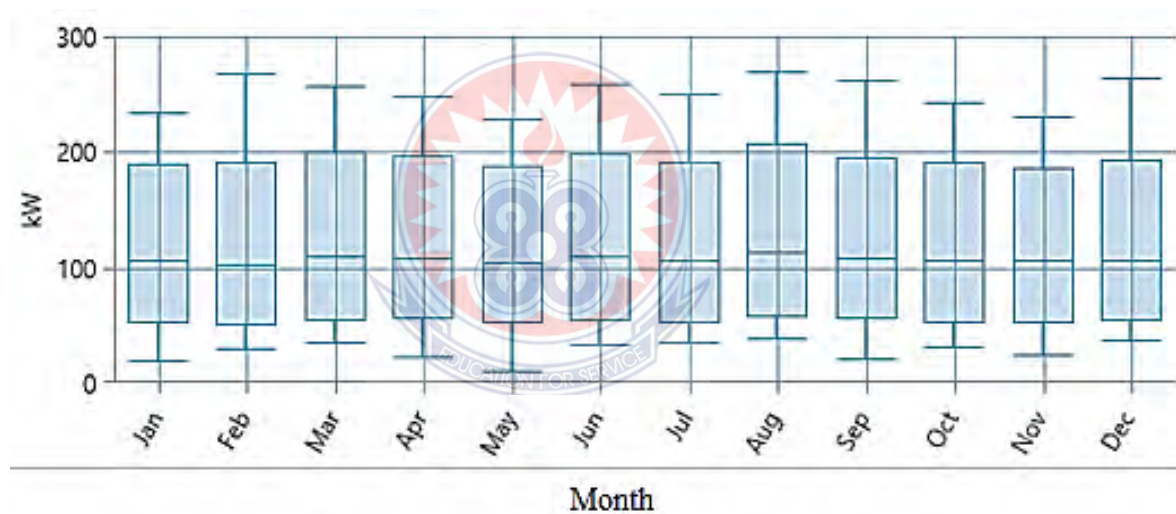


Figure 4.2: Monthly load based on a 24-hour load profile

According to the results, the highest total load demand was recorded in the month of August in the electrical power supply system. However, Figure 4.3 showed that the highest load profile for a single day occurred on February 16th. This is a significant finding, as the electricity billing system takes into account demand charges, which are calculated based on the highest peak power in kilowatt-hours (kWh) or megawatts (MW). This highlights

the importance of monitoring and managing peak power demand, as it can have a significant impact on electricity costs.

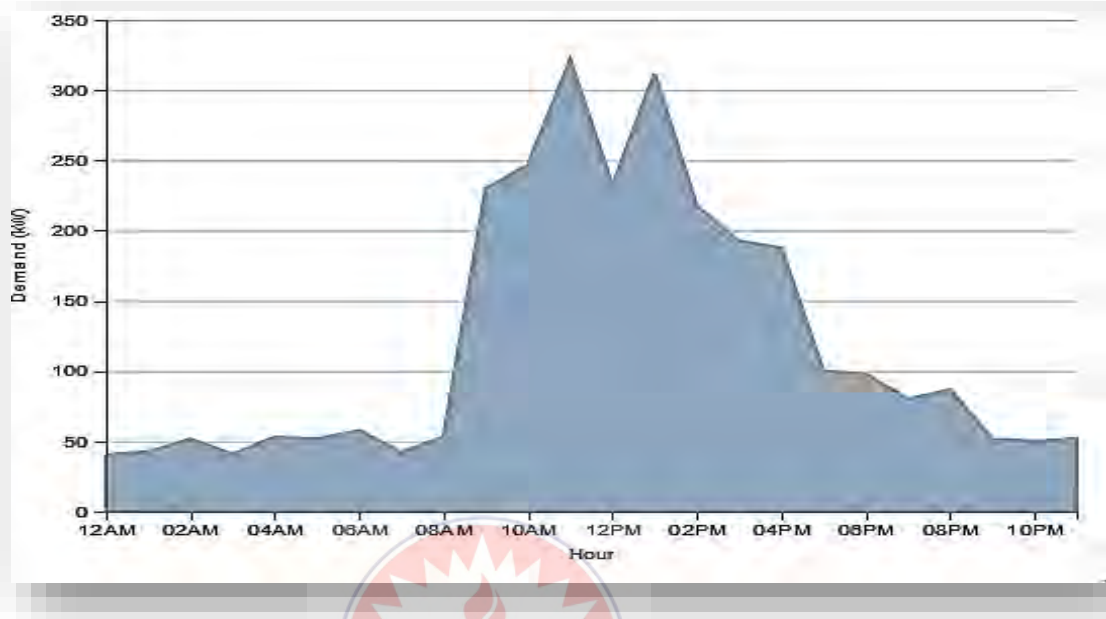


Figure 4.3: The day when the highest load demand occurs

An experimental study used electricity bill data as primary data to predict the system load requirements based on the electrical load demand for the commercial HOMER grid simulation. The authors chose this approach because the tropical climate of the selected site suggested that the average year-round electrical load would not greatly differ from the utility bill. Therefore, the projected average electrical load of the selected facility was adopted based on the electricity bill data. (Riayatsyah et al., 2022).

For accurate simulation results for this study, the healthcare facility's load requirements were evaluated by examining all available electrical equipment at their time of individual operations.

A similar study to the one described in the results evaluated the healthcare facility's load requirements by examining the operation times of all available electrical equipment. The average daily energy requirement was found to be 11,970 kWh for residential buildings, 2,114.4 kWh for commercial buildings, and 1,382.6 kWh for the municipality gross. The total energy consumed was 15,467 kWh per day with a peak load of 1725.5 kW and a derating factor of 0.73. (Mezigebu et al., 2020).

4.2. Assessment of renewable resources.

The town of Kasoa in Ghana, West Africa is blessed with an abundance of sunlight throughout the year. The solar radiation data for KPC at the location of $5^{\circ} 32.0'$ N latitude and $0^{\circ} 25.6'$ W longitude was sourced from NASA's Meteorological and Solar Energy Wave Site. The highest recorded insolation of 5.410 kWh/m²/day occurred in March, followed by February, April, January, December, and November. Conversely, the lowest insolation was recorded as 4.970 kWh/m²/day in May, and the following months in decreasing order of insolation were June, August, September, July, and October. The highest clearness index value of 0.555 was observed in January, followed by December, February, November, March, and a value of 0.515 for the month of April. The location's wind speed ranged from 3.12 to 4.900 m/s and average annual wind speed was 3.78m/s with the 50m height using the anemometer. The wind turbine speed-generation is illustrated in Figure 4.4 which was adopted for this study.

A study conducted in the Khulna district of Bangladesh (22.5° N, 89.5° E) utilized data on wind speed and solar radiation obtained from the NASA Surface Meteorology and Solar

Energy database. The results of the study showed that the wind speed in the area ranged from 2.64 m/s to 4.33 m/s, with the highest wind speed recorded in the month of June. Additionally, the annual average solar radiation in the region was estimated to be 4.56 kWh/m²/day (Nurunnabi et al., 2015) confirms the metrological data used for this current study. The wind speed data collected at an altitude of 50 meters above sea level in the Khulna region was utilized as the basis for the selection of the meteorological data from NASA for the chosen KPC site.

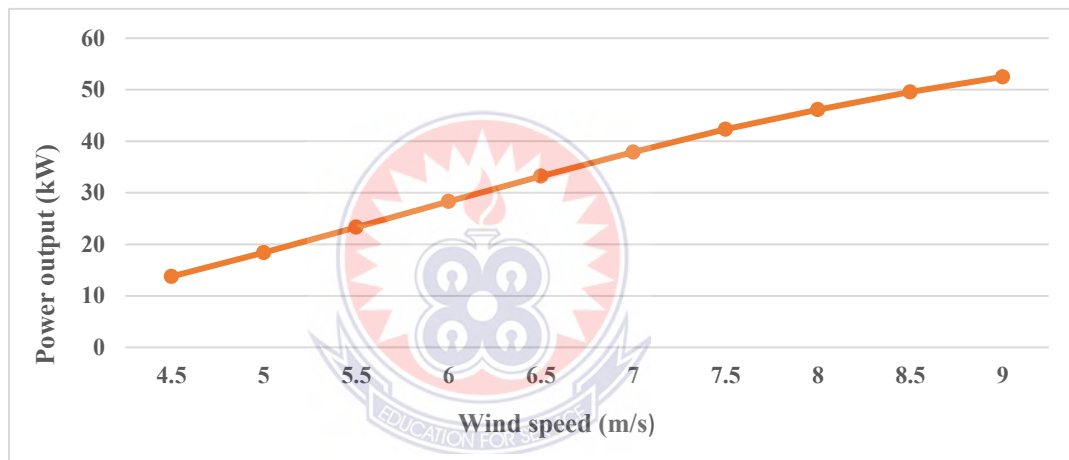


Figure 4.4: Wind turbine power curve

In Nigeria, a study was conducted wherein the wind resource data was procured from the NASA Surface Meteorology and Solar Energy web portal. The study determined the average annual wind speed in the area to be 4.40 meters per second, measured at a height of 10 meters via an anemometer. Additionally, the average annual solar radiation for the area was obtained from the same NASA Surface Meteorology and Solar Energy web portal, yielding a result of 5.51 kilowatt-hours per square meter per day, as reported by (Rilwan et al., 2017).

4.3. Base case Results

The results of the base case simulation were obtained through the utilization of a grid-only generation scheme to meet the energy demands of the facility. The annual operational and maintenance costs, represented by the utility bill, were calculated to be US\$213,439.90. The net present cost was determined to be US\$7,004,608, and the levelised cost was calculated to be US\$0.2414. A representation of the monthly utility bills for the months of January through December is provided in Figure 4.5, yielding the following results respectively: US\$17,846, US\$15,900, US\$18,636, US\$17,644, US\$17,720, US\$17,734, US\$17,959, US\$18,803, US\$17,780, US\$18,090, US\$17,242, and US\$18,087.

Table 4.1 presents the monthly utility bills. It was noted that the highest monthly utility bill for the year was recorded in August, amounting to US\$18,803, while the lowest utility bill was observed in February, totalling US\$15,900. To verify the accuracy of the results, the Homer Grid tool was utilized to estimate the "behind the meter" electricity bills by cross-checking the baseline electricity costs, including energy and demand charges, listed in the report with actual electricity bills. It is worth noting that an electric utility bill may consist of various charges, such as an energy charge for the total monthly energy consumption in kilowatt-hours, a demand charge for the highest monthly peak power in kilowatts or megawatts, and a fixed charge that remains constant regardless of consumption or peak demand.

The HOMER Grid software integrates with the utility rate database provided by Geniality, ensuring the attainment of the most accurate and current results possible. HOMER Grid

stands as the unique demand charge reduction and optimization tool that takes into account the utilization of generators as a means of peak shaving, adhering to HOMER's technology-agnostic approach (HOMER, 2021).

Table 4.2 demonstrates the environmental impact of carbon dioxide (CO₂) emissions, as a result of an exclusive reliance on the national grid to supply various KPC loads. The data illustrates an annual emission total of 558.8 tons of CO₂, which constitutes a significant contribution to greenhouse gas emissions (Intergovernmental Panel on Climate Change, 2014). The persistence of global warming has become a source of concern, and the utilization of fossil fuels, particularly those based on carbon, is seen to incur substantial costs both economically and environmentally for individual and commercial consumers (Stern N., 2006). As such, the exploitation of Renewable Energy Sources (RES) has emerged as a potential alternative energy source, and this research was motivated by the need to explore these possibilities (International Energy Agency, 2019).

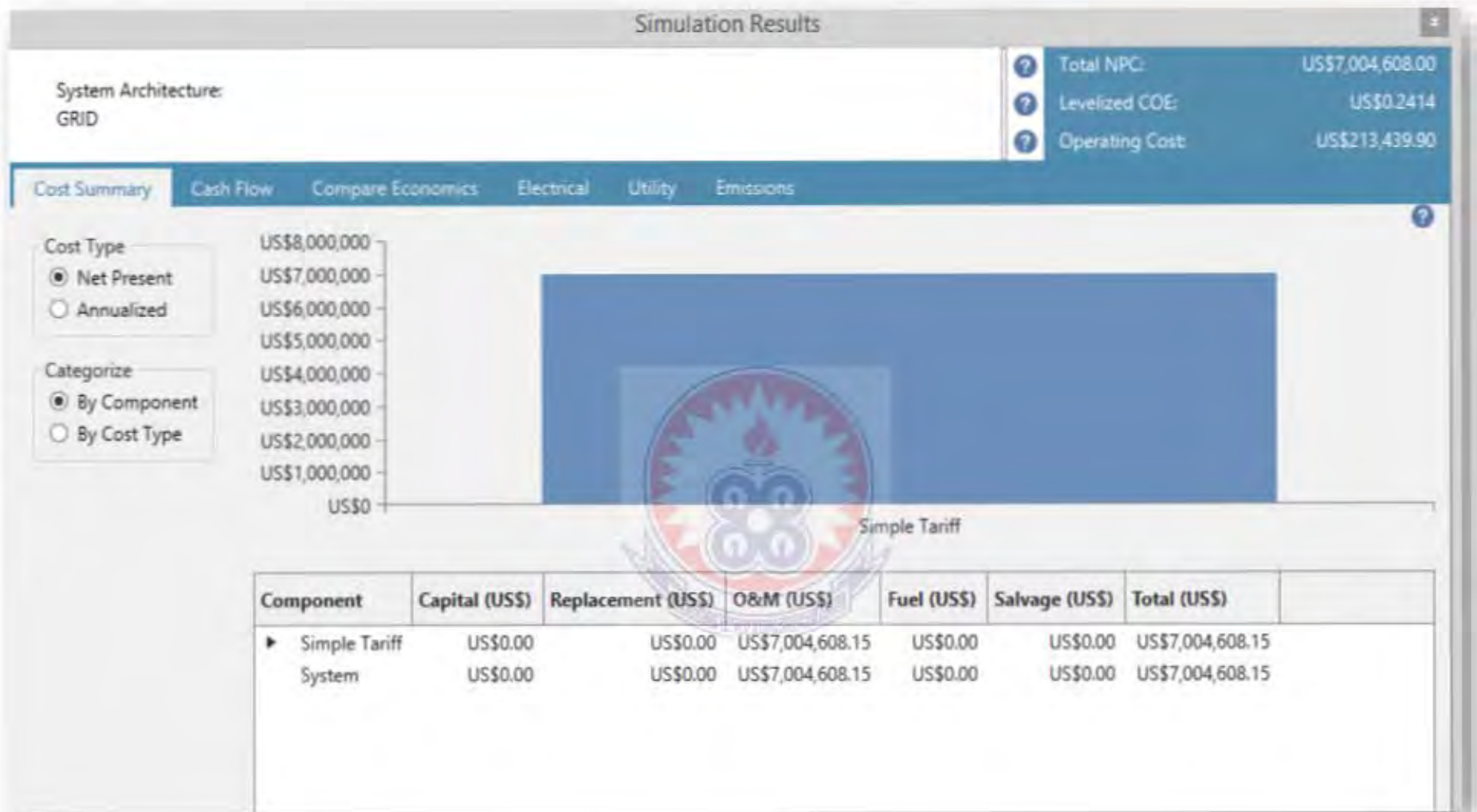


Figure 4.5: Grid system Results

Table 4.1. Monthly bills (Predicted)

	Jan	Feb	Mar	Apr	May	June	July	Aug	Sep	Oct	Nov	Dec
Energy Charges	\$17,746	\$15,792	\$18,530	\$17,540	\$17,622	\$17,632	\$17,852	\$18,696	\$17,674	\$17,988	\$17,145	\$17,983
Consumption	73,942 kWh	65,799 kWh	77,208 kWh	73,083 kWh	73,424 kWh	73,465 kWh	74,384 kWh	77,902 kWh	73,641 kWh	74,951 kWh	71,437 kWh	74,929 kWh
Sales	0 kWh	0 kWh	0 kWh	0 kWh	0 kWh	0 kWh	0 kWh	0 kWh	0 kWh	0 kWh	0 kWh	0 kWh
Demand Charges	US\$98	US\$106	US\$104	US\$102	US\$96	US\$100	US\$104	US\$105	US\$104	US\$99	US\$95	US\$102
Peak Demand	287 kW	321 kW	313 kW	302 kW	277 kW	296 kW	314 kW	315 kW	311 kW	292 kW	272 kW	305 kW
Fixed charges (US\$)	US\$2	US\$2	US\$2	US\$2	US\$2	US\$2	US\$2	US\$2	US\$2	US\$2	US\$2	US\$2
Monthly Total	US\$17,846	US\$15,900	US\$18,636	US\$17,644	US\$17,720	US\$17,734	US\$17,959	US\$18,803	US\$17,780	US\$18,090	US\$17,242	US\$18,087
Annual Total	\$213,440											

Table 4.2: Monthly Carbon dioxide Emissions

	Jan	Feb	Mar	Apr	May	June	July	Aug	Sep	Oct	Nov	Dec
Monthly Total (metric tons)	47 t	42 t	49 t	46 t	46 t	46 t	47 t	49 t	47 t	47 t	45 t	47 t
Annual Total (metric tons)	559 t/yr.											

The findings on the cost and savings, economic and environmental impact of the sole grid dependency architecture, as summarized in Table 4.3, suggest that the current scenario is suboptimal for KPC. This is supported by a comparison of the "behind-the-meter" August electricity bill of US\$18,803 provided by HOMER Grid with the actual ECG bill of GhC3,160.17 (US\$19,443) for September 2021, which was found to be approximately the same (as documented in Appendix D).

Table 4.3: Cost and savings, Economic and Environmental impact result for Base case

Description	Base Case
Costs and Savings	
CAPEX	US\$0
OPEX	US\$213,440
Annual Total Savings (US\$)	US\$0
Annual Utility Bill Savings	US\$0
Annual Demand Charges (US\$/yr.)	US\$1,215/year
Annual Energy Charge	US\$212,225/year
Annual Electricity Bill	US\$213,440
Economic Metrics	
Discounted Payback time (years)	0
Simple payback time (years)	0
LCOE (US\$/kWh)	US\$0.241
IRR (%)	0
Net Present Cost(US\$)	US\$7,004,608
Environmental Impact	
CO ₂ Emitted (metric ton / year)	558.8t/year

The results of the grid-only architecture simulation showed that the yearly consumption of electricity from the grid was 88,165 kWh, representing 100% of the AC primary load consumption of 884,165 kWh, with no excess production or presence of renewable energy sources. The monthly performance of the grid system architecture was summarized in Figure 4.6, which depicted the grid purchase (represented in black) for each month from January to December. The figure displayed that there was a high demand and supply of

energy from the grid during the hours of 8am to 5pm, with a relatively stable demand during the off-peak hours between 6pm to 7am.

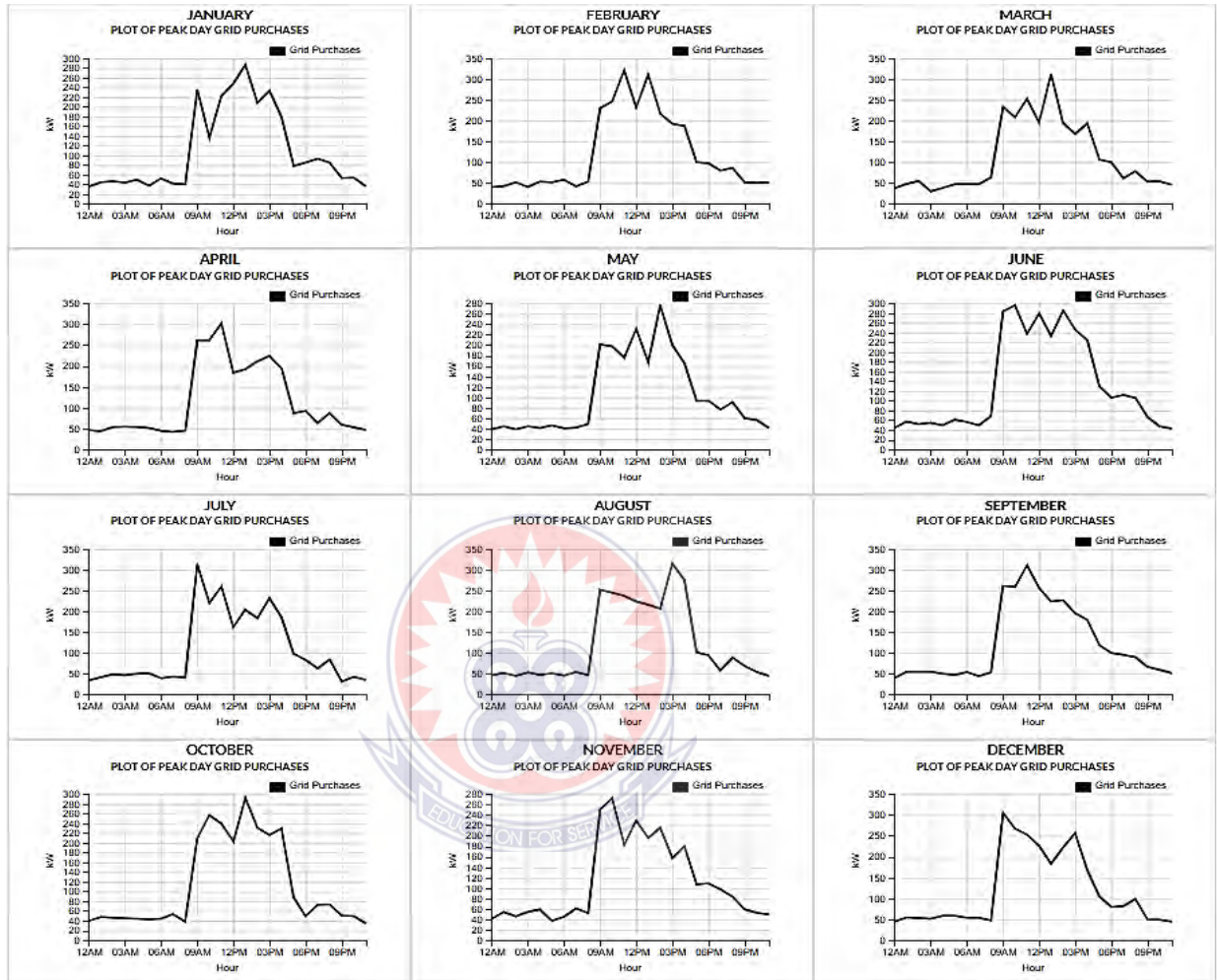


Figure 4.6: Summary of monthly grid purchases

The optimized component details are tabulated in Table 4.4 with the base case as reference is identified in blue. The HOMER grid evaluates the cost for a list of system configurations and their capacities and selects the system based on the lowest CoE and renewable energy fraction. It also determines the viability of hybridised energy systems over time in the simulation process.

Table 4.4: Optimisation Results of the proposed system

Export Optimization Results Categorize

Left Double Click on a particular system to see its detailed Simulation Results.

Architecture						Cost				System						
						Jin310 (kW) ▾	EOXM21 ▾	Li ASM (#) ▾	GRID (kW) ▾	Youn250 (kW) ▾	NPC (US\$) ⓘ ▾	LCOE (US\$/kWh) ⓘ ▾	Operating cost (US\$/yr) ⓘ ▾	CAPEX (US\$) ▾	Ren Frac (%) ⓘ ▾	Total Fuel (L/yr) ▾
						562	2		999,999	278	US\$3.31M	US\$0.0882	US\$52,380	US\$1.59M	77.6	0
						578	2	1	999,999	274	US\$3.32M	US\$0.0880	US\$51,755	US\$1.62M	78.0	0
						746			999,999	346	US\$3.66M	US\$0.0936	US\$64,513	US\$1.54M	72.1	0
						721		14	999,999	356	US\$3.68M	US\$0.0949	US\$66,065	US\$1.51M	71.8	0
							7		999,999		US\$4.55M	US\$0.108	US\$93,709	US\$1.47M	61.4	0
							7	23	999,999	238	US\$4.56M	US\$0.109	US\$93,651	US\$1.48M	61.6	0
									999,999		US\$7.00M	US\$0.241	US\$213,440	US\$0.00	0	0
								15	999,999	252	US\$7.03M	US\$0.242	US\$213,767	US\$10,452	0.0000300	0

4.3. Optimization Results

The results of the optimization process are presented in the "Optimization Results" table, which includes only the feasible simulation outcomes for the selected sensitivity case (non-feasible systems were excluded from the presentation). The categorization and filtering of the results were performed based on the system type. After conducting an analysis of the feasible systems, eight different scenarios were evaluated amongst various configured energy systems to identify the five optimal system designs that effectively meet the institution's energy demand requirements.

4.3.1. Optimisation Details

4.3.2. Case 1: Solar+wind+storage: LI ASM battery+grid

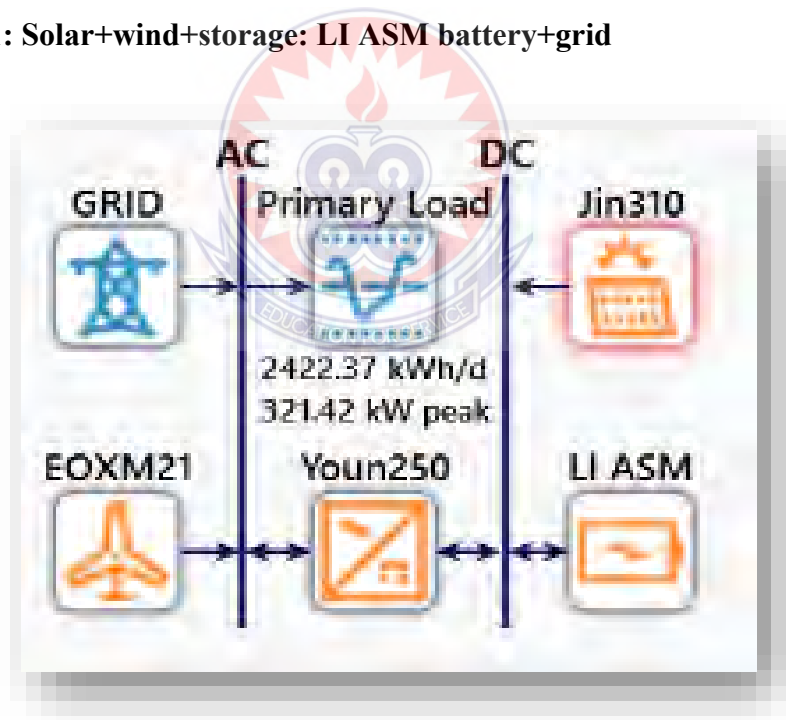


Figure 4.7: Optimised system architecture

The optimization outcomes for the case study location of KPC indicated that the integration of Solar Photovoltaic (PV), Wind energy storage utilizing a Lithium-ion battery and Grid

power generation components was found to be more economically favourable in comparison to relying solely on the conventional national grid system. The results of this study align with the growing consensus among researchers that renewable energy sources integrated with energy storage systems can provide cost-effective and sustainable energy solutions. (Poudineh, R., & Powell, D. 2017), (Zeng, L., Long, Q., & Fang, Y. 2019).

Table 4.5 presents the aggregated expenses associated with the installation and operational costs of three key components of the renewable energy system, including the Jinko Solar module (US\$963,834), the Eocycle Turbine (US\$630,000), and the battery storage system (US\$213,900). Furthermore, the annual operation and maintenance expenses incurred by each component, including Jinko Solar (US\$4,952), the Eocycle Turbine (US\$10,500), and the battery storage system (US\$1,278), were also accounted for and culminated in a total operational cost of US\$16,730.

Table 4.5: Optimized system components cost and O&M

Component	Price	Installation Size	Total Installed Cost	Annual Expenses
Jinko Solar310JKM310PP-72B	US\$1.95/watt	495 kW	US\$963,834	US\$4,952/yr.
Eocycle EOX M-21 [100kW]	US\$210,000.00/ea.	3 ea.	US\$630,000	US\$10,500/yr.
Generic 1kWh Li-Ion [ASM]	US\$300.00/ea.	713 ea.	US\$213,900	US\$1,278/yr.

4.3.2.1 Electricity generation and consumption

Table 4.5 showcases the comprehensive cost analysis of the renewable energy system's three critical components, including the Jinko Solar module (US\$963,834), the Eocycle Turbine (US\$630,000), and the battery storage system (US\$213,900). Additionally, this analysis takes into consideration the annual operation and maintenance costs incurred by

each component, such as Jinko Solar (US\$4,952), the Eocycle Turbine (US\$10,500), and the battery storage system (US\$1,278), resulting in a total operational cost of US\$16,730

Table 4.6 in this study presents evidence of the cost reduction achieved through the implementation of an optimized energy system model. This finding aligns with prior research on grid-connected Solar PV and Wind Battery Storage systems, as demonstrated in a study by (Shantu et al.,2017), which reported a minimum cost of energy of US\$0.0618 and a renewable energy fraction of 98%. The optimized energy system in this study achieved a renewable energy fraction of 90.4%, with solar PV contributing 61% or 700,177kWh per year and wind turbine contributing 29.4% or 337,377kWh per year. These results highlight the potential benefits of integrating renewable energy sources into energy systems, which are consistent with the growing consensus among researchers in the field.

Table 4.6: Optimized system components

Component	Name	Size	Electricity Production (kWh/Year)	Percentage
PV	Jinko Solar	495kW	700,177	61.0%
Wind Turbine	GT [100kW]	100kW	337,377	29.4%
Utility	Simple Tariff	US\$0.23/kWh	110,695	9.64%
Storage				
Total			1,148,249	100%

The results, depicted in Figure 4.13, demonstrate the electricity consumption for a period of one year, amounting to 884,165 kWh or 87.2% of the total energy consumption. Additionally, the figure indicates that a portion of the generated electricity, totalling 129,332 kWh or 12.8%, was sold back to the grid, resulting in an excess of 42,590 kWh

per year. These findings provide insight into the balance between energy consumption and generation in the studied system.

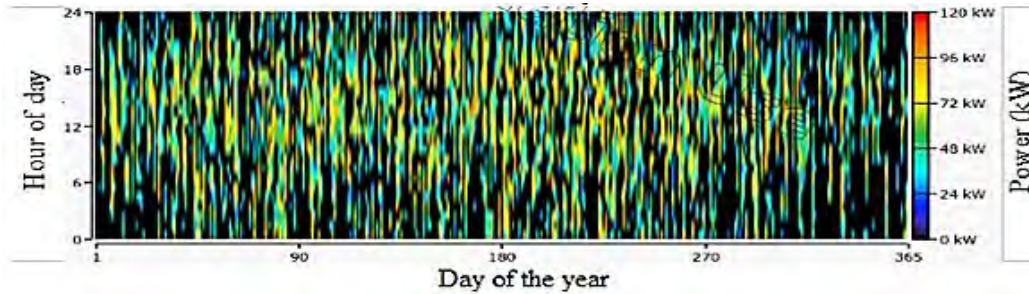


Figure 4.8: Wind turbine electricity generation output

The wind turbine power output is graphically represented in a heat map format in Figure 4.8, while the Solar PV power output is visualized in Figure 4.9. These visual representations provide a comprehensive understanding of the power generation capabilities of the wind turbine and Solar PV components of the energy system.

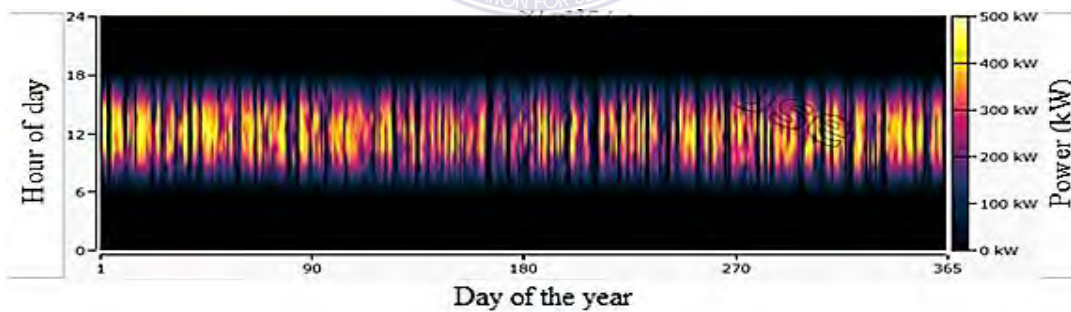


Figure 4.9: Solar PV electricity generation output

The visual representation of the wind turbine power output is presented through a heat map in Figure 4.8, while the Solar PV power output is depicted in a similar manner in Figure 4.9. To provide a clear depiction of the energy exchange between the studied system and

the grid, Figures 4.10 and 4.11 present the energy purchased from and sold to the grid, respectively. The results from the optimized model demonstrate that there was a higher amount of energy sold to the grid compared to the energy purchased from the grid, which provides insight into the balance between energy generation and consumption in the studied system.

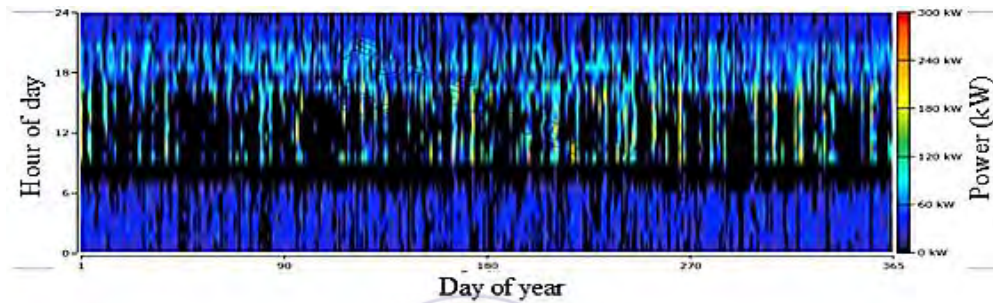


Figure 4.10: Energy purchased from Grid

This is confirmed since the image is divided and within each square, the heat map showed the relative intensity of values captured by your eye tracker by assigning each value a colour representation. The energy purchase from grid and the solar PV that are highest in their value will be given a “hot” colour, while those that are lower in their value will be given a “cold” colour.

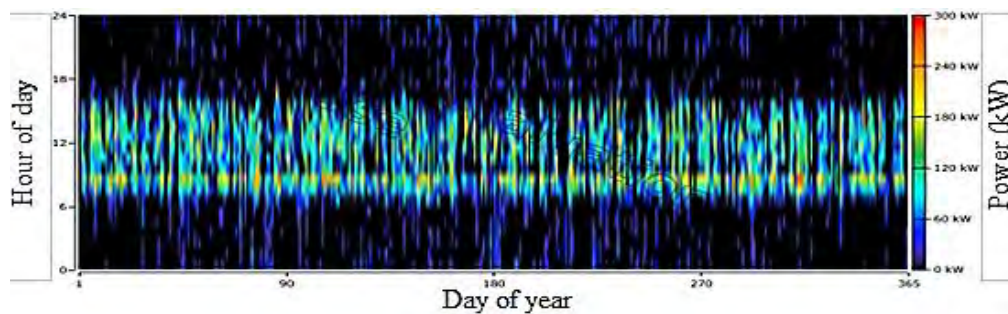


Figure 4.11: Energy sold to the Grid.



Figure 4.12: Monthly electricity production of solar PV, wind turbine GT100 and grid

The monthly performance of the optimized system is depicted in Figure 4.12 and summarizes the yearly electricity production of 42,590 kWh/yr. from the wind turbine GT100, solar photovoltaic (PV), and grid system components. Figure 4.13 displays a graphical representation of the peak load against time of day, with the total renewable power output being indicated in green. The grid purchases are represented in black, while the power output from the solar PV is depicted in yellow and the wind turbine power output is depicted in sea blue.

Figure 4.13 provides a comparison of the grid purchases of the winning system and the base case, with the former being represented in black and the latter in red for each month of the year. Additionally, the figure presents the characteristic of the battery state of charge versus time for each month. The annual performance of the winning system demonstrates a substantial generation of renewable energy power supplied to KPC's load, primarily between the hours of 6 a.m. and 6 p.m. from January to December. The grid purchases of the system and the baseline grid purchases are largely conducted between the hours of 12 a.m. and 9 p.m. Furthermore, the figure indicates high battery charge capacity during the same hours in February, March, April, May, August, September, October, November, and December, with the lowest battery charge capacity observed in January, June, and July.

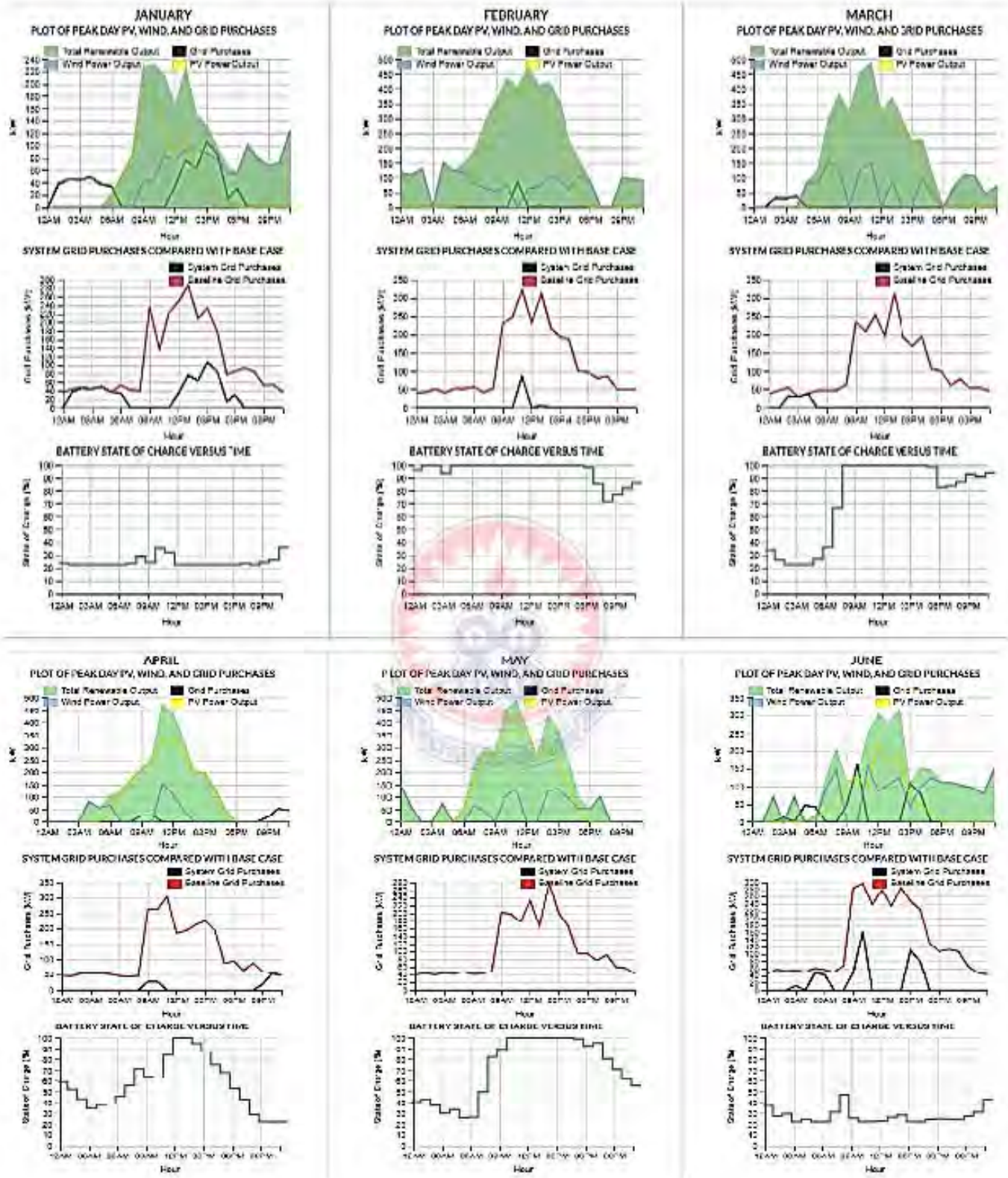


Figure 4.13: Summary monthly performance of the optimized system

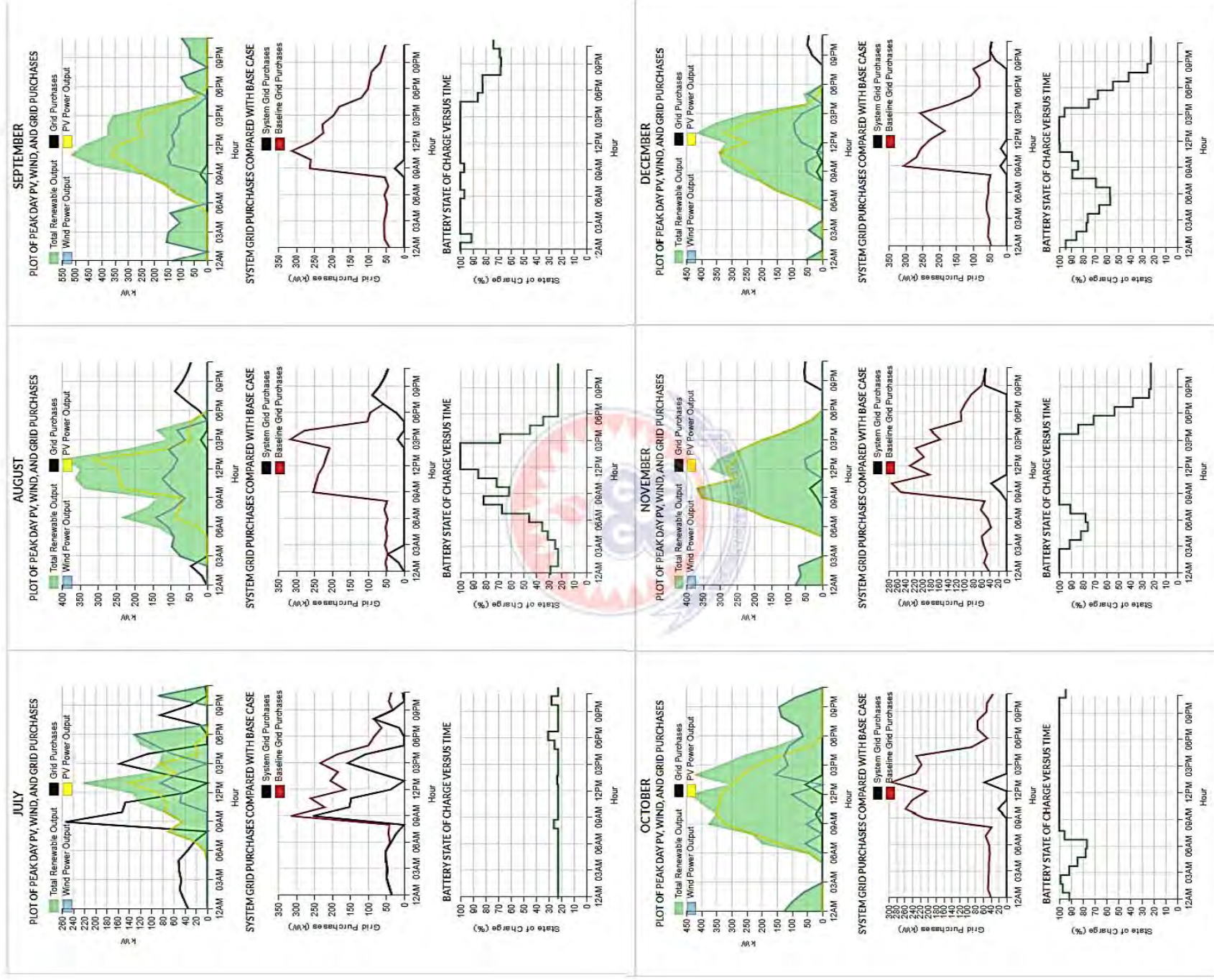


Figure 4.13: Summary monthly performance of the optimized system (Continuation)

4.3.2.2. Economic Evaluation

The renewable energy system's economic performance was analysed using techno-economic analysis. The system's operational expenses and the original investment and replacement costs included in calculating the economic advantages of the proposed system. All costs that arise over the system's lifetime were included in this analysis. To identify the most beneficial system in the HOMER grid model, the TNPC was used, and was utilised in the optimisation process to rank all scenarios with various setups and discover the smallest one. In some cases where renewable energy needed to be promoted, the levelised CoE and the fraction of renewable energy were also used in selecting an optimized system.

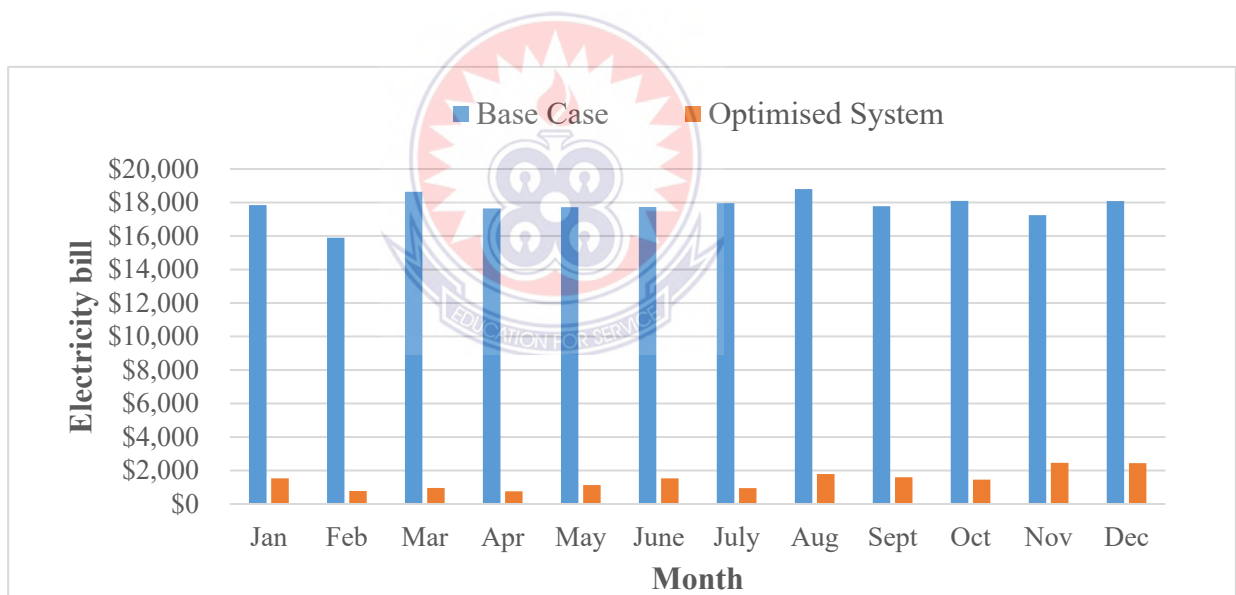


Figure 4.14: Monthly utility bill savings

The annual monthly savings on utility bills are illustrated in Figure 4.14. This is substantiated by the optimized utility bills (predicted) depicted in Table 4.7, which corresponds to a reduction in greenhouse gas emissions of 70 metric tons per year, as presented in Table 4.8.

Table 4.7: Optimized monthly bills (predicted)

	Jan	Feb	Mar	Apr	May	June	July	Aug	Sep	Oct	Nov	Dec
Energy Charges	\$1,447	\$701	\$905	\$705	\$1,057	\$1,448	\$866	\$1,706	\$1,520	\$1,384	\$2,381	\$2,365
Cosumption	10,334 kWh	5,005 kWh	6,461 kWh	5,034 kWh	7,553 kWh	10,219 kWh	6,182 kWh	12,106 kWh	10,854 kWh	9,884 kWh	13,933 kWh	13,128 kWh
Sales	10,526 kWh	12,149 kWh	11,210 kWh	12,418 kWh	10,690 kWh	10,048 kWh	10,263 kWh	11,997 kWh	11,296 kWh	11,248 kWh	9,629 kWh	7,859 kWh
Demand Charges	\$83	\$75	\$53	\$50	\$71	\$79	\$84	\$81	\$79	\$69	\$79	\$70
Peak Demand	250 kW	215 kW	118 kW	108 kW	199 kW	232 kW	253 kW	244 kW	233 kW	188 kW	233 kW	195 kW
Fixed charges (\$)	\$2	\$2	\$2	\$2	\$2	\$2	\$2	\$2	\$2	\$2	\$2	\$2
Monthly Total	\$1,532	\$778	\$959	\$757	\$1,130	\$1,529	\$951	\$1,789	\$1,601	\$1,454	\$2,462	\$2,437
Annual Total	\$17,379											

Table 4.8: Monthly Carbon dioxide Emissions

	Jan	Feb	Mar	Apr	May	June	July	Aug	Sep	Oct	Nov	Dec
Monthly Total (metric tons)	6.5 t	3.2 t	4.1 t	3.2 t	4.8 t	6.5 t	3.9 t	7.7 t	6.9 t	6.2 t	8.8 t	8.3 t
Annual Total (metric tons)	70.0 t/yr.											

The TNPC of the system was US\$3,098,562 and the total savings for the entire 25 years of the project's lifespan was US\$4,901,516 as stated in the Table 4.8. Similarly, Figure 4.15 showcases the economic and cash flow analysis, including a capital cost of US\$1,843,122.44, an operating cost of US\$754,496.62, an operation and maintenance cost of US\$1,138,355.23, and a salvage value of US\$305,698.49.

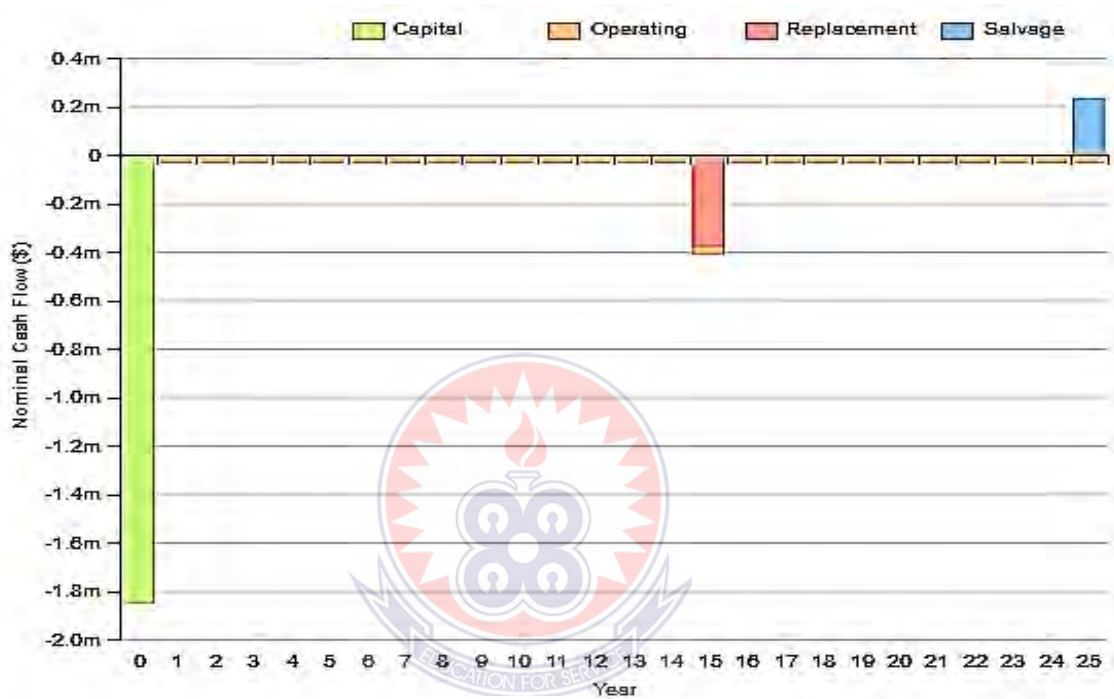


Figure 4.15: Economic and chronological cash flow

The emissions in question consist of carbon dioxide, sulphur dioxide, and nitrogen oxides, which are the prevalent pollutants produced by the utility grid. The optimized system exhibits a lower environmental impact compared to a grid-only system. The optimization results demonstrate that the system can effectively mitigate carbon dioxide emissions from 558.8 metric tons per year to 70.0 tons per year. This study demonstrates that photovoltaic systems generate more energy compared to wind turbines, yet the combination of both photovoltaic and wind energy sources provides a more optimized system in satisfying the

energy demands of the facility. In a similar investigation, it was found that wind turbines were capable of producing more energy than photovoltaic panels due to local climate conditions. The implementation of both photovoltaic and wind energy sources was deemed essential for the system as it simultaneously reduces carbon and other harmful gas emissions while minimizing operation and maintenance costs (Guiju et al., 2020).

A comparative analysis of various standalone hybrid energy systems was conducted in the remote area of Barwani, India and the results indicated that the integration of photovoltaic (PV), wind, storage, and diesel generator (DG) systems was the most economically advantageous and ecologically sustainable solution among the hybrid system combinations evaluated (Sawle et al., 2016). The comprehensive cost-effectiveness evaluation, economic metrics, and the potential environmental impact in comparison to the baseline scenario are depicted in Table 4.9.

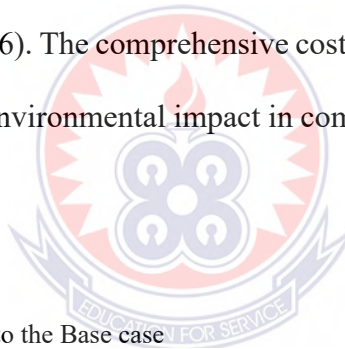


Table 4.9: Case 1 in relation to the Base case

Description	Base Case	Solar+Wind+Storage:LI Battery+Grid ASM
Costs and Savings		
CAPEX	US\$0	US\$1,849,194
OPEX	US\$213054	US\$38,070
Annual Total Savings (US\$)	US\$0	US\$175,370
Annual Utility Bill Savings	US\$0	US\$196,061
Annual Demand Charges (US\$/yr.)	US\$829/year	US\$871/year
Annual Energy Charge	US\$212,225/year	US\$16,508/year
Annual Electricity Bill	US\$213,054	US\$17,379
Projected lifetime savings over 25years	US\$0	US\$4,901,516
Economic Metrics		
Discounted Payback time (years)	0	9.3
Simple payback time (years)	0	10.3
LCOE (US\$/kWh)	US\$0.241/kWh	US\$0.093/kWh
IRR (%)	0	7.87%
Net Present Cost(US\$)	US\$7,004,608	US\$3,098,562
Environmental Impact		
CO ₂ Emitted (metric ton / year)	558.8t/year	70.0t/year

4.3.3. Case 2: Solar+wind+grid

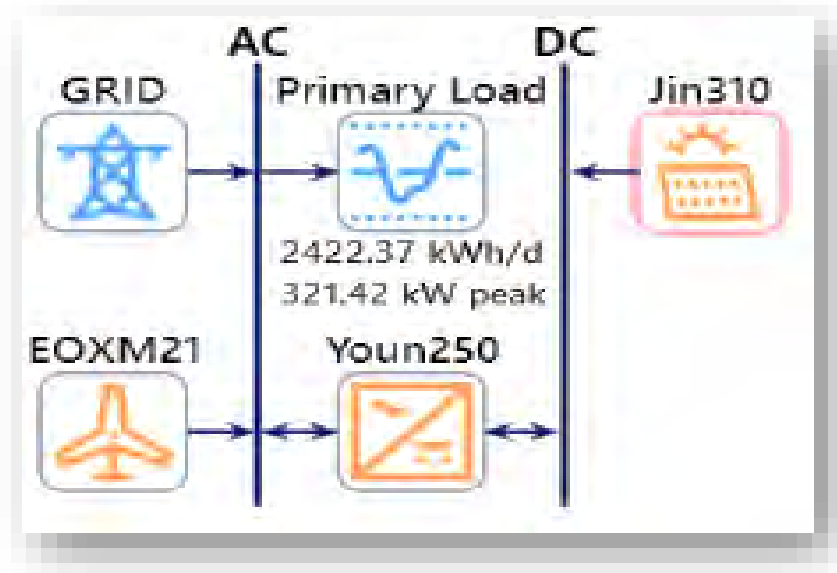


Figure 4.16: Case 2 Schematic diagram

In the second optimized scenario, a hybrid energy generation system that consisted of photovoltaics (PV), wind, and grid-connected generation was analysed, without incorporating energy storage. The model involved the implementation of Jinko Solar PV panels, which had an installation cost of US\$1,089,454, and an Eocycle wind turbine, with an installation cost of US\$420,000 (Table 4.10). The annual operational expenses for the Jinko Solar PV system were calculated to be US\$5,597/year, while the annual operational expenses for the Eocycle wind turbine were estimated to be US\$7,000/year, resulting in a total annual cost of US\$12,597.

Table 4.10: Case 2 installation and annual Expenses

Component	Price	Installation Size	Total Cost	Installed	Annual Expenses
Jinko Solar310JKM310PP-72B	US\$1.95/watt	560 kW	US\$1,089,454		US\$5,597/yr.
Eocycle EOX M-21 [100kW]	US\$210,000.00/ea.	2 ea.	US\$420,000		US\$7,000/yr.

The results of the simulation study indicated that photovoltaics was the predominant source of electricity generation, with an annual output of 791,434 kilowatt-hours (kWh), accounting for 62.1% of the total energy supply for the KPC facility.

The utility grid contributed to 20.2% of the total energy supply with 257,231 kWh, while the wind turbine generated 17.7% of the total energy supply with 224,918 kWh. The details of the component size and annual electricity production, along with the overall electricity production of 1,273,582 kWh, are presented in Table 4.11.

Table 4.11: Case 2 System components and electricity production

Component	Name	Size	Electricity Production (kWh/Year)	Percentage
PV	Flat-plate PV	682kW	791,434	62.1%
Wind Turbine	GT [100kW]	100kW	224,918	17.7%
Utility	Simple Tariff	US\$0.23/kWh	257,231	20.2%
TOTAL			1,273,582	100%

The system's TNPC is US\$3,313,462, and the levelised CoE is US\$0.088/kWh, as opposed to US\$7,004,608 and US\$ 0.241/kWh for the base system.

Table 4.12 displays the cost summary, economic effect, and environmental impact for the project's 25-year lifespan. In a related study, it was shown that the optimised Solar Wind and Grid architecture might lower energy costs. The optimised system suggests integrating 682 kW of generic flat solar PV and 100 kW of wind turbines, which would lower the levelised CoE from \$0.060 per kWh to \$0.0446 per kWh (Riyatsyah et al., 2022).

Table 4 12: Case 2 in relation to the Base case

Description	Base Case	Solar+Wind+Grid
Costs and Savings		
CAPEX	US\$0	US\$1,591,066
OPEX	US\$213054	US\$52,484
Annual Total Savings (US\$)	US\$0	US\$160,956
Annual Utility Bill Savings	US\$0	US\$174,810
Annual Demand Charges (US\$/yr.)	US\$829/year	US\$928/year
Annual Energy Charge	US\$212,225/year	US\$37,702/year
Annual Electricity Bill	US\$213,054	US\$38,630
Projected lifetime savings over 25years	US\$0	US\$4,370,258
Economic Metrics		
Discounted Payback time (years)	0	8.9
Simple payback time (years)	0	9.8
LCOE (US\$/kWh)	US\$0.241/kWh	US\$0.088/kWh
IRR (%)	0	8.72%
Net Present Cost(US\$)	US\$7,004,608	US\$3,313,462
Environmental Impact		
CO ₂ Emitted (metric ton / year)	558.8t/year	162.6t/year

The results of the second optimized Case, comprising of a hybrid energy generation system incorporating photovoltaics, wind, and grid-connected generation, are presented in the form of performance graphs and cash flow analysis in Appendix E, as obtained through the utilization of the HOMER tool. Additionally, the monthly utility bills and monthly carbon dioxide emissions resulting from this scenario are presented in Appendix F.

4.3.4 Case 3: Solar+storage: LI ASM battery+grid

Case 3 optimized model comprises of solar PV, storage: LI ASM battery and grid generation schemes. The model involved the installation of Jinko solar PV panels with a cost of US\$1,476, and an ASM battery system at a cost of US\$344,400. The operational expenses for the solar PV system were estimated to be US\$7,584 per year, and US\$3,902 per year for the battery storage system, as depicted in Table 4.13.

Table 4.13: Case 3 Installation and annual expenses

Component	Price	Installation Size	Total Installed Cost	Annual Expenses
Jinko Solar310JKM310PP-72B	US\$1.95/watt	758 kW	US\$1,476,141	US\$7,584/yr.
Generic 1kWh Li-Ion [ASM]	US\$300.00/ea.	1,148 ea.	US\$344,400	US\$3,902/yr.

A substantial proportion, 1,072,323 kWh, of the electricity produced was derived from the implementation of photovoltaic solar panels, constituting 89% of the overall energy generation, with the grid only contributing approximately 11%. The comprehensive breakdown of electricity production over the course of 25 years is presented in Table 4.14, showcasing an annual total electricity generation of 1,204,955 kWh.

Table 4.14: Case 3 System components and Electricity production

Component	Name	Size	Electricity Production (kWh/Year)	Percentage
PV	Flat-plat PV	682kW	1,072,323	89.0%
Utility	Simple Tariff	US\$0.23/kWh	132,612	11.0%
Total			1,204,955	100%

The simulation outcome demonstrated that the Total Net Present Cost (TNPC) of the system was US\$3,430,276, with the Levelised Cost of Energy (CoE) of US\$1.06/kWh, as opposed to the baseline system which incurred a TNPC of US\$7,004,608 and CoE of US\$0.241/kWh. The optimal configuration of the solar, storage, and grid architecture enhances the dependability of the electrical supply. Healthcare facilities are essential services, and their operations can be severely impacted by frequent power outages, a prevalent issue in sub-Saharan countries, including Ghana. The results of a similar study conducted in Nigeria (Rilwan et al., 2017) corroborated the findings of this study, where the Grid/PV/Battery system was identified as the optimal solution, with the lowest TNPC of US\$8,901/kWh and CoE of US\$0.096/kWh. This system is vital to healthcare facilities,

as the renewable energy sources are capable of supplying power to critical loads during periods of intermittent grid supply.

The summary of costs in the present study indicates that the capital expenditure of US\$1,843,123 resulted in an annual operational expenditure of US\$48,363. This was accompanied by an economic payback period of 10 years and an environmental impact of 83.8 metric tons of carbon dioxide emissions per year over the course of the 25-year project lifespan. These findings are displayed in Table 4.15.

Table 4.15: Case 3 in relation to the Base case

Description	Base Case	Solar+Storage:LIASM Battery +Grid
Costs and Savings		
CAPEX	US\$0	US\$1,843,123
OPEX	US\$213054	US\$48,363
Annual Total Savings (US\$)	US\$0	US\$165,077
Annual Utility Bill Savings	US\$0	US\$190,238
Annual Demand Charges (US\$/yr.)	US\$829/year	US\$857/year
Annual Energy Charge	US\$212,225/year	US\$22,344/year
Annual Electricity Bill	US\$213,054	US\$23,202
Projected lifetime savings over 25years	US\$0	US\$4,755,952
Economic Metrics		
Discounted Payback time (years)	0	9.3
Simple payback time (years)	0	10.3
LCOE (US\$/kWh)	US\$0.241/kWh	US\$1.06/kWh
IRR (%)	0	7.44%
Net Present Cost(US\$)	US\$7,004,608	US\$3,430,276
Environmental Impact		
CO ₂ Emitted (metric ton / year)	558.8t/year	83.8t/year

The performance of the optimized Case 3 system incorporating wind energy, battery storage, and grid-connected generation is presented in graphical form, covering the period from January to December, along with the relevant cash flow analysis obtained from the HOMER tool. This information can be found in Appendix G. Additionally, the simulation results for the monthly utility bills and the corresponding monthly carbon dioxide emissions are presented in Appendix H.

4.3.5 Case 4: Solar+Grid

Case 4 optimized model comprises of solar and grid generation schemes without storage component. Concerns of global warming and for a long time system operation with no pollution, the PV Solar system installations have proven to be more economical and environmentally friendly. Installation cost for Jinko solar of US\$1,451,082 with grid resulted an annual expenses of US\$7,455 at a price of US\$1.95/watt (Table 4.16).

Table 4.16: Case 4 Installation and Annual expenses

Component	Price	Installation Size	Total Installed Cost	Annual Expenses
JinkoSolar310JKM310PP-72B	US\$1.95/watt	746 kW	US\$1,451,082	US\$7,455/yr.

The simulation results demonstrate that the photovoltaic component generated a substantial amount of electricity annually, accounting for 76% of the total energy production with an estimated output of 1,054,139 kWh, while the grid-connected generation contributed a comparatively smaller portion, representing 24% with an estimated output of 332,679 kWh.

This data is presented in detail in Table 4.17, which depicts the component size and annual electricity production.

Table 4.17: Case 4 Component size and Annual electricity production

Component	Name	Size	Electricity Production (kWh/Year)	Percentage
PV	Flat-plat PV	682kW	1,054,139	76.0%
Utility	Simple Tariff	US\$0.23/kWh	332,679	24.0%
Total			1,386,818	100%

The simulation outcomes indicate that the grid-connected photovoltaic (PV) generation scheme demonstrated a Levelised Cost of Energy (LCOE) of US\$0.094/kWh, which was significantly lower than the LCOE of US\$0.241/kWh obtained from a grid-only dependency. This observation was consistent with the findings of a similar study (Pawar, Nagorao; Nema, Pragma , 2018), which revealed that the grid-connected PV scheme had a lower COE of US\$0.0316/kWh compared to US\$0.100/kWh for grid-only systems.

The results of this study indicate that the implementation of grid-connected PV systems can result in a significant reduction in energy costs compared to grid-only systems. In this study, the grid-connected PV system was found to have a simple payback time of 10 years, with a Total Net Present Cost (TNPC) of US\$3,660,097 and annual savings of US\$148,846 as outlined in Table 4.18.

Table 4.18: Case 4 In relation to the Base case

Description	Base Case	Solar+Wind+Battery: ASM Battery+Grid	LI
Costs and Savings			
CAPEX	US\$0	US\$1,540,269	
OPEX	US\$213054	US\$64,594	
Annual Total Savings (US\$)	US\$0	US\$1,48846	
Annual Utility Bill Savings	US\$0	US\$162,197	
Annual Demand Charges (US\$/yr.)	US\$829/year	US\$916/year	
Annual Energy Charge	US\$212,225/year	US\$50,327/year	
Annual Electricity Bill	US\$213,054	US\$38,213	
		4,054,930	
Economic Metrics			
Discounted Payback time (years)	0	9.0	
Simple payback time (years)	0	10.0	
LCOE (US\$/kWh)	US\$0.241/kWh	US\$0.094/kWh	
IRR (%)	0	8.36%	
Net Present Cost(US\$)	US\$7,004,608	US\$3,660,097	
Environmental Impact			
CO ₂ Emitted (metric ton / year)	558.8t/year	210.3t/year	

The performance graph and cash flow analysis of the optimized Case 4 Solar Photovoltaic (PV) and Grid system, generated by the HOMER tool, are presented in Appendix J. The simulation results detailing the monthly utility bills and carbon dioxide emissions are depicted in Appendix K.

4.3.6. Case 5: Wind+Storage: LI ASM Battery+Grid

The optimized Case 5 model, which is comprised of wind, energy storage in the form of a LI ASM battery, and grid generation schemes, is demonstrated in terms of component size and associated costs in Table 4.19.

The implementation of this model involves the installation of an Eocycle wind turbine at a cost of US\$1,680,000, and the integration of a LI ASM battery with an installation cost of US\$197,400. The annual expenses incurred for the wind turbine and battery storage are US\$28,000 and US\$1,178, respectively, as indicated in Table 4.19.

Table 4.19: Case 5 Installation and Annual expenses

Component	Price	Installation Size	Total Installed Cost	Annual Expenses
Eocycle EOX M-21 [100kW]	\$210,000.00/ea.	8 ea.	\$1,680,000	\$28,000/yr.
Generic 1kWh Li-Ion [ASM]	\$300.00/ea.	658 ea.	\$197,400	\$1,178/yr.

The results of the optimized Case 5 model, which comprised of a wind generation scheme, LI ASM battery storage, and grid generation scheme, are presented in Table 4.20. The system demonstrated an annual electricity generation capacity of 1,386,818kWh, with 72.8% of the total energy output, or 899,671kWh, derived from the wind turbine alone and the remaining 27.2% (336,421kWh) sourced from the national grid. This finding is

supported by prior research conducted which confirmed the cost-effectiveness and efficiency of wind energy systems for the island of Gokceada in Turkey. The study concluded that the cost of energy for wind energy systems was lower, with a COE of approximately 17 US cents, and further reduced to 2 US cents with sales. The NPC was also significantly reduced through the use of grid connections (Demiroren et al., 2010).

Table 4.20: Case 5 Component size and Electricity production

Component	Name	Size	Electricity Production (kWh/Year)	Percentage
Wind Turbine	GT [100kW]	100kW	899,671	72.8%
Utility	Simple Tariff	US\$0.23/kWh	336,421	27.2%
Total			1,386,818	100%

The findings of the Case 5 architecture demonstrated a reduced project lifetime savings of US\$3,914,409 and a relatively high levelised cost of energy (LCOE) of US\$0.116/kWh, despite some annual utility bill savings of US\$156,576 in comparison to the base case scenario. The optimized Case 5 configuration also revealed the highest net present cost at an amount of US\$4,485,805, accompanied by yearly carbon dioxide emissions as depicted in Table 4.21.

The graphical representation of the performance of the optimized Case 5 Wind, Battery Storage, and Grid System from January to December, as well as the cash flow analysis derived from the optimized results obtained using the HOMER tool, are presented in Appendix L. Additionally, the simulation results for Case 5, showcasing the monthly utility bills and monthly carbon dioxide emissions, are displayed in Appendix M.

Table 4.21: Case 5 in relation to the Base case

Description	Base Case	Wind+Battery:LIASM +Grid
Costs and Savings		
CAPEX	US\$0	US\$1,916,466
OPEX	US\$213054	US\$78,291
Annual Total Savings (US\$)	US\$0	US\$135,149
Annual Utility Bill Savings	US\$0	US\$156,576
Annual Demand Charges (US\$/yr.)	US\$829/year	US\$1,151/year
Annual Energy Charge	US\$212,225/year	US\$55,712/year
Annual Electricity Bill	US\$213,054	US\$56,864
Project lifetime savings over 25 years		US\$3,914,409
Economic Metrics		
Discounted Payback time (years)	0	13.0
Simple payback time (years)	0	17.1
LCOE (US\$/kWh)	US\$0.241/kWh	US\$0.116/kWh
IRR (%)	0	4.31%
Net Present Cost(US\$)	US\$7,004,608	US\$4,485,805
Environmental Impact		
CO ₂ Emitted (metric ton / year)	558.8t/year	212.6t/year

4.4. Results on Technical Analyses at point of common couple for grid-connected PV/Wind generation scheme with Battery storage

The results for the ETAP PCC analysis for this study shows performance of voltage and current flows, losses, and stability of the power system at the point where it connects to the external power grid. The analysis considers the characteristics of the buses, branches, generators, power grids, and loads connected to the system.

The study results of Load Flow analysis for grid-connected Solar PV, Wind and Battery storage PCC using ETAP software is illustrated in Figure 4.16. In other study the results suggests that the power system is operating in a steady-state condition with no significant imbalances between the load and generation (Md Saleh et.al., 2017).

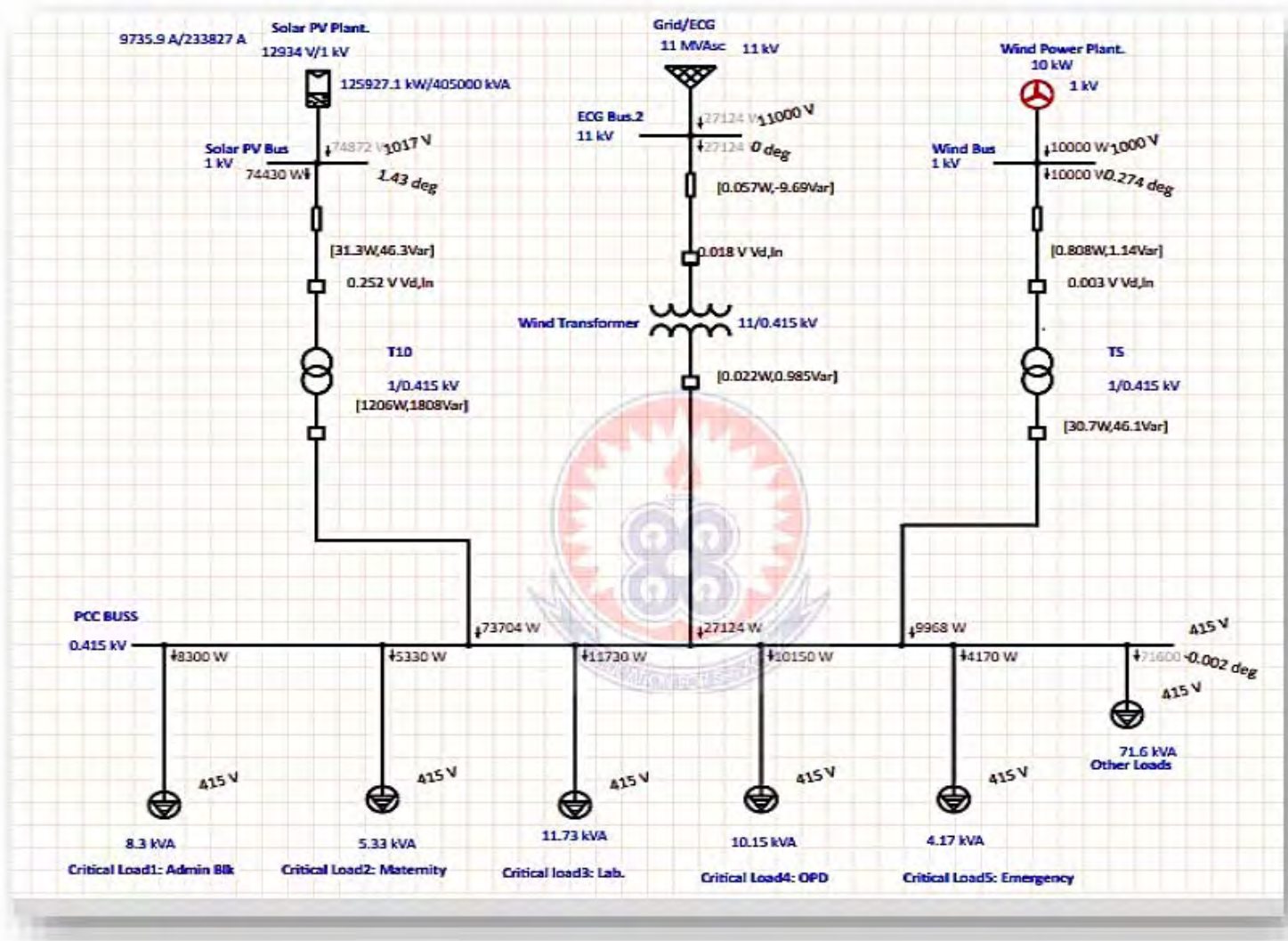


Figure 4.17: Results of PCC from ETAP

4.4.1 PCC Branch characteristics

In the same scenario, this current research results for Bus 1(Wind, ECG and Solar PV Bus), including kW flow, kvar flow, amp flow, power factor, voltage drop, kW losses, and kvar losses for the Wind Bus, ECG Bus.2, and Solar PV Bus, are presented in Table 4.22. The Wind Bus is consuming reactive power (inductive) with a power factor of -85%, which is leading to a slight voltage drop. The ECG Bus.2 is supplying reactive power (capacitive) with a high power factor of 96.59%, resulting in no voltage drop. The Solar PV Bus is also consuming reactive power (inductive) but with a very high power factor of 99.99%, causing a minimal voltage drop.

The kW losses for all three buses are relatively low, with the highest losses occurring at the Solar PV Bus due to the high kW flow. The kvar losses for the Wind Bus and Solar PV Bus are also low, but the ECG Bus.2 is generating capacitive reactive power, resulting in a negative kvar loss.

Overall, the power flow and losses for the Wind Bus, ECG Bus.2, and Solar PV Bus are within acceptable limits, and the power factors are generally high, indicating a good balance between active and reactive power in the system. The minimal voltage drops also suggest that the system is well-designed and operating efficiently.

Again the research data (Table 4.22) provides the electrical characteristics of three buses, i.e., Bus33 for wind, Bus30 for Grid/ECG, and Bus27 for Solar PV. Bus33 has a kW flow of 10, a kvar flow of -6.2, and an amp flow of 6.791. The power factor is -84.99%, indicating the presence of a significant reactive component. The voltage drop is minimal,

at 0.01%, but there are noticeable losses in kW and kvar, at 0.0307 and 0.0461, respectively.

Bus30 has a kW flow of 74.91, a kvar flow of 0.924, and an amp flow of 42.56. The power factor is high, at 99.99%, indicating a near unity power factor. However, the voltage drop is significant, at 1.64%. The kW and kvar losses are also high, at 1.21 and 1.81, respectively.

Bus27 has a kW flow of 27.12, a kvar flow of 7.27, and an amp flow of 1.474. The power factor is 96.59%, indicating a relatively low reactive component. There is no voltage drop, and there are no kW losses. However, there is a small kvar loss of 0.001.

Overall, the analysis indicates that Bus30 has the highest power flow, but it is also associated with significant losses and voltage drop. Bus27 has the lowest power flow but with minimal losses and voltage drop. Bus33 has a low power flow with moderate losses and voltage drop.

4.4.2. PCC Bus and Power flow characteristics

The analysis of the measured data shows that the ECG Bus.2 is drawing a significant amount of power from the PCC, with a kW flow of 27.12. This is also reflected in the high amp flow of 154.5 at the PCC Bus. However, the power factor at this bus is relatively high at 96.59%, indicating efficient power consumption.

The Solar PV Bus is generating a significant amount of power with a kW flow of 74.87. However, the kvar flow is 0, indicating a leading power factor. This can be attributed to the nature of solar PV generation, which has a relatively high power factor.

The Wind Bus is drawing a relatively low amount of power with a kW flow of 10. However, the kvar flow is 6.2, indicating a lagging power factor. This can be corrected by installing reactive compensation devices such as capacitors.

The analysis of the power system with a PCC voltage of 415V indicates efficient power consumption at the ECG Bus.2 with a high power factor. The Solar PV Bus is generating a significant amount of power with a leading power factor. The Wind Bus is drawing a relatively low amount of power with a lagging power factor that can be corrected with the installation of reactive compensation devices.

4.4.4. Discharged Voltage and Current to Hospital loads

The study results report the critical loads and associated power consumption for various sections of the building. The critical loads and their power consumption in kilowatts (kW) and amperes (Amp) as shown in Figure 4.17. These findings provide insight into the power requirements for critical and other loads within the building, which can inform decisions related to energy management and system design.

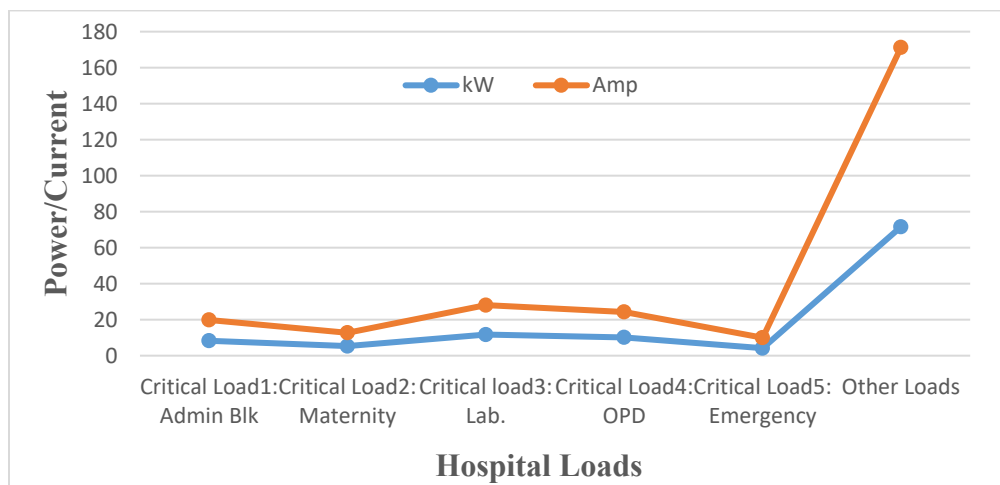


Figure 4.17: Power and Load performance at PCC

Table 4.22: Results from ETAP PCC Branch characteristics

Bus 1	kW Flow	kvar Flow	Amp Flow	% PF	% Voltage Drop	kW Losses	kvar Losses
Wind Bus	10	-6.2	6.791	-85	0	0.0008	0.0011
ECG Bus.2	27.12	7.27	1.474	96.59	0	0.0001	-0.0097
Solar PV Bus	74.4	1.09	42.27	99.99	0.04	0.0313	0.0463
Bus33	10	-6.2	6.791	-84.99	0.01	0.0307	0.0461
Bus30	74.91	0.924	42.56	99.99	1.64	1.21	1.81
Bus27	27.12	7.27	1.474	96.59	0	0	0.001

Table 2.23: Results from ETAP PCC Load performance

ID	Rating/Limit	Rated V	kW	Amp	Vterminal
Critical Load1: Admin Blk	8.3 kVA	415	8.3	11.55	415
Critical Load2: Maternity	5.33 kVA	415	5.33	7.415	415
Critical load3: Lab.	11.73 kVA	415	11.73	16.32	415
Critical Load4: OPD	10.15 kVA	415	10.15	14.12	415
Critical Load5: Emergency	4.17 kVA	415	4.17	5.801	415
Other Loads	71.6 kVA	415	71.6	99.61	415

Table 4.24: Results from ETAP PCC Buss characteristics

Bus ID	Voltage	kW Loading	kvar Loading	Amp Loading
Bus27	11	27.12	7.27	1.474
Bus30	1.016	74.4	1.09	42.27
Bus33	1	10	6.2	6.791
ECG Bus.2	11	27.12	7.26	1.474
PCC BUSS	0.415	110.8	7.27	154.5
Solar PV Bus	1.017	74.87	0	42.51
Wind Bus	1	10	6.2	6.791

4.5. Emissions Reduction and Monetary Savings of Optimised Case

In Ghana as of 2020, the total greenhouse gas (GHG) emissions of 42.15 MtCO₂e, the energy sector ranks second with approximately 35.63% (Environmental Protection Agency, Ghana, 2020). Out of the total energy sector contribution, the country's electricity generation alone provides 19% of the GHG emissions (United State AID, 2016). In 2000, the lowest level of emissions from electricity generation in the country was achieved at 490,000 metric tons of CO₂ equivalent (Doris Dokua, 2022).

As of 2020, carbon emissions from the power sector in Ghana reached 6.5 million metric tons of carbon dioxide equivalent. This followed a steadily increasing trend visible since 2015 and represented the highest volume of emissions within the observed period.

The result from this study as stated early shows a current less optimal case (Grid only) for KPC has a high carbon emission of 588.8t/year but significant reduced emission of 70t/year by the most optimised Solar PV, wind. Storage and grid generation architecture which represents about 78%. The potential energy created by the purpose of the renewable energy system to replace energy from fossil fuels is used to calculate the emission reduction. This is measured in terms of emissions per unit of energy consumed (Antwi-Agyei, P., Andrew, J.D., Agyekum, P.T., Lindsay, C.S., 2018).

The result of this study also confirms the many attempts have being made to reduce carbon emissions by many countries. Two of such significant attempts are the 2015 Paris Climate Change Agreement and the United Nations Sustainable Development Goals (SDGs) (Alignment between nationally determined contributions and the sustainable development goals for West Africa. Clim. Policy).

4.5.1. Monetary Savings potential from Carbon price reform

The Effective Carbon Rate (ECR) encompasses the total monetary value assigned to the emissions of carbon dioxide (CO₂) resulting from energy utilization. This value is arrived at by considering the taxes and emissions trading schemes, net of fuel subsidies. An increase in the ECR stimulates both producers and consumers to adopt cleaner energy sources or reduce energy consumption, thus mitigating the emissions of CO₂ and local pollution. The rise in ECR also contributes to the public revenue through the levying of taxes and auctioning of permits.

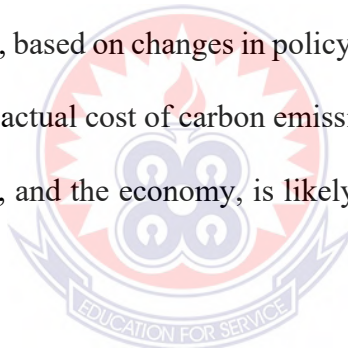
In the scenario where the ECRs are elevated to attain a level of EUR 30/tCO₂ for all fossil fuels, a crucial question arises regarding the extent to which tax revenues would increase. The benchmark of EUR 30 per tonne of CO₂ emitted is considered a low-end approximation of the harm caused to the environment.

For the purpose of ensuring that the most vulnerable groups, who are also likely to be disproportionately impacted by climate change, have access to clean energy, an equitable reform package is imperative.

The implementation of carbon price reform in Ghana has the potential to increase the country's tax revenues. According to a study conducted by the Organisation for Economic Co-operation and Development (OECD, 2018), a potential increase of 0.2% of Gross Domestic Product (GDP) could be realized if the Effective Carbon Rate (ECR) were raised to reach the benchmark rate of EUR 30/tCO₂ for all fossil fuels. This increase, while below the averages set by the OECD and TEU-SD, represents a significant opportunity for Ghana. Furthermore, the study finds that a reform of fuel subsidies in Ghana could lead to an

estimated increase of 0.1% of GDP in tax revenues. In total, a carbon price reform in Ghana has the potential to raise tax revenues by an amount equivalent to 0.3% of the country's GDP.

The assessment of monetary savings associated with reducing carbon emissions involves quantifying the cost per metric ton of CO₂. Based on the benchmark of 30 Euros per tonne, the results of this study indicate that the grid-only generation scheme results in emissions costs of 17,664 Euros. In contrast, the most optimized generation scheme results in a reduced emission cost of 2,100 Euros, translating to a monetary savings of 15,564 Euros (approximately US\$18,454). It is noteworthy that the cost of carbon emissions per metric ton may fluctuate over time, based on changes in policy or market conditions. Furthermore, it is acknowledged that the actual cost of carbon emissions to society, considering impacts on health, the environment, and the economy, is likely to be significantly higher than the market price of carbon.



4.6. Rate of Depreciation of the Optimal Case

The rate of depreciation for the optimal case, which is integrated within the HOMER Grid framework, is a crucial aspect to consider when evaluating the financial viability of the system. The results of this study shows that optimal case is characterized by a capital expense of US\$1,849,194 and operational expenses of US\$38,070. Accurately determining the rate of depreciation is imperative in order to calculate the net present cost of the system and assess its economic viability over time. Methods for determining the rate of depreciation are widely discussed in literature, with various techniques and models

available, including the straight-line method, declining balance method, sum-of-the-years' digits method, and accelerated cost recovery system (ACRS) (De Silva, 2019).

Table 4.25: HOMER Cost summary and Rate of Depreciation (Optimised Case 1)

Component	Capital (US\$)	Replacement (US\$)	O&M (US\$)	Salvage	Total
Bonus Depreciation	(123,662.06)	0.00	0.00	0.00	(123,662.06)
Eco cycle Wind Turbine [100kW]	630,000.00	0.00	344,585.98	(173,644.98)	800,941.00
Generic Battery 1kWh Li ASM	213,900.00	289,264.11	41,947.01	(117,913.21)	427,197.91
Jinko Solar PV	963,833.87	0.00	162,506.09	0.00	1,126,339.96
Simple Tariff	0.00	0.00	570,347.15	0.00	570,347.15
Younics Converter Y.	165,121.90	223,299.85	0.00	(91,024.09)	297,397.66
Optimised System	1,849,193.71	512,563.96	1,119,386.22	(382,582.29)	3,098,561.60

The rate of depreciation for the entire project is determined by using the assumed depreciating lifetime of the project to be 25 years. The equation for the Total Capital Cost can be expressed as the sum of various cost components, which are -123,662.06, 630,000.00, 213,900.00, 963,833.87, 0.00, 165,121.90, and 1,849,193.71, resulting in a total cost of US\$ 3,698,387.42. Additionally, the salvage value of the project is estimated to be US\$ 382,582.29 HOMER provides (Table 4.25).

The research study computed the rate of depreciation, which yielded a result of US\$132,632.21 per year. Thus: Rate of Depreciation = (Total Capital Cost - Salvage Value) / Depreciable Life. The Capital cost was US\$3,698,387.42, the salvage value was US\$382,582.29, and depreciable life was 25 years. Therefore, the rate of depreciation for the entire project is US\$132,632.21 per year and US\$ 11,052.68 per month.

CHAPTER FIVE

SUMMARY OF FINDINGS, CONCLUSION AND RECOMMENDATIONS

The main focus of this chapter is to present a clear and concise summary of the results, to draw meaningful conclusions based on the findings, and to offer practical recommendations for future work.

5.1. Summary of Findings

The purpose of this study was to design a grid-connected renewable power generation system suitable for a public commercial healthcare facility in Ghana (KPC). The research aimed to address the need for a more sustainable energy source for the facility, with a focus on reducing reliance on fossil fuels and improving the overall energy efficiency of the healthcare facility. The study involved conducting a detailed analysis of the energy consumption patterns at KPC, evaluating different renewable energy sources, and finally, proposing an optimized grid-connected renewable energy generation system.

5.1.1. Load profile

The first specific objective of this study was to conduct load profile in order to accurately determine the estimated energy loads utilized within the public commercial healthcare facility in Ghana (Kasoa Polyclinic). The energy audit was largely successful in achieving this objective through the use of load time series analysis. The results of the load time series analysis showed that the total daily energy demand of the healthcare facility was 1,284.822 kWh.

Among the various units within the facility, the medical laboratory had the highest energy demand with 304.255 kWh per day, whereas the reproductive and child health unit had the least energy demand of 12.350 kWh per day. The simulation results obtained through the use of the HOMER tool scaled the total daily energy demand to 2,422.37 kWh, with a scaled peak load of 321.42 kW.

5.1.2. Economic analysis

The second specific objective of this study was to model an optimal grid-connected renewable energy system using the HOMER Grid software environment. The simulation results first showed the base case results; it was found that the annual utility bill ('behind the metre bill) which also represented the operation and maintenance costs, was US\$213,439.90, NPC of US\$7,004,608, LCoE of US\$0.2414 and carbon emissions of 558.8t/year. This represented the current grid connected power supply architecture for KPC which is less optimal situation and to which this study aimed at designing an optimal solution. From the optimization results table (Table 4.4), the results were categorized and filtered by system to determine the five optimal system designs (Cases) that best suits the institution's load demand requirement.

Case 1 or the winning case (solar+wind+storage: LI ASM battery+grid) total installation cost of US\$1,807,734 yielded high annual electricity bill savings of US\$196,061, lowest LCOE of US\$0.093/kWh, lowest TNPC of US\$3,098,562 and lowest carbon dioxide emissions of 70.0 tons per year as compared to the base case.

Secondly, Case 2 (Solar+wind+grid) was next optimal solution with installation cost of US\$1,509,454 yielded annual electricity bill savings of US\$174,810, LCOE of US\$0.088/kWh, TNPC of US\$3,313,462 and carbon dioxide emissions of 162.6t per year and compared to the base case.

The third case results, Case 3 (Solar+Storage:battery LI ASM+grid) was next optimal solution which had total installation cost US\$1,820,541 yielded annual electricity bill savings of US\$190,238, LCOE of US\$0.106/kWh, TNPC of US\$3,430,276 and carbon dioxide emissions of 83.8t per year and compared to the base case.

Next case results was the Case 4 (Solar+Grid) had installation cost of US\$1,451,082 yielded annual electricity bill savings of US\$162,197 LCOE of US\$0.094/kWh, TNPC of US\$3,660,097 and carbon dioxide emissions of 210.3t per year and compared to the base case.

Case 5 (Wind +Storage:battery LI ASM +grid) results represented the least optimal solution with installation cost of US\$1,877,400 yielded an annual electricity bill savings of US\$156,576 LCOE of US\$0.116/kWh, TNPC of US\$4,485,805 and carbon dioxide emissions of 212.6t per year and compared to the base case.

The most optimized grid-connected architecture was solar, wind, storage and grid with simple payback period of approximately 10 years followed by solar, wind and grid scheme, followed by solar, storage and grid scheme, followed by solar and grid, with wind, storage and grid scheme presenting the least optimized system.

Detailed five optimized grid-connected renewable energy systems are tabulated in Appendix B with the first being the winning system architecture.

The third objective of this study was to determine the optimal size of a wind turbine, solar photovoltaic, and energy storage (batteries) to meet load standard. The results of this study showed that a solar size of 495 kW (US\$1.95/watt) resulted in a total installation cost of US\$963,834, a wind turbine installation size of 3 pieces (\$210,000.00/each) resulted in a total installation cost of US\$630,000, and a storage battery bank size of 713 pieces (\$300.00/each) resulted in a total installation cost of US\$213,900 and can be operated with annual expenses of US\$16,730 and a simple payback period of approximately 10 years.

5.1.3. Monetary savings of Carbon Emissions

The Monetary Savings Potential from Carbon Price Reform can be significant. A well-designed policy can lead to reduced carbon emissions, increased innovation in low-carbon technologies, and efficient use of energy and resources. The cost of carbon emissions per ton varies widely and is typically set through a tax, cap-and-trade system, or a carbon tax.

The cost of carbon emissions per ton may also change over time. An increase in the Effective Carbon Rate (ECR) to EUR 30/tCO₂ for all fossil fuels could result in tax revenue increase worth 0.3% of GDP in Ghana. The study suggests that reducing emissions through grid-connected renewable power generation could result in a monetary saving of 15,564 Euros (US\$18,454). The actual cost of carbon emissions to society is likely higher than the market price of carbon.

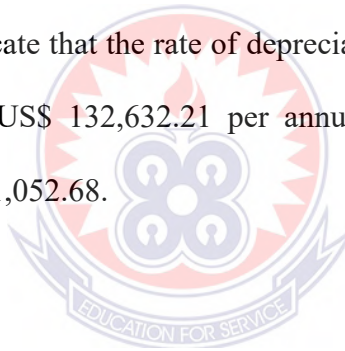
5.1.4. Technical impact of Point of Common Couple on Optimised Case

In this study, the analysis of the power system with a PCC voltage of 415V indicates efficient power consumption at the ECG Bus.2 with a high power factor. The Solar PV Bus is generating a significant amount of power with a leading power factor. The Wind Bus is drawing a relatively low amount of power with a lagging power factor that can be corrected with the installation of reactive compensation devices.

The minimal voltage drops also suggest that the system is well-designed and operating efficiently.

5.1.5 Rate of Depreciation of Optimised Case

The research findings indicate that the rate of depreciation over the project lifespan of 25 years is estimated to be US\$ 132,632.21 per annum, which translates to a monthly depreciation rate of US\$ 11,052.68.



5.2. Conclusion

This study presents the feasibility and reliability of grid-connected solar/wind power generation systems and focuses on a typical urban health facility in Kasoa, central region of Ghana. An energy audit was carried out to record the load profile which was used to determine the hourly load for this selected site. Wind speed, temperature and solar radiation data from NASA's Surface Meteorology and Solar Energy website were used along with hourly loading data for the clinic to run the HOMER grid simulation. The adopted simulation tool is the HOMER Grid and is the only demand charge reduction and optimization tool that considers generators as a shaving method, in keeping with HOMER's technology-agnostic tradition. This simulation tool combines engineering and economics

to quickly perform complex calculations that allow design results to be compared and options to be considered to minimize project risk and reduce energy expenditure.

The optimization result showed that five schemes for combining renewable energies out of eight schemes were discussed with grid architecture as the base case. The grid-connected hybrid system (solar and wind with battery storage) was found to be efficient, economical and environmentally friendly in meeting KPC's load than relying only on the grid. The economics results showed that a grid-connected solar PV and wind turbine system with battery as storage had the lowest levelised CoE of US\$0.093/kWh and the highest renewable energy fraction of 90.4% over the project lifetime of 25 years, in contrast to the reference grid only (base case) of US\$0.241 kWh which had none renewable energy penetration.

Again, the grid-only architecture highest electricity bill (predicted bill by HOMER grid) was GhC3,160.17 (US\$18,803) in the month of August (Table 4.1), can be termed as 'behind-the-metre electricity bill'. The ECG served bill for the month of September 2021 for KPC was compared to the result of this finding. This actual bill (Appendix D) was GhC3,267.84 (US\$19,433), hence in approximation, confirmed HOMER Grid predicted month bill result of GhC3,160.17 (US\$18,803).

Again, the TNPC of the system was US\$3,098,562, which approximately represented about 50% of the TNPC of the grid alone architecture and saving the environment from high carbon dioxide level of 558.8 tons to reduced level of 70.0 tons per year if the hybrid grid-connected solar/wind/storage and grid generation system were adopted. Project life savings

were US\$4,901,516 for the entire 25 years with a simple payback time of approximately 10 years.

These results were confirmed to have multiple benefits of employing a hybrid renewable grid connected systems as described in previous studies (Al-Badi, 2011). In conclusion, the results of this study show that grid-connected PV, wind and grid with storage generation systems are feasible and provide the required reliability, cost effectiveness and protection of the environment.

The integration of renewable energy sources into the grid has become increasingly important as society shifts towards a more sustainable energy mix. Grid-connected solar photovoltaic (PV) and wind generation systems have emerged as leading technologies in this transition. This study utilized the HOMER grid software to analyse and compare the optimal system design for grid-connected solar PV and wind generation.

The results of this study showed that the optimal grid-connected solar PV and wind generation system is influenced by various factors such as location, technology cost, and system size. The HOMER software allowed for a comprehensive evaluation of the economic and technical feasibility of these systems. It was found that in locations with high solar irradiation and wind speed, a combination of solar PV and wind generation was the most cost-effective option.

This study also highlights the importance of considering the intermittences of renewable energy sources when designing a grid-connected system. HOMER's capacity to analyse the time-varying nature of wind and solar resources allowed for a more realistic evaluation of

the system's performance. It was found that the integration of energy storage can mitigate the intermittence of renewable energy sources and improve system reliability.

In conclusion, this study demonstrates the potential of utilizing HOMER as a tool for optimizing grid-connected solar PV and wind generation systems. The results of this study provide valuable insights for policymakers and practitioners in the renewable energy industry. It is suggested that further research be conducted to explore the potential for integrating other renewable energy sources and to examine the effect of different policy and regulatory frameworks on the feasibility of these systems (Bolinger and Wiser, 2016). The impact of generation addition and rejection is broadly discussed and over all study outcome is summarized as the renewable generations (Solar and wind) units have no negative impact on the stability of the system. It is also found that hybrid power system including solar and wind generation can meet up the load demand which other research outcomes present the same (Md Saleh et. al 2017).

5.3. Recommendations

This study can be employed as a benchmark in sizing hybrid solar PV, wind, battery storage and grid systems for other hospitals having similar load and climate conditions. For hospitals, microgrids add value every day, and not just when the power goes out. Microgrids go beyond diesel-based backup power systems by enabling the use of renewable energy, fuel cells and energy storage. They help maximize resilience, reduce costs, and ensure sustainability with advanced energy analysis capabilities that help optimize and balance the use of grid and on-site energy resources. They also comply with all applicable national and local regulations. Now is the perfect time for hospital

administrators to adopt a microgrid solution. The technology has matured, making solutions more affordable and easier to implement than ever before.

5.3.1. Suggestion for Further Studies

This study considered only solar and wind energy as renewable energy resources with battery bank as storage. Flywheels can be considered as a probable energy storage system in future analyses. Adding other sources of renewable energy to determine optimal configurations and to assess the sensitivity of the optimal system is also suggested for future studies.

This study was limited to grid connected solar and wind generation systems but could be extended for the addition of biomass energy. Renewable energy technology components accurate cost data has to be developed and computed for optimization, especially when considering various sensitivity cases analysis The complete potential of these approaches has not been proven fully, and hence further studies are needed.

Based on the current research landscape, the following recommendations can be made for further research on the topic of optimal grid-connected solar PV and wind with battery storage using HOMER grid software:

- i. Integrating more renewable energy sources: While the current research focuses primarily on solar PV and wind energy, it would be interesting to explore the integration of other renewable sources such as hydro and geothermal energy with battery storage systems.
- ii. Improving battery storage performance: A major challenge in integrating renewable energy sources with battery storage is ensuring the efficient and cost-

effective operation of the battery system. Further research could focus on improving the performance of battery storage systems and evaluating their impact on the overall system performance.

- iii. Optimizing for different grid configurations: The current research has primarily focused on rural and island grid configurations. Further research could focus on optimizing renewable energy systems for different types of grid configurations such as urban grids, microgrids, and large-scale centralized grids.
- iv. Evaluating the impact of policy and regulatory factors: Policy and regulatory factors play a critical role in the adoption and implementation of renewable energy systems. Further research could evaluate the impact of different policy and regulatory measures on the economic and technical performance of renewable energy systems with battery storage.
- v. Incorporating demand-side management: Incorporating demand-side management strategies into the design of renewable energy systems with battery storage can help to optimize the overall system performance. Further research could focus on incorporating demand-side management strategies into HOMER models to evaluate their impact on the overall system performance.

These recommendations can provide guidance for further research on the topic of optimal grid-connected solar PV and wind with battery storage using HOMER grid software.

REFERENCES

- Agbossou, K., Kelouwani, S., Anouar, A. & Kolhe, M (2004). Energy management of hydrogen-based stand-alone renewable energy system by using boost and buck converters. In Industry Applications Conference, 2004. 39th IAS Annual Meeting. Conference Record of the 2004 IEEE, 4, 2786-2793.
- Aichhorn, A., Greenleaf, M., Li, H. & Zheng, J (2012). A cost effective battery sizing strategy based on a detailed battery lifetime model and an economic energy management strategy. IEEE Power & Energy Society General Meeting, 1-8.
- Akinyele D., J. Belikov, and Y. Levron, “Challenges of Microgrids in Remote Communities: A STEEP Model Application,” *Energies*, vol. 12, no. 2, pp. 2–35, 2018
- Akuffo F.O., (2007) Generating electricity from sunlight: global trends and developments in Ghana. Surface meteorology and solar energy data and information, 2014. Available from: <https://eosweb.larc.nasa.gov/sse>
- Al-Alawi, A., S. M & Islam, M (2007). Predictive control of an integrated PV-diesel water and power supply system using an artificial neural network. *Renewable Energy*, 32, 1426-1439.
- Al-Badi, A. H (2011). Hybrid (solar and wind) energy system for Al Hallaniyat Island electrification. *International Journal of Sustainable Energy*, 30(4), 212–222. doi:10.1080/1478646X.2010.503276
- Alexandre B., de Souza Paulo Hroeff, and K. Arno, “A method to evaluate the effect of complementarity in time between hydro and solar energy on the performance of hybrid hydro PV generating plants,” *Renewable Energy Science Direct*, vol. 45, pp. 24–30, 2012.

Alhamad, I (2018). A feasibility study of roof-mounted grid-connected PV solar system under Abu Dhabi net metering scheme using HOMER in 2018 Advances in Science and Engineering Technology International Conferences, pages 1-4, doi: 10.1109/ICASET AT., 2018.8376793.

Alignment between nationally determined contributions and the sustainable development goals for West Africa. Clim. Policy. <https://doi.org/10.1080/14693062.2018.1431199>.

Arefifar S.A., Mohamed, Y.A.R.I. & EL-Fouly, T.H.M (2013). Optimum microgrid design for enhancing reliability and supply-security. IEEE Trans. Smart Grid, 4(3), 1567-1575.

Argaw N., “Estimation of solar radiation energy of Ethiopia from sunshine data,” Int. J. Sol. Energy, vol. 18, no. 2, pp. 103–113, 2014.

Awopone K. A., Ahmed F Zobaa, Walter Banuenumah.: “Optimising Energy Systems of Ghana for Long-Term Scenarios” Energy Poly 2017.

Badawe M. E., T. Iqbal, and G. K. Mann, “Optimization and a Comparison between Renewable Energy Systems for a Telecommunication Site,” in 2012 25th IEEE Canadian Conference on Electrical and Computer Engineering (CCECE), pp. 1–5, April 2012.

Baharudin N., T. Mansur, R. Ali, Y. Yatim, and A. Wahab, “Optimization Design and Economic Analysis of Solar Power System with Sea Water Desalination for Remote Areas,” in ICIEA 2007: Second IEEE Conference on Industrial Electronics and Applications, pp. 1594–1599, June 2007.

- Bahramara, S.; Moghaddam, M.P.; Haghifam, M.R. Optimal planning of hybrid renewable energy systems using HOMER: A review. *Renew. Sustain. Energy Rev.* 2016, 62, 609–620.
- Bajpai P., N. Prakshan, and N. Kishore, “Renewable Hybrid Stand-alone Telecom Power System Modelling and Analysis,” in *TENCON 2009-2009 IEEE Region 10*
- Bank of Ghana Website <https://www.bog.gov.gh/economic-data/>, Date Assessed December, 2021.
- Barbosa P.G., Rolim, L.G.B. & Watanabe, E.H. et al., (1998). Control strategy for grid-connected dc-ac converters with load power factor correction. *IEE Proceedings on Generation, Transmission and Distribution*, 145, 487-491.
- Barsoum N., W. Y. Yiin, T. K. Ling, and W. Goh, “Modelling and Cost Simulation of Stand-Alone Solar and Biomass Energy,” in *Second Asia International Conference on Modelling and Simulation*, pp. 1–6, 2008.
- Bekele G., and B. Palm, “Feasibility Study for a Standalone Solar-Wind-based Hybrid Energy System for Application in Ethiopia,” *Applied Energy*, vol. 87, pp. 487–495, 2010.
- Block C, Neumann D, Weinhardt C. A market mechanism for energy allocation in microgrids. In: *Proceedings of the 41st annual Hawaii international conference on system sciences*. IEEE; 2008. 172–172.
- Bolinger, M., & Wiser, R. (2016). 2016 Wind Technologies Market Report. DOE/GO-102016-4861.
- Boqtob O., H. El Moussaoui, H. El Markhi, and T. Lamhamdi, “Optimal sizing of grid connected microgrid in Morocco using Homer Pro,” *2019 Int. Conf. Wiret at., Technol. Embed. Intell. Syst. WITS 2019*, pp. 1–6, 2019

- Burkart R.M. and J. W. Kolar, “Comparative Life Cycle Cost Analysis of Si and SiC PV Converter Systems Based on Advanced η - ρ - σ Multi objective Optimization Techniques,” IEEE Trans. Power Electron., vol. 32, no. 6, pp. 4344– 4358, 2017.
- Conference, pp. 1–6, January 2009.
- Dali, M., Belhadj, J. & Roboam, X (2010). Hybrid solar-wind system with battery storage operating in grid-connected and standalone mode: Control and energy management - Experimental investigation. Energy, 35, 2587-2595.
- Dalton G., D. Lockington, and T. Baldock, “Feasibility Analysis of Stand-alone Renewable Energy Supply Options for a Large Hotel,” Renewable Energy, vol. 33, pp.1475-1490, 2008.
- Darbyshire, J (2010). Multi-Function Power Electronic Interface for Hybrid Mini-Grid Systems. PhD, School of Electrical and Computer Engineering Curtin University of Technology.
- Dehbonei, H., Nayar, C. V. & Chang, L (2003). A new modular hybrid power system in IEEE International Symposium on Industrial Electronics, 2003ISIE '03.985-990, 2.
- Demiroren A and U. Yilmaz, “Analysis of change in Electric Energy Cost with using Renewable Energy Sources in Gokceada, Turkey: An island example,” Renewable and Sustainable Energy, vol. 14, pp. 323–333, 2010.
- Djohra Saheb Koussa, “Mustapha Koussa GHGs (greenhouse gases) emission and economic analysis of a GCRES (grid-connected renewable energy system) in the arid region, Algeria” <http://dx.doi.org/10.1016/j.energy.2016.02.103> 0360-5442/© 2016 Elsevier Ltd. All rights reserved

- Doris Dokua Sasu Statistics on power sector carbon emission in Ghana- Published: May 9, 2022. <https://www.statista.com/statistics/1307146/power-sector-carbon-emissions-in-ghana>
- Dufo-López, R., Bernal-Agustín, J. L. & Contreras, J (2007). Optimization of control strategies for stand-alone renewable energy systems with hydrogen storage. *Renewable Energy*, 32, 1102-1126.
- Edalati S., M. Ameri, M. Iranmanesh, H. Tarmahi, and M. Gholampour, “Technical and economic assessments of grid-connected photovoltaic power plants: Iran case study,” *Energy*, vol. 114, no. 2016, pp. 923–934, 2016.
- Electronics (IICPE), 1-5.
- Elhassan Z. A., M. F. Zain, K. Sopian, and A. Abass, “Design and Performance of Photovoltaic Power System as a Renewable Energy Source for Residential in Khartoum”, *International Journal of the Physical Sciences*, vol.7 pp., 2012.
- El-tous, Y (2012). A study of a grid-connected PV household system in Amman and the effect of the incentive tariff on the economic feasibility. *International Journal Applied Science Technology*, 2(2), pages 100-105.
- Energy, P. On Farm Power Generation—Wind Power; *Applied Horticultural Research: Eveleigh, NSW, Australia*, 2021.
- Engineering, vol. 3, pp. 219–227, September 2010.
- EPA-Ghana, “Ghana’s fourth national communication to the United Nations Framework Convention on Climate Change,” 2020, <https://www.epa.gov.gh>.
- Feed-in Tariffs. *Energypedia.info*. https://energypedia.info/wiki/Feed-in_Tariffs, accessed 2nd January 2020

Ghana Electricity Plan, 2020: ‘An Outlook of the Power Supply Situation for 2020 and Highlights of Medium Term Power Requirements’

Giraja Shankar Chaurasia, Amresh Kumar Singh, Sanjay Agrawal, & N.K. Sharma, 2017
A meta-heuristic firefly algorithm based smart control strategy and analysis of a grid connected hybrid photovoltaic/wind distributed generation system. *Solar Energy*, 150(), 265–274. doi:10.1016/j.solener.2017.03.079.

Guiju Zhang, Caiyuan Xiao & Navid Razmjoo. “Optimal Operational Strategy of Hybrid PV/Wind Renewable Energy System Using Homer: A Case Study” *International Journal of Ambient Energy*: <https://doi.org/10.1080/01430750.2020.1861087>.

Gyamfi S, Modjinou M, Djordjevic S (2015) Improving electricity supply security in Ghana—the potential of renewable energy. *Renewable and Sustainable Energy Reviews* 43: 1035-1045.

Halabi, L.M.; Mekhilef, S.; Olatomiwa, L.; Hazelton, J. Performance analysis of hybrid PV/diesel/battery system using HOMER: A case study Sabah, Malaysia. *Energy Convers. Manag.* 2017, 144, 322–339.

HOMER Grid software, Version 1.8.9; HOMER Grid: Boulder, CO, USA, 2021.

Huang, X., & Sauer, P. W. (2015). "Power system black start capability." *IEEE Transactions on Power Systems*, 30(2), 744-751. Available at: <https://ieeexplore.org/abstract/document/6775187>.
IECON '03. 1296-1301, 2.

Intergovernmental Panel on Climate Change (2014). *Climate Change 2014: Synthesis Report*. Available at: <https://www.ipcc.ch/report/ar5/syr/>

International Council on Large Electric Systems (CIGRE). "Glossary of terms used in power system restoration." (2016). Available at:

<https://www.cigre.org/publications/other/Glossary-of-terms-used-in-power-system-restoration>

International Energy Agency (2019). Renewable Energy Sources. Available at:

<https://www.iea.org/reports/renewable-energy-sources>

Iqbal, M.T (2003). Modelling and control of a wind fuel cell hybrid energy system. *Renewable Energy*, 28(2): 223-237.

Iqbal, M.T (2003). Simulation of a small wind fuel cell hybrid energy system [J]. *Renewable Energy* 28, 511–522.

Islam MT, Shahir S, Uddin TI, (2014) Current energy scenario and future prospect of renewable energy in Bangladesh. *Renewable and Sustainable Energy Reviews* 39: 1074-1088

IURC Staff (2002). Distributed Generation White Paper 1, Page 1-13.

Jih-Sheng, L (2007). Power conditioning systems for renewable energies. In International Conference on Electrical Machines and Systems, ICEMS, 209-218.

Jimenez, A., (2018). ‘Chefornak Energy Configuration Options Energy Infrastructure Optimization to Reduce Fuel Cost and Dependence in Chefornak.’ [https://www.nret at.gov](https://www.nret.at.gov).

Johnson N., P. Lilienthal, and T. Schoechle, “Modelling Distributed Premises-based Renewables Integration using HOMER,” Research Gate, pp. 5–8, December 2011.

Karim D.A., and I. Mahmoud, “Design of Isolated Hybrid Systems Minimizing Costs and Pollutant Emissions,” *Renewable Energy*, vol. 44, pp. 215–224, 2012.

Kazem H.A., T. Khatib, and K. Sopian, “Sizing of a standalone photovoltaic/battery system at minimum cost for remote housing electrification in Sohar, Oman,” *Energy Build.*, vol. 61, pp. 108–115, 2013.

- Khadem S.K., “Feasibility study of Wind Home System in Coastal Region of Bangladesh,”
Journal of Science, vol. 55, no. 2, pp. 263–268, 2007.
- Khalesi, H., & Mohamed, Y. A. R. I. (2016). Control of grid-connected renewable energy systems: problems and solutions. *Renewable and Sustainable Energy Reviews*, 56, 210-223.
- Khan, H., I.; BiBi, R. The role of innovations and renewable energy consumption in reducing environmental degradation in OECD countries: An investigation for Innovation Claudia Curve. *Environ. Sci. Pollut. Res.* 2022, 29, 43800–43813.
[CrossRef] [PubMed]
- Khan, M.J. & Iqbal, M.T (2005). Dynamic modelling and simulation of a small wind–fuel cell hybrid energy system *Renewable Energy* 30, 421–439.
- Khanniche, S. (2006). *Power Electronics for Renewable Energy Systems*. Available from: www.welshenergysectortraining.org/renewable%20energy%20Swansea.ppt.
- Kusakana K., J. Munda, and A. Jimoh, “Feasibility Study of a Hybrid PV-Micro Hybrid system for Rural Electrification,” in *IEEE AFRICON*, pp. 1–5, September 2009.
- Lau K. Y., M. F. M. Yousof, S. N. M. Arshad, M. Anwari, and A. H. M. Yatim, “Performance analysis of hybrid photovoltaic/diesel energy system under Malaysian conditions,” *Energy*, vol. 35, no. 8, pp. 3245–3255, 2010.
- Lilienthal P., “The HOMER Micro power Optimization Model at.,” [https://www.nret at., gov/docs/fy04osti/35406.pdf](https://www.nret.gov/docs/fy04osti/35406.pdf), October 2004.
- Lim P., and C. Nayar, “Solar Irradiance and Load Demand Forecasts in the Supervisory Control for Off-grid Hybrid Energy System,” *IACSIT International Journal of Engineering and Technology*, vol. 4, no. 4, pp. 451–455, August 2012.

- Lim, P. Y., Nayar, C. V. & Rajakaruna, S (2010). Simulation and components sizing of a stand-alone hybrid power system with variable speed generator. In 9th International Conference on Environment and Electrical Engineering (EEEIC), 465-468.
- Liserre, M., & Wright, G. (2010). "Microgrids." Springer Science & Business Media. Available at: <https://link.springer.com/book/10.1007/978-3-540-92662-3>
- Liu G., M. Rasul, M. Amanullah, and M. Khan, "Techno-Economic Simulation and Optimization of Residential Grid-Connected PV System for the Queensland Climate," *Renewable Energy*, vol. 45, pp. 146–155, 2012.
- Lu, X., & Blaabjerg, F. (2020). "Review of microgrid control techniques: Topologies, control methods, and future trends." *IEEE Journal of Emerging and Selected Topics in Power Electronics*, 8(1), 14-33. Available at: <https://ieeexplore.org/abstract/document/8799076>
- Manwell J. F and J. G. McGowan, Lead acid battery storage model for hybrid energy systems, *Solar Energy*, Vol. 50, pp. 399–405, 1993,
- Markus Hirschbold and Andy Haun "How new microgrid designs help hospitals increase resilience, cut costs, and improve sustainability". Life is on Part Number 998-20588515 Rev 0 © 2019 Schneider Electric.
- Matinn, M. A., Deb, A. & Nasir, A., (2013). Optimum Planning of Hybrid Energy System using HOMER for Rural Electrification. *International Journal of Computer Applications* (0975 – 8887), 66(13).
- Mcgowan, J.G. & Manwell, J.F (1999). Hybrid Wind/PV/Diesel system Experience *Renewable Energy* 6(3), 928-933.
- Md Saleh Ebn Sharif, Md Monower Zahid Khan, Md Moniruzzaman & Anamika Bose, (2017). Design, Simulation and Stability Analysis of Wind-PV-Diesel Hybrid

Power System Using ETAP. American Journal of Modern Energy 2017; 3(6):121-130. <http://www.sciencepublishinggroup.com/j/ajme> doi: 10.11648/j.ajme.20170306.12 ISSN: 2575-3908 (Print); ISSN: 2575-3797 (Online)

Meziegebu Getinet Yenalem, Livingstone, M.H. Ngoo, Dereje Shiferaw, & Peterson Hinga: Optimal Sizing of Grid-Connected Micro grid System using HOMER in Bahir Dar City, Ethiopia, International Journal of Power Systems <http://www.ias.org/ias/journals/ijps>, Volume 5, 2020

Mitchess, K., Nagrial, M. & Rizk, J (2006). Optimisation of Renewable Energy Systems presented at the ICREPQ.

Mitra I., and S. G. Chaudhuri, “Remote Village Electrification Plan through Renewable Energy in the Islands of Indian Sundarbans.” <https://www.homerenergy.com/webcast-downloads/ises-remic2-v2.pdf>, 2016.

Mubarick Issahaku, Adam Sandow Saani and Khadija Sarquah; “Feasibility Studies of a Grid-Connected Solar PV system for a Restaurant in Ghana using HOMER Pro” www.researchgate.net/publication/354153058, August 2021

Muljadi, E. & Bialasiewicz, J. T (2003). Hybrid power system with a controlled energy storage in The 29th Annual Conference of the IEEE Industrial Electronics Society,

Murthy, S. S., Mishra, S., Mallesham, G. & Sekhar, P. C (2010). Voltage and Frequency control of wind diesel hybrid system with variable speed wind turbine. IEEE Magazine 20-23.

Nagaraj, R (2012). Renewable energy based small hybrid power system for desalination applications in remote locations. IEEE 5th India International Conference on Power NASA meteorological and solar energy wave site. 2022

- NASA, Wind Research: International wind resource maps, 2004. Available from: [http://www.nret at. Gov/wind/international _wind _resources.html#ghana](http://www.nret.at.gov/wind/international_wind_resources.html#ghana).
- Nayar, C. V (2010). High Renewable Energy Penetration Diesel Generator systems electricalindia.[http://www.regenpower.com/images/cms/docs/SpecialDocs/1006_ Electrical pdf](http://www.regenpower.com/images/cms/docs/SpecialDocs/1006_Electrical.pdf)
- Norouzi, N., Alipour, M., & Alidoost, F., 2021. The Pahlev Reliability Index: A measurement for the resilience of power generation technologies versus climate change. *Nucl. Eng. Technol.* 2021, 53, 1658–1663. [CrossRef]
- Ntziachristos, L., Kouridis, C., Samaras, Z. & Pattas, K (2005). A wind-power fuel-cell hybrid system study on the non-interconnected Aegean islands grid. *Renewable Energy* 30, 1471–1487.
- Nurunnabi, M. & Roy, N. K (2015). “Grid connected hybrid power system design using HOMER. 2015 International Conference on Advances, Dhaka, pp. 18-21. of a hybrid solar PV-grid powered air-conditioner for daytime office use in hot humid climates—a case study in Kumasi city, Ghana *Solar energy*, 165, pages 65-74. doi: 10.1016/j.solener.2018.03.013.
- Opoku R., Mensah-Darkwa, K. and Samed Muntaka, A., 2018, Techno-economic analysis Organization for Economic Cooperation and Development. Renewable energy feed-in tariffs. <https://stats.oecd.org/Index.aspx> Data Set Code RE FIT, accessed 13 January 2020.
- Ozerdem, B. & Turkeli, H.M (2005). Wind energy potential estimation and micro sitting onIzmir Institute of Technology Campus Turkey, *Renewable Energy* 30, 1623–1633.

- Panickar, P. S., Rahman, S. & Islam, S. M (2001). A Neuro-Fuzzy Model for the Control Operation of a Wind-Diesel-Battery Hybrid Power System. Presented at the AUPEC, Perth, Australia.
- Papaefthymiou G, Dragoon K. Towards 100% renewable energy systems: uncapping power system flexibility. *Energy Policy* 2016; 92:69–82.
- Pawar, Nagorao; Nema, Pragma (2018). [IEEE 2018 IEEE International Conference on Computational Intelligence and Computing Research (ICCIC) - Madurai, India (2018.12.13-2018.12.15)]. Techno-Economic Performance Analysis of Grid Connected PV Solar Power Generation System Using HOMER Software
- Pena, R., Cardenas, R., Proboste, J., Clare, J. & Asher, G (2008). Wind-Diesel Generation Using Doubly Fed Induction Machines. *IEEE Transactions on Energy Conversion*, 23, 202-214.
- Poudineh, R., & Powell, D. (2017). The economics of energy storage and its integration with renewable energy. *Renewable and Sustainable Energy Reviews*, 76, 1054-1069. doi:10.1016/j.rser.2017.03.115.
- Public Utilities Regulatory Commission (2012). Feed-in tariffs. <http://www.purc.com.gh/>
- Public Utilities Regulatory Commission (PURC, 2021). Approved electricity and water tariffs for the year 2020. <http://www.purc.com.gh>, accessed 9th August 2022. Time: 3:51am purc/node/193, accessed 23 January 2021
- Quansah, D., Adaramola, M. and Anto, E. 2017. Cost-competitiveness of distributed grid-connected solar photovoltaics in Ghana: case study of a 4kWp polycrystalline system. *Clean Technology Environmental Policy*, 19(10), pages 2,431-2,442. doi: 1007/s10098-017-1432-z.

- Rajoriya A., and E. Fernandez, “Sustainable Energy Generation using Hybrid Energy System for Remote Hilly Rural Area in India,” *International Journal of Sustainable*
- Razak, N. A., Othman, M. M. & Musirin, I (2010). Optimal sizing and operational strategy of hybrid renewable energy system using homer.2010 4th International Power Engineering and Optimization Conference (PEOCO), Shah Alam, 495-501.
- Regen Power Pty. Ltd (2010). Hybrid renewable energy penetration micro-grid power system using a variable speed constant frequency generator. Available from: <http://www.dailylife.com.sg/HybridGen%20Writeup%20ver3.pdf>
- Rehman S., I. Amin, F. Ahmad, S. Shaahid, and A. M. Shehri, “Feasibility study of hybrid retrofits to an isolated off-grid diesel power plant,” *Renewable and Sustainable Energy Reviews*, vol. 11, no. 4, pp. 635–653, 2007.
- Riayatsyah T. M. I, T. A. Geumpana, I. M. Rizwanul Fattah, Samsul Rizal and T. M. Indra Mahlia “Techno-Economic Analysis and Optimisation of Campus Grid-Connected Hybrid Renewable Energy System Using HOMER Grid” *Sustainability* 2022, 14, 7735. <https://doi.org/10.3390/su14137735>.
- Rilwan Usman, Adamu Gidado (2017) “Feasibility analysis of a grid connected pv/wind options for rural healthcare centre using homer” *European Journal of Engineering and Technology* Vol. 5 No. 3, 2017 ISSN 2056-586
- Ruther, R., Schmid, A. L., Beyer, H. G., Montenegro, A. A. & Oliveira, H. F (2003). Cutting on diesel, boosting PV: the potential of hybrid diesel/PV systems in existing mini-grids in the Brazilian Amazon. In 3rd World Conference on Photovoltaic Energy Conversion, 2620-2623.

- Sawle Yashwant, S.C. Gupta and Aashish Kumar Bohre ‘PV-wind hybrid system: A review with case study. Cogent Engineering (2016), 3: 1189305
<http://dx.doi.org/10.1080/23311916.2016.1189305>.
- Sedghi, M. & Ahmadian, A., (2016). Student Member, IEEE, and Masoud Aliakbar-Golkar. Optimal Storage Planning in Active Distribution Network Considering Uncertainty of Wind Power Distributed Generation.
- Setiawan, A. A (2009). Development of a modular AC coupling minigrid hybrid system for sustainable power supply in remote areas and disaster response and reconstruction. Electrical and Computer Engineering, Curtin University of Technology.
- Shalchi, A., & Guerrero, J. M. (2011). Overview of control and grid synchronization for distributed power generation systems. IEEE Transactions on Industrial Electronics, 58(4), 1239-1250.
- Shantu Ghose, Adel El Shahat, Rami J. Haddad. “Wind-Solar Hybrid Power System Cost Analysis using HOMER for Statesboro, Georgia” 978-1-5386-1539-3/17/US\$31.00 ©2017 IEEE.
- Singh B., “Control Strategies for DFIG Based Grid Connected Wind Energy Conversion System,” International Journal of Grid Distribution Computing, vol. 7, pp. 49–60, 2014.
- Stern, N. (2006). The Economics of Climate Change: The Stern Review. Cambridge University Press.
- Suresh G., “Photovoltaic based flexible microgrid,” Int. J. Multidiscip. Res. Mod. Educ., vol. II, no. II, pp. 535–544, 2016.

Tarman, P. B (1996). Fuel cells for distributed power generation. *Journal of Power Sources*, 61(1), 87-89.

The Organisation for Economic Co-operation and Development (OECD 18) Taxing Energy use for sustainable development. <https://www.oecd.org/tax/tax-policy/taxing-energy-use-ghana.pdf>

Türkyay B.E., and A. Y. Telli, “Economic Analysis of Stand-alone and Grid Connected Hybrid Energy Systems,” *Renewable Energy Science Direct*, vol. 36, pp. 1931 - 1943, 2011.

US Department of Energy. "Microgrid." (2021). Available at: <https://www.energy.gov/eere/technology-to-market/microgrid>.

Uyterlined, M.A., van-Sambeek, E.J.W. & Cross, E.D (2002). Decentralised Generation: Development of Eu Policy Energy Research Centre of the Netherlands, 10, 9-69.

Vania, N. & Kharea, V (2013). Rural Electrification System based on Hybrid Energy System Model Optimization using HOMER. *CJBAS*, 01(01), 19-25.

Varying Climatic Conditions’ *FME Transactions* (2016) VOL.44, 71-82

Vukman V. Bakić, Milada L. Pezo, Saša M. Stojković. ‘Technical and Economic Analysis of Grid-Connected PV/Wind Energy Stations in the Republic of Serbia Under

Wichert, B (2000). Control of photovoltaic-diesel hybrid energy systems. PhD, Dept. Elect. & Comp. Eng., Curtin University of Technology, Perth.

Wilkins Engineering Ltd. <http://www.shop.wilkinsengineering.com>. Assessed 11th August 2022. 5:25pm.

www.welshenergysectortraining.org/renewable%20energy%20Swansea.ppt.

- Xu L., X Ruan, A., Mao, C. & Zhang, B (2013). An improved optimal sizing method for wind-solar-battery hybrid power system. *IEEE Trans. Sustainable Energy*, 4(3), 774-785.
- Yamegueu, D., Azoumah, Y., Py, X. & Zongo, N (2011). Experimental study of electricity generation by Solar PV/diesel hybrid systems without battery storage for off-grid areas. *Renewable Energy*, 36, 1780-1787.
- Yanning, Z., Longyun, K., Binggang, C., Chung-Neng, H. & Guohong, W. (2009). Renewable energy distributed power system with wind power and biogas generator. *EEE Transmission & Distribution Conference & Exposition: Asia and Pacific*, 1-6.
- Zeng, L., Long, Q., & Fang, Y. (2019). Energy storage systems for renewable energy integration: A review of key issues and future directions. *Renewable and Sustainable Energy Reviews*, 106, 355-370. doi:10.1016/j.rser.2018.12.001
- Zhang, X., & Liu, X. (2015). Converter technology in grid-connected photovoltaic power systems. *Renewable and Sustainable Energy Reviews*, 43, 785-798. <https://doi.org/10.1016/j.rser.2014.10.047>.

APPENDICES

60Appendix A: Table of sourced load profile of chosen health institution

ELECTRICAL APPLIANCES	POWER (W)	QTY	TOTAL POWER	TIME OF USAGE	USAGE HOURS	ENERGY	LOAD kWh/d	kWh
A. ADMINISTRATION BLOCK								
Panel Light	12	4	48	08:00-16:00	8	384	0.384	0.048
Panel Light	24	4	96	08:00-16:00	8	768	0.768	0.096
Ceiling Fan	80	6	480	08:00-16:00	8	3840	3.84	0.48
Air Conditioner (1.5Hp)	1119	5	5595	08:00-16:00	8	44760	44.76	5.595
Desktop Computers	200	4	800	08:00-17:00	9	7200	7.2	0.8
Printer (Printer & Scanner)	50	3	150	08:00-13:00	5	750	0.75	0.15
Photocopier	183	3	549	09:00-12:00	3	1647	1.60	0.549
Fridge (Table top)	100	4	400	00:00-23:00	24	9600	9.6	0.4
Money Counter	80	1	80	08:00-17:00	9	720	0.72	0.08
Laptop Computer	50	2	100	09:00-14:00	5	500	0.5	0.1
							70.089	
B. MEDICAL STORES								
Panel Light	24	4	96	08:00-15:00	7	672	0.672	0.096
LED bulb	15	2	30	08:00-16:00	8	240	0.24	0.03
Air Conditioner (2.5Hp)	1492	2	2984	00:00-23:00	24	71616	71.616	2.984
Air Conditioner (1.5Hp)	1119	1	1119	08:00-15:00	7	7833	7.833	1.119
32 Inches Television	28	1	28	08:00-16:00	8	224	0.224	0.028

Fridge (Double Door)	150	1	150	00:00-23:00	24	3600	3.6	0.15
Fridge (Table Top)	100	1	100	00:00-23:00	24	2400	2.4	0.1
Ceiling Fan	80	2	160	08:00-16:00	8	1280	1.28	0.16

87.865**C. PHARMACY**

Panel Light	12	4	48	00:00-23:00	24	1152	1.152	0.048
Ceiling Fan	80	3	240	08:00-18:00	10	2400	2.4	0.24
Air Conditioner (2.5Hp)	1492	3	4476	08:00-18:00	10	44760	44.76	4.476
Air Conditioner (1.5Hp)	1119	1	1119	00:00-23:00	24	26856	26.856	1.119
32 Inches Television	28	1	28	08:00-22:00	14	392	0.392	0.028
Desktop Computers	200	5	1000	08:00-22:00	14	14000	14	1
Laptop Computer	50	3	150	08:00-17:00	9	1350	1.35	0.15

90.91**D. REPRODUCTION AND CHILD HEALTH (RCH)**

LED bulb	40	8	320	08:00-15:00	7	2240	2.24	0.32
LED bulb	15	1	15	08:00-16:00	8	120	0.12	0.015
Ceiling Fan	80	3	240	08:00-15:00	7	1680	1.68	0.24
Air Conditioner (1.5Hp)	1119	1	1119	08:00-14:00	6	6714	6.714	1.119
32 Inches Television	28	1	28	08:00-15:00	7	196	0.196	0.028
Desktop Computers	200	1	200	08:00-15:00	7	1400	1.4	0.2

12.350**E. OUT PATIENT DEPARTMENT (OPD)**

LED bulb	40	23	920	00:00-23:00	24	22080	22.08	0.92
Ceiling Fan	80	12	960	08:00-22:00	14	13440	13.44	0.96
32 Inches Television	28	2	56	08:00-22:00	14	784	0.784	0.056
Air Conditioner (2.5Hp)	1492	3	4476	08:00-20:00	12	53712	53.712	4.476
Fridge (Table Top)	100	1	100	00:00-23:00	24	2400	2.4	0.1

Desktop Computers	200	5	1000	00:00-23:00	24	24000	24	1
Ceiling Fan (Short blade)	40	1	40	08:00-22:00	14	560	0.56	0.04
Door Bell	1300	2	2600	00:00-20:00	20	52000	52	2.6

168.976**F. EMERGENCY WARDS**

LED bulb	40	6	240	00:00-23:00	24	5760	5.76	0.24
Ceiling Fan	80	1	80	08:00-16:00	8	640	0.64	0.08
Ceiling Fan (Short blade)	40	1	40	08:00-16:00	8	320	0.32	0.04
Desktop Computers	60	2	120	00:00-23:00	24	2880	2.88	0.12
Air Conditioner (2.5Hp)	1492	1	1492	08:00-16:00	8	11936	11.936	1.492
Fridge (Table Top)	100	1	100	00:00-23:00	24	2400	2.4	0.1
32 Inches Television	28	1	28	00:00-23:00	24	672	0.672	0.028
Big Wall Fan	690	3	2070	00:00-21:00	22	45540	45.54	2.07

70.148**G. RECORDS DEPARTMENT**

LED bulb	40	4	160	08:00-15:00	7	1120	1.12	0.16
Ceiling Fan	80	2	160	08:00-15:00	7	1120	1.12	0.16
Air Conditioner (1.5Hp)	1119	1	1119	08:00-16:00	8	8952	8.952	1.119
Desktop Computers	200	5	1000	08:00-22:00	14	14000	14	1
Laptop Computer	50	1	50	08:00-16:00	8	400	0.4	0.05
Lamination Machine	600	1	600	08:00-18:00	10	6000	6	0.6
Fridge (Table Top)	100	1	100	00:00-23:00	24	2400	2.4	0.1
Air Conditioner (2.5Hp)	1492	3	4476	08:00-20:00	12	53712	53.712	4.476
32 Inches Television	28	2	56	08:00-22:00	14	784	0.784	0.056

88.488**H. MALE WARD**

LED bulb	40	5	200	00:00-23:00	24	4800	4.8	0.2
----------	----	---	-----	-------------	----	------	-----	-----

LED bulb	15	6	90	00:00-23:00	24	2160	2.16	0.09
Ceiling Fan	80	1	80	08:00-20:00	12	960	0.96	0.08
Air Conditioner (2.5Hp)	1492	2	2984	08:00-16:00	8	23872	23.872	2.984
Desktop Computers	200	1	200	08:00-22:00	14	2800	2.8	0.2
Fridge (Table Top)	100	1	100	00:00-23:00	24	2400	2.4	0.1
Ceiling Fan (Short blade)	40	1	40	08:00-20:00	12	480	0.48	0.04

37.472**I. FEMALE WARD**

LED bulb	40	5	200	00:00-23:00	24	4800	4.8	0.2
LED bulb	15	6	90	00:00-23:00	24	2160	2.16	0.09
Ceiling Fan	80	4	320	08:00-20:00	12	3840	3.84	0.32
Desktop Computers	200	1	200	08:00-22:00	14	2800	2.8	0.2
Fridge (Table Top)	100	1	100	00:00-23:00	24	2400	2.4	0.1
32 Inches Television	28	2	56	08:00-21:00	13	728	0.728	0.056

16.728**J. EYE & ANTENENTAL CLINIC (ANC)**

LED bulb	40	13	520	08:00-16:00	8	4160	4.16	0.52
LED bulb	15	4	60	08:00-20:00	12	720	0.72	0.06
Ceiling Fan	80	16	1280	08:00-16:00	8	10240	10.24	1.28
Fridge (Table Top)	100	3	300	00:00-23:00	24	7200	7.2	0.3
Desktop Computers	200	5	1000	08:00-16:00	8	8000	8	1
Air Conditioner (1.5Hp)	1119	1	1119	08:00-16:00	8	8952	8.952	1.119
Ceiling Fan (Short blade)	40	2	80	08:00-22:00	14	1120	1.12	0.08
32 Inches Television	28	1	28	08:00-16:00	8	224	0.224	0.028
Snellen Chart	220	1	220	08:00-17:00	9	1980	1.98	0.22

42.596

K. LABORATORY								
LED bulb	40	4	160	18:00-06:00	12	1920	1.92	0.16
LED bulb	15	3	45	00:00-23:00	24	1080	1.08	0.045
Ceiling Fan	80	4	320	08:00-15:00	7	2240	2.24	0.32
Desktop Computers	200	4	800	08:00-17:00	9	7200	7.2	0.8
Air Conditioner (2.5Hp)	1492	1	1492	00:00-23:00	24	35808	35.808	1.492
Deep Freezer	1000	1	1000	00:00-23:00	24	24000	24	1
32 Inches Television	28	1	28	08:00-15:00	7	196	0.196	0.028
Chemistry Analyser	100	1	100	00:00-23:00	24	2400	2.4	0.1
GeneXpert Analyser	150	1	150	00:00-23:00	24	3600	3.6	0.15
Glove box	500	1	500	08:00-17:00	9	4500	4.5	0.5
Glycated Machine	500	1	500	08:00-17:00	9	4500	4.5	0.5
Haematology Analyser	450	1	450	08:00-17:00	9	4050	4.05	0.45
Blood Roller	680	2	1360	08:00-17:00	9	12240	12.240	0.68
Hot air Oven	250	1	250	08:00-23:00	24	6000	6	0.25
Centrifuge	500	1	500	00:00-23:00	24	12000	12	0.5
Electrophoresis Tank	500	1	500	00:00-23:00	24	12000	12	0.5
Microscope	120	2	240	08:00-23:00	15	3600	3.6	0.24
Water bath	450	1	450	08:00-17:00	9	4050	4.05	0.45
Electrolyte Analyser	60	1	60	00:00-23:00	24	1440	1.44	0.06
UPS	3500	1	3500	00:00-23:00	24	84000	84	3.5
							226.704	
L. SCAN & DENTAL UNIT								
LED bulb	40	4	160	08:00-16:00	8	1280	1.28	0.16
LED bulb	15	5	75	08:00-15:00	7	525	0.525	0.075
Ceiling Fan	80	3	240	08:00-16:00	8	1920	1.92	0.24
Air Conditioner (1.5Hp)	1119	2	2238	08:00-15:00	7	15666	15.666	2.238

Air Conditioner (2.5Hp)	1492	1	1492	08:00-15:00	7	10444	10.444	1.492
Desktop Computers	200	2	400	08:00-15:00	7	2800	2.8	0.4
Mindray	8000	1	8000	08:00-16:00	8	64000	64	8
Air Compressor	4950	1	4950	08:00-16:00	8	39600	39.6	4.95
Auto Clave	6000	2	12000	08:00-16:00	8	96000	96	12
Dental Chair	3000	1	3000	08:00-16:00	8	24000	24	3
Microwave	600	1	600	08:00-12:00	4	2400	2.4	0.6
Distiller	3000	1	3000	08:00-14:00	6	18000	18	3
Fridge (Table Top)	100	2	200	00:00-23:00	24	4800	4.8	0.2
Ceiling Fan (Short blade)	40	1	40	08:00-16:00	8	320	0.32	0.04
X-Ray Machine	2500	1	2500	08:00-17:00	9	22500	22.5	2.5

304.255**M. MATERNITY WARD**

Panel Light	12	12	144	00:00-23:00	24	3456	3.456	0.144
LED bulb	15	5	75	08:00-15:00	7	525	0.525	0.075
Ceiling Fan	80	8	640	00:00-23:00	24	15360	15.36	0.64
32 Inches Television	28	1	28	08:00-22:00	14	392	0.392	0.028
Fridge	1000	1	1000	00:00-23:00	24	24000	24	1
Air Conditioner (1.5Hp)	1119	1	1119	08:00-20:00	12	13428	13.428	1.119
Desktop Computers	200	1	200	00:00-23:00	24	4800	4.8	0.2
Panel Light	24	5	120	00:00-23:00	24	2880	2.88	0.12
Pressing Iron	1000	2	2000	08:00-10:00	2	4000	4	2

68.841**Polyclinic Total Load (A+B+C+D+E+F+G+H+I+J+K+L+M)****1,284.822**

Appendix B: Summary of cost and savings, Economic metrics and Environmental impact of Optimized systems

	Base Case	Solar + Wind + Storage: LI ASM + GRID	Solar + Wind + GRID	Solar + Storage: LI ASM + GRID	Solar + GRID	Wind + Storage: LI ASM + GRID
Costs and Savings						
CAPEX	US\$0	US\$1,849,194	US\$1,591,066	US\$1,843,123	US\$1,540,269	US\$1,916,466
OPEX	US\$213,440	US\$38,070	US\$52,484	US\$48,363	US\$64,594	US\$78,291
Annual Total Savings (US\$)	US\$0	US\$175,370	US\$160,956	US\$165,077	US\$148,846	US\$135,149
Annual Utility Bill Savings (US\$)	US\$0	US\$196,061	US\$174,810	US\$190,238	US\$162,197	US\$156,576
Annual Demand Charges (US\$/yr.)	US\$1,215/yr.	US\$871/yr.	US\$928/yr.	US\$857/yr.	US\$916/yr.	US\$1,151/yr.
Annual Energy Charges (US\$/yr.)	US\$212,225/yr.	US\$16,508/yr.	US\$37,702/yr.	US\$22,344/yr.	US\$50,327/yr.	US\$55,712/yr.
Economic Metrics						
Discounted payback time (yrs.)		9.3	8.9	9.3	9	13
Simple payback time (yrs.)		10.3	9.8	10.3	10	17.1
LCOE (US\$/kWh)	US\$0.241/kWh	US\$0.093/kWh	US\$0.088/kWh	US\$0.106/kWh	US\$0.094/kWh	US\$0.116/kWh
IRR %		7.87%	8.72%	7.44%	8.36%	4.31%
Net Present Cost (US\$)	US\$7,004,608	US\$3,098,562	US\$3,313,462	US\$3,430,276	US\$3,660,097	US\$4,485,805
Environmental Impact						
CO ₂ Emissions* (metric ton/yr.)	558.8 t/yr.	70.0 t/yr.	162.6 t/yr.	83.8 t/yr.	210.3 t/yr.	212.6 t/yr.

Appendix C: HOMER Grid Electric load setup window

Electric Load (X)

Name:

Year to model: 2021

January Profile:

Hour	Load (kW)
0	18.550
1	23.220
2	23.220
3	23.220
4	23.220
5	23.220
6	23.220

Show All Months...

Daily Profile

Time step size: 60 minutes Peak month: None Crest factor: 2.58

Random Variability:
 Day-to-day (%): Timestep (%):


Load Metrics:

Metric	Baseline	Scaled
Average (kWh/day)	1,284.8	2,422.3
Average(kW)	53.53	100.93
Peak (kW)	170.48	321.42
Load factor	.31	.31

System Diagram:

AC: GRID, Primary Load (2422.37 kWh/d, 321.42 kW peak), Jin310
 DC: EOXM21, Youn250, LI ASM
 Search Space, Sensitivity

Appendix D: ECG bill for the month of September 2021



ELECTRICITY COMPANY OF GHANA LIMITED
 VAT REG: 714 V 000395
 P.O. Box GP 521
 Accra, Ghana
 PHONE: 0302-611611
 WEB: <http://www.ecggh.com/>
 EMAIL: ecgho@ghana.com

Electricity bill Period: 29 Days Page 1 of 1
 Reading cycle
 Bill Number: 2006919680843
 Bill Date: 04/10/2021 Month: Sep 2021
 Due Date: 18/10/2021 (Pay by this date to avoid disconnection)
 Tariff: E02 - Non Residential (postpaid)
 Contracted Demand(KVA) 3.6

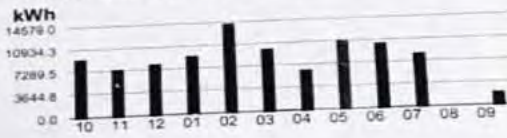
Customer Information

Recipient Name: KASOA HEALTH CENT
 Digital Address: 00-000-0000
 Delivery Address: Street 1 - Kasoa South - WALENTU, WALENTU, KASOA SOUTH CENTRAL

Meter Number: 15325885
 Account Number: 706364421
 Customer Name: KASOA HEALTH CENT
 Service Address: Street 1 - Kasoa South - WALENTU WALENTU, KASOA SOUTH CENTRAL

Consumption History (12 months)

Geographical Code: 08-10-828-075-245-2290
 Issuing Center: Kasoa South District



Meter No.	Energy type	From	To	Previous Reading	Current Reading	Diff.	Multiplier	Consumption	E/A
15325885	Active energy (kWh)	12/08/2021	10/09/2021	227347	229550	2203	1.00	2203	A

Calculation Information


Additional information	From	To	Item	Units	Price	Amount
	13/08/2021	10/09/2021	Energy first threshold (EFT)	286 kWh	0.7979	228.20
	13/08/2021	10/09/2021	Energy second threshold (EST)	286 kWh	0.8491	242.84
	13/08/2021	10/09/2021	Energy third threshold (ETT)	1631 kWh	1.3398	2,185.21
	13/08/2021	10/09/2021	Service Charge	29 days	0.4086	11.85
	13/08/2021	10/09/2021	National Electrification Levy	2656.25Ghc	0.0200	53.13
	13/08/2021	10/09/2021	Street Light	2656.25Ghc	0.0300	79.69
	13/08/2021	10/09/2021	VAT	2668.10Ghc	0.1250	333.51
	13/08/2021	10/09/2021	NHL & GETFUND	2668.10Ghc	0.0500	133.41


Current Bill:	3,267.84
Previous Balance:	302,927.08
Amount Payable:	306,194.92

Payment Information. Last payment date: 10/03/2020 and Payment Amount: 358,530.65

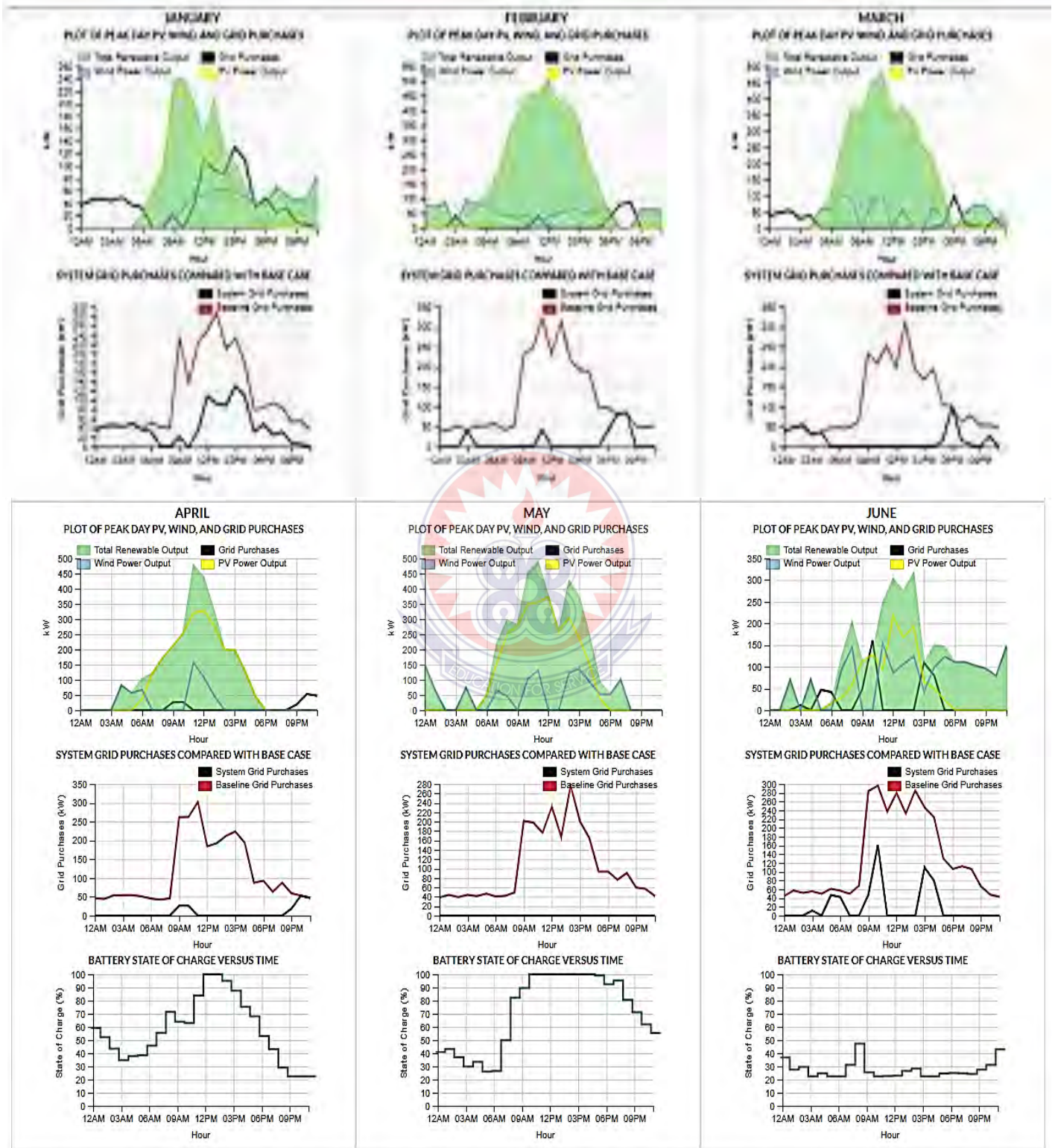
Please See Over

Customer Name: KASOA HEALTH CENT
 Bill Date: 04/10/2021
 Account No: 706364421
 Bill No: 2006919680843
 Amount Payable: 306194.92

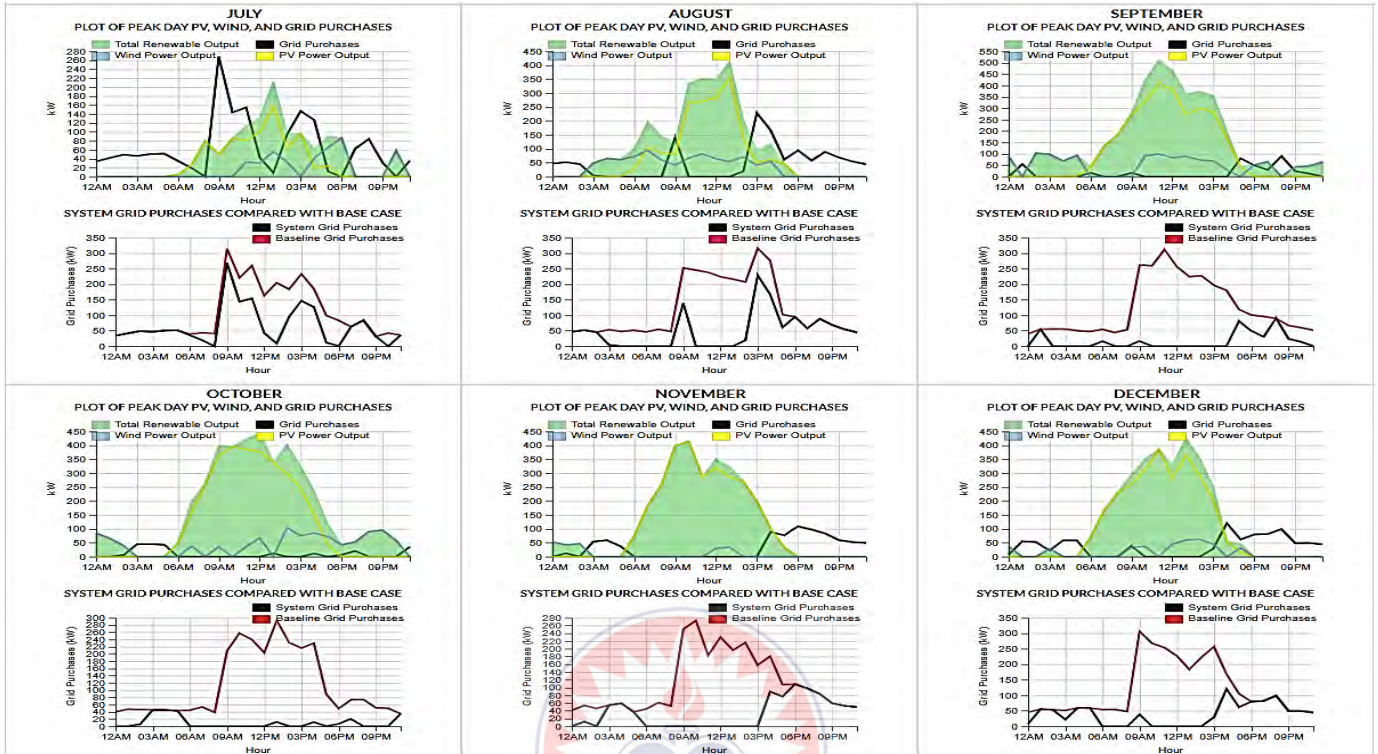




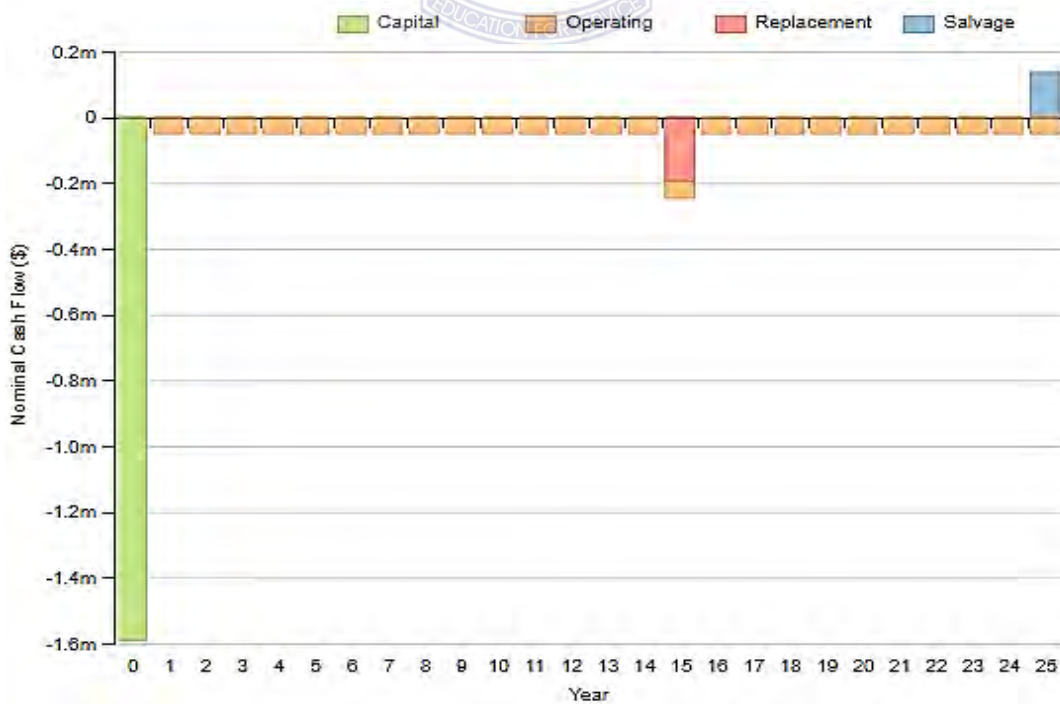
Appendix E: Case 2 system performance summary



Appendix E: Case 2 system performance (continuation)

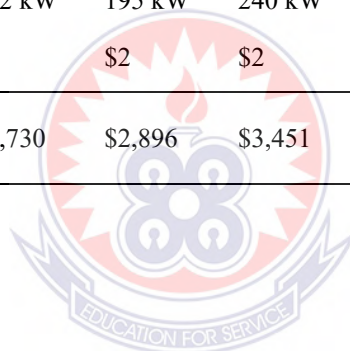


Cash flow summary for Case 2



Appendix F: Case 2 monthly bills (Predicted)

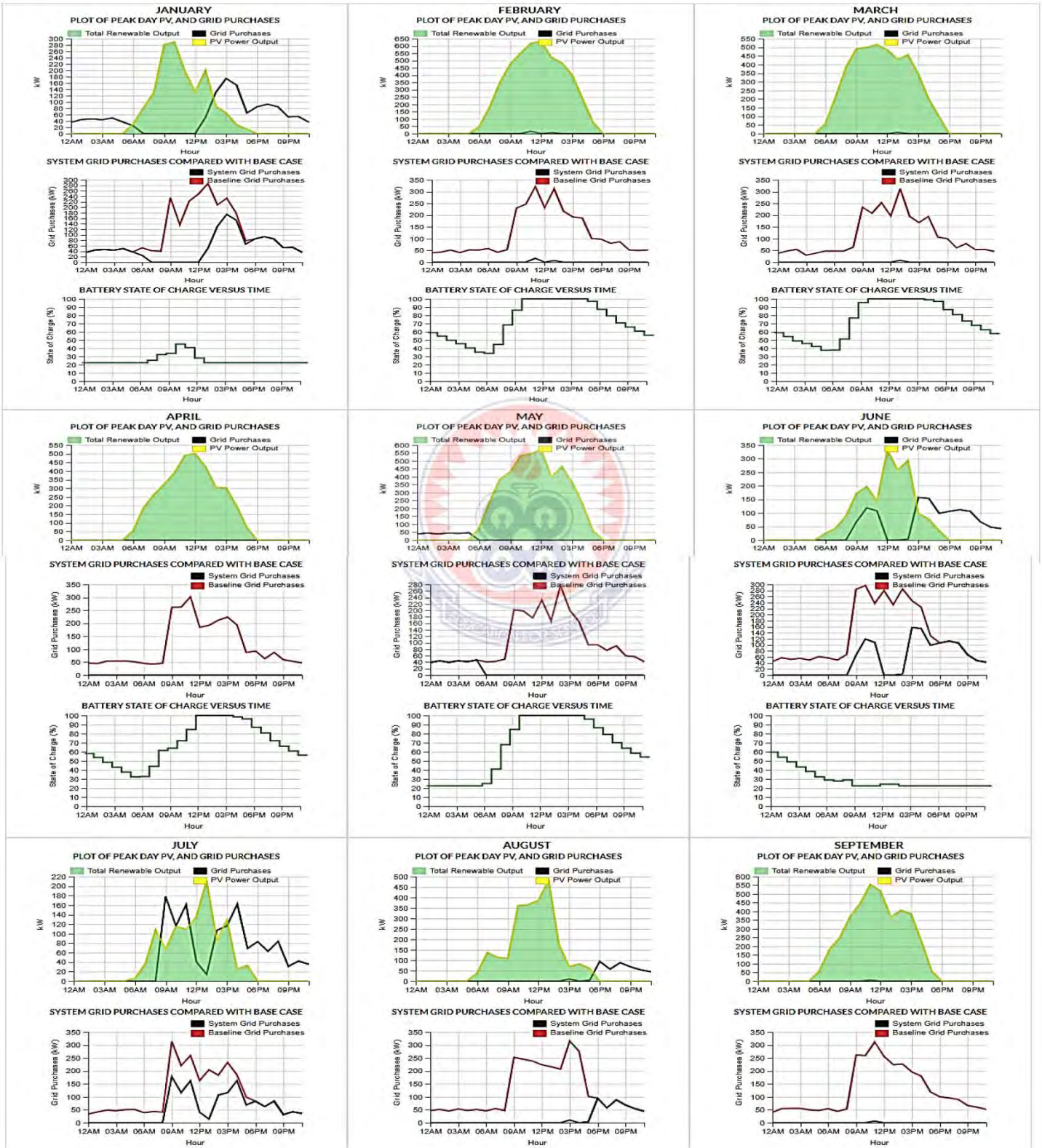
	Jan	Feb	Mar	Apr	May	June	July	Aug	Sep	Oct	Nov	Dec
Energy Charges	\$3,278	\$2,144	\$2,748	\$2,652	\$2,822	\$3,367	\$2,742	\$3,730	\$3,496	\$3,007	\$3,835	\$3,855
Cosumption	23,417 kWh	15,313 kWh	19,629 kWh	18,946 kWh	20,155 kWh	21,980 kWh	19,588 kWh	24,337 kWh	23,222 kWh	21,480 kWh	24,930 kWh	24,232 kWh
Sales	23,508 kWh	21,756 kWh	23,608 kWh	24,766 kWh	22,341 kWh	19,083 kWh	20,950 kWh	21,109 kWh	20,775 kWh	22,380 kWh	21,479 kWh	19,613 kWh
Demand Charges	\$84	\$76	\$64	\$76	\$72	\$82	\$89	\$82	\$83	\$69	\$80	\$71
Peak Demand	250 kW	212 kW	163 kW	212 kW	195 kW	240 kW	269 kW	241 kW	244 kW	185 kW	231 kW	194 kW
Fixed charges (\$)	\$2	\$2	\$2	\$2	\$2	\$2	\$2	\$2	\$2	\$2	\$2	\$2
Monthly Total	\$3,365	\$2,222	\$2,814	\$2,730	\$2,896	\$3,451	\$2,833	\$3,814	\$3,581	\$3,079	\$3,917	\$3,928
Annual Total	\$38,630											



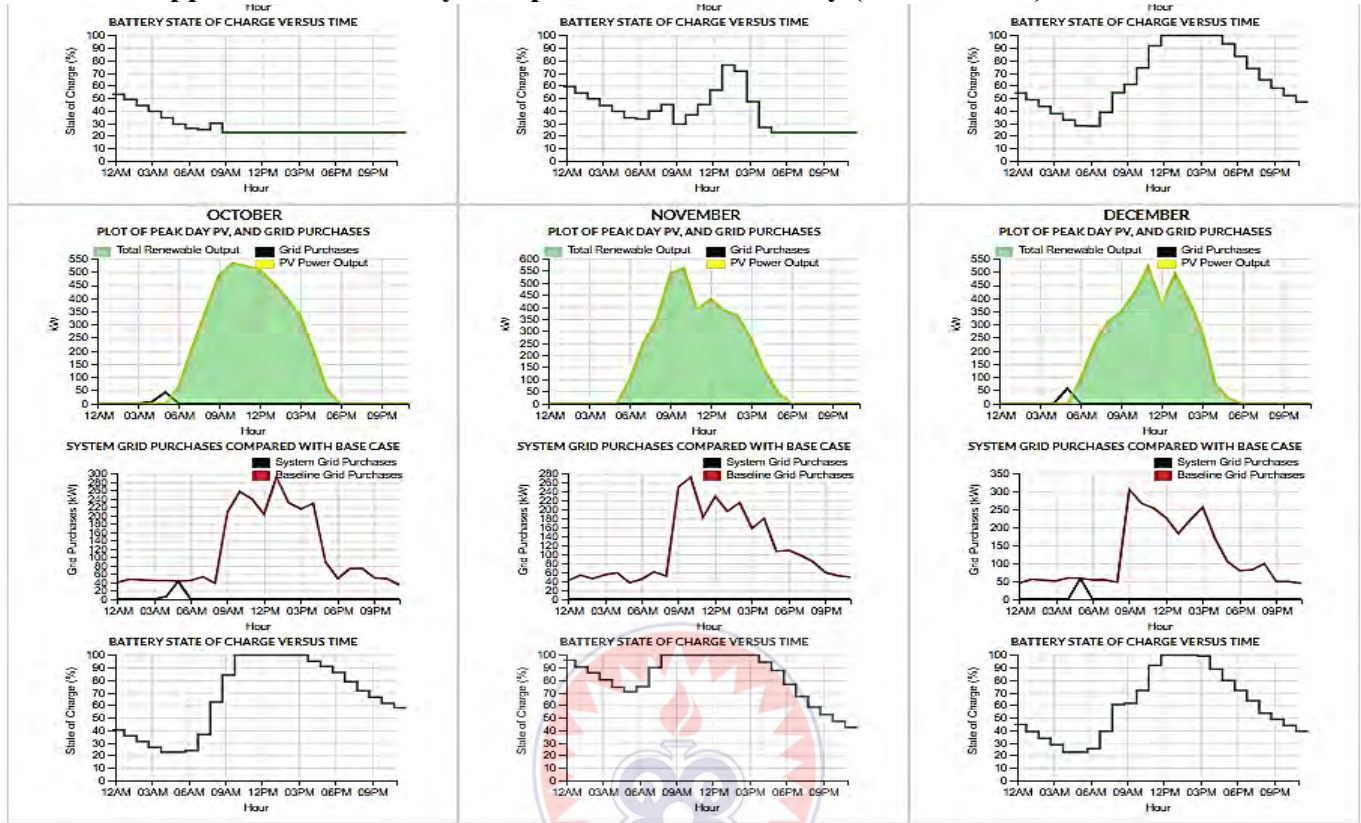
Case 2 monthly carbon dioxide emissions

	Jan	Feb	Mar	Apr	May	June	July	Aug	Sep	Oct	Nov	Dec
Monthly Total (metric tons)	15 t	9.7 t	12 t	12 t	13 t	14 t	12 t	15 t	15 t	14 t	16 t	15 t
Annual Total (metric tons)	163 t/yr.											

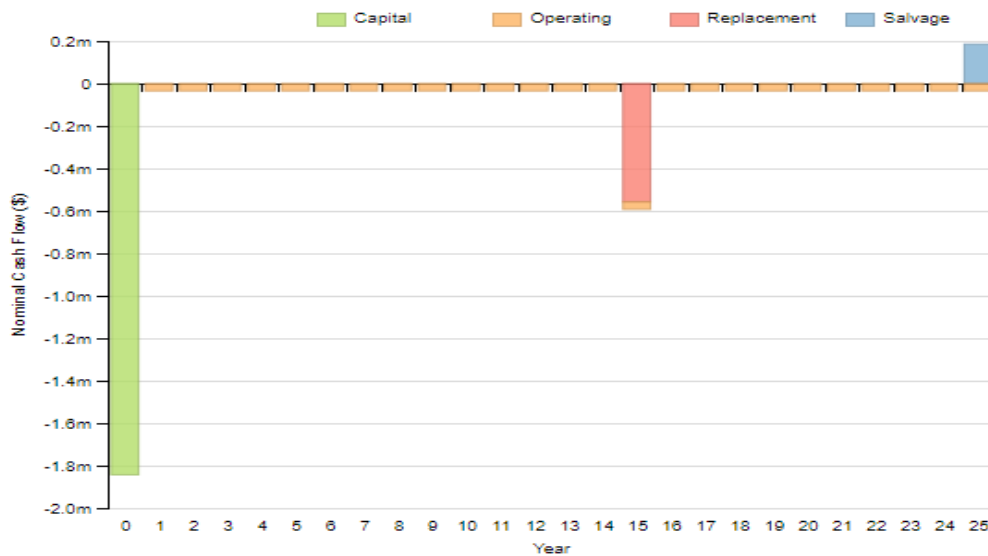
Appendix G: Case 3 system performance summary



Appendix G: Case 3 system performance summary (continuation)



Cash flow summary for Case 3



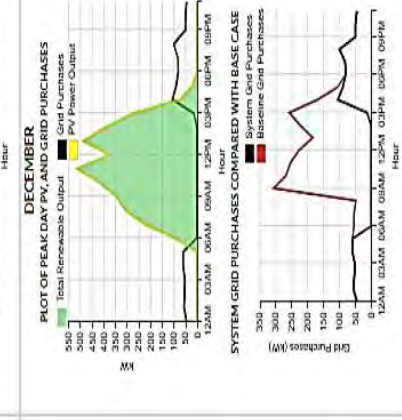
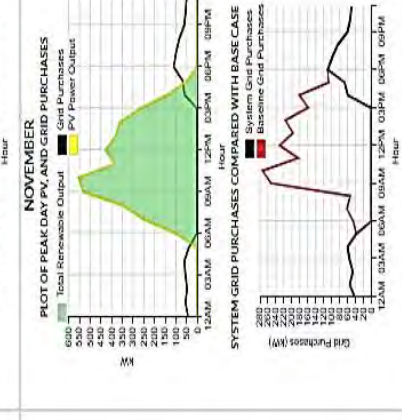
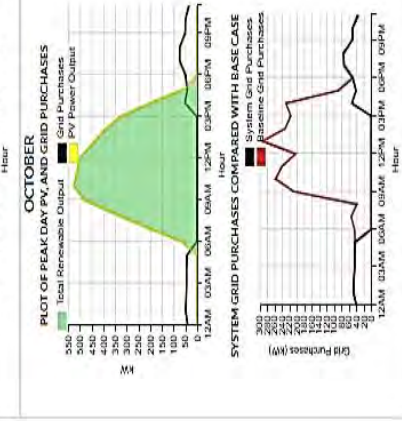
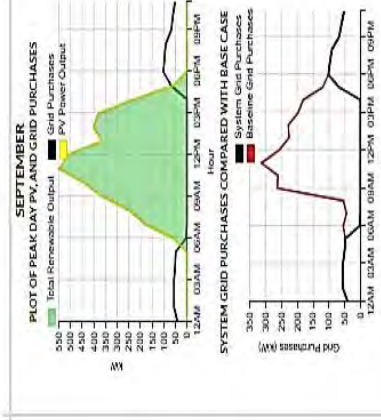
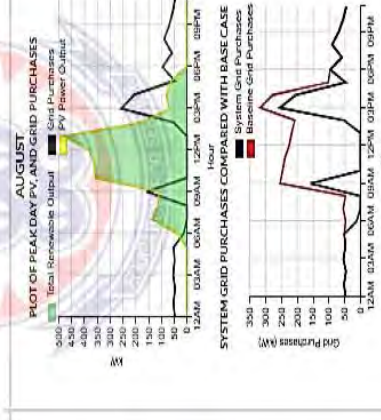
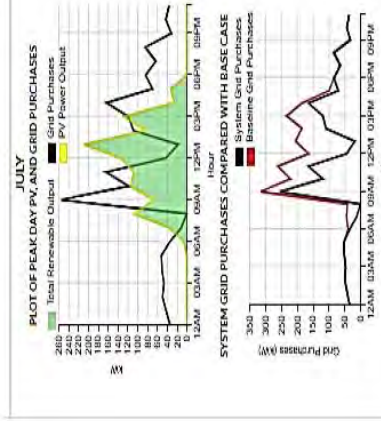
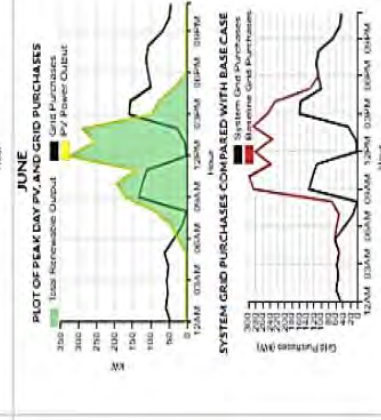
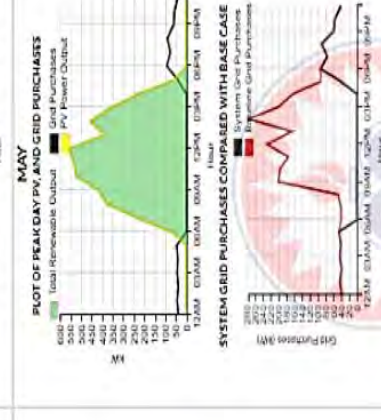
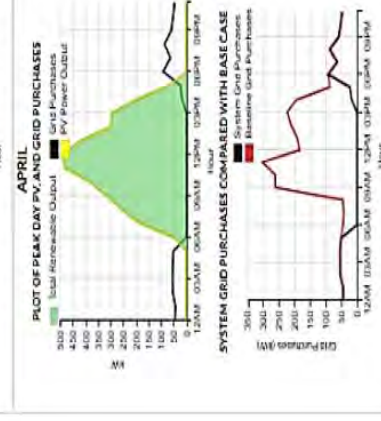
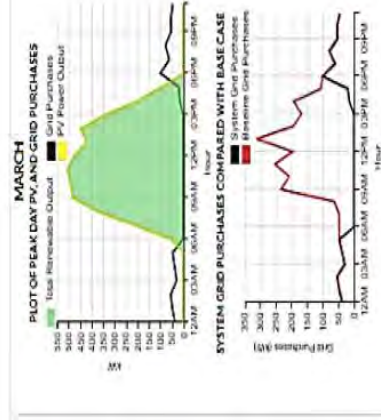
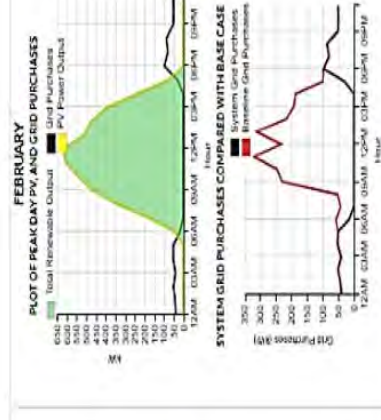
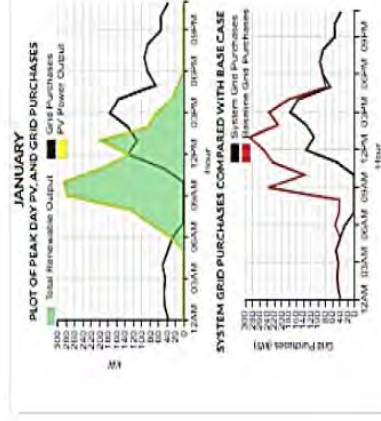
Appendix H: Case 3 monthly bills (Predicted)

	Jan	Feb	Mar	Apr	May	June	July	Aug	Sep	Oct	Nov	Dec
Energy Charges	\$1,364	\$808	\$1,422	\$782	\$1,330	\$2,929	\$2,336	\$3,574	\$3,322	\$1,324	\$1,703	\$1,426
Cosumption	9,743 kWh	5,768 kWh	9,874 kWh	5,589 kWh	9,000 kWh	14,632 kWh	12,457 kWh	17,323 kWh	16,865 kWh	9,454 kWh	11,719 kWh	10,188 kWh
Sales	10,791 kWh	10,142 kWh	9,474 kWh	8,859 kWh	8,303 kWh	5,829 kWh	6,538 kWh	5,836 kWh	7,254 kWh	9,512 kWh	11,100 kWh	10,716 kWh
Demand Charges	\$67	\$64	\$70	\$79	\$68	\$78	\$67	\$77	\$79	\$64	\$75	\$68
Peak Demand	187 kW	175 kW	200 kW	241 kW	190 kW	234 kW	185 kW	231 kW	239 kW	175 kW	223 kW	193 kW
Fixed charges (\$)	\$2	\$2	\$2	\$2	\$2	\$2	\$2	\$2	\$2	\$2	\$2	\$2
Monthly Total	\$1,433	\$874	\$1,495	\$864	\$1,400	\$3,009	\$2,405	\$3,653	\$3,403	\$1,390	\$1,780	\$1,497
Annual Total	\$23,202											

Case 3 monthly carbon dioxide emissions

	Jan	Feb	Mar	Apr	May	June	July	Aug	Sep	Oct	Nov	Dec
Monthly Total (metric tons)	6.2 t	3.6 t	6.2 t	3.5 t	5.7 t	9.2 t	7.9 t	11 t	11 t	6 t	7.4 t	6.4 t
Annual Total (metric tons)	83.8 t/yr											

Appendix I: Case 4 system performance summary

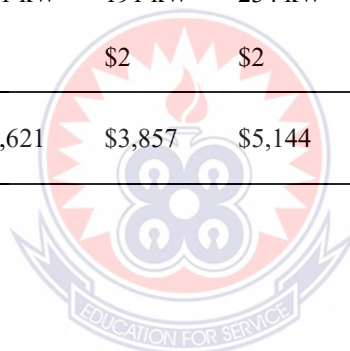


Appendix I (continuation) Cash flow summary for Case 4



Appendix J: Case 4 monthly bills (predicted)

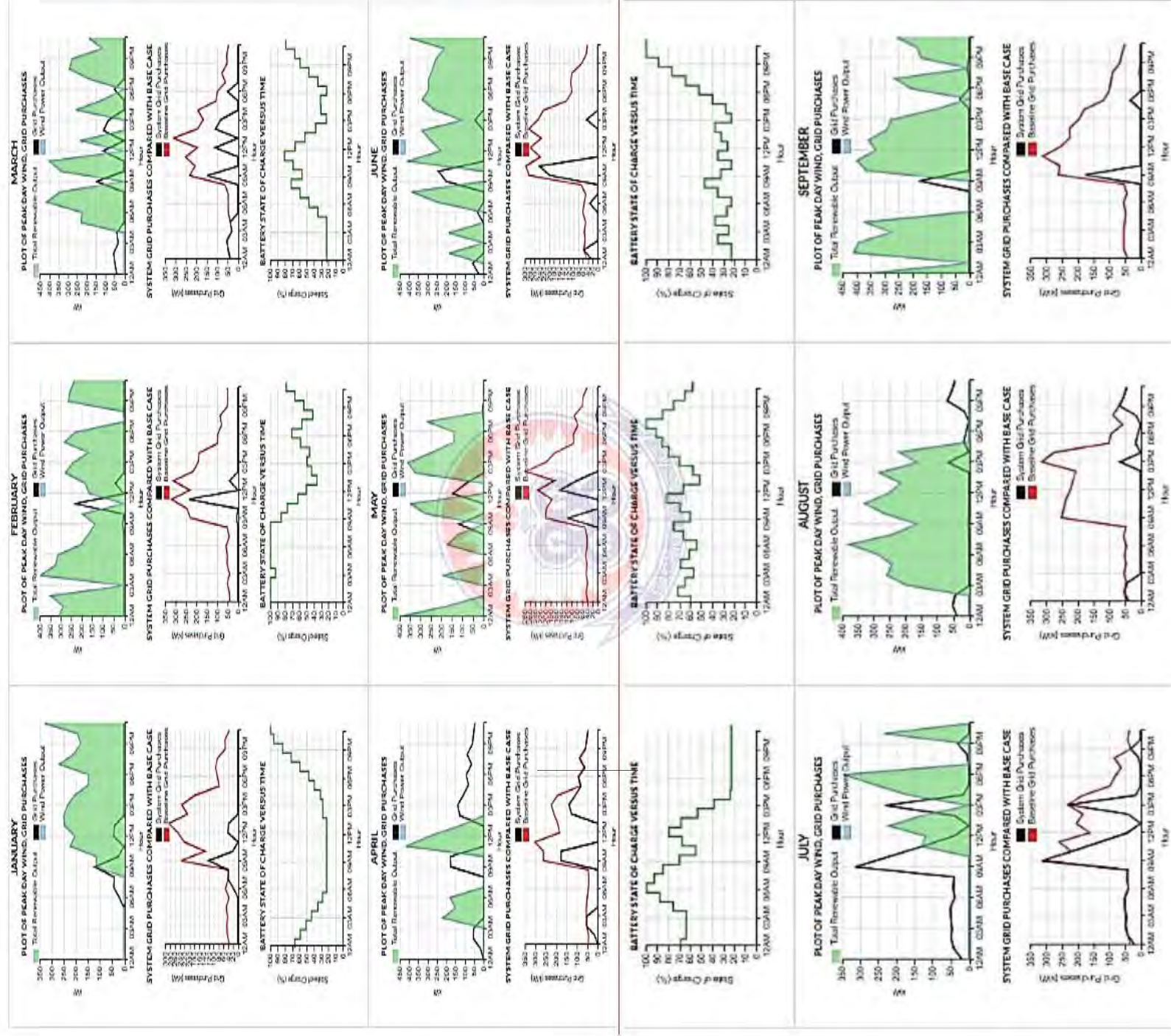
	Jan	Feb	Mar	Apr	May	June	July	Aug	Sep	Oct	Nov	Dec
Energy Charges	\$3,847	\$3,058	\$3,803	\$3,538	\$3,786	\$5,062	\$4,610	\$5,695	\$5,382	\$3,801	\$3,924	\$3,795
Cosumption	27,479 kWh	21,845 kWh	27,033 kWh	25,271 kWh	26,820 kWh	29,819 kWh	28,297 kWh	32,251 kWh	31,633 kWh	27,152 kWh	27,971 kWh	27,108 kWh
Sales	29,359 kWh	26,152 kWh	26,853 kWh	28,092 kWh	26,508 kWh	20,944 kWh	21,814 kWh	20,450 kWh	22,096 kWh	27,410 kWh	27,889 kWh	27,840 kWh
Demand Charges	\$82	\$72	\$72	\$81	\$69	\$79	\$84	\$84	\$80	\$66	\$77	\$70
Peak Demand	247 kW	203 kW	200 kW	241 kW	191 kW	234 kW	254 kW	254 kW	240 kW	176 kW	224 kW	193 kW
Fixed charges (\$)	\$2	\$2	\$2	\$2	\$2	\$2	\$2	\$2	\$2	\$2	\$2	\$2
Monthly Total	\$3,931	\$3,133	\$3,876	\$3,621	\$3,857	\$5,144	\$4,696	\$5,781	\$5,465	\$3,869	\$4,003	\$3,86
Annual Total	\$51,243											



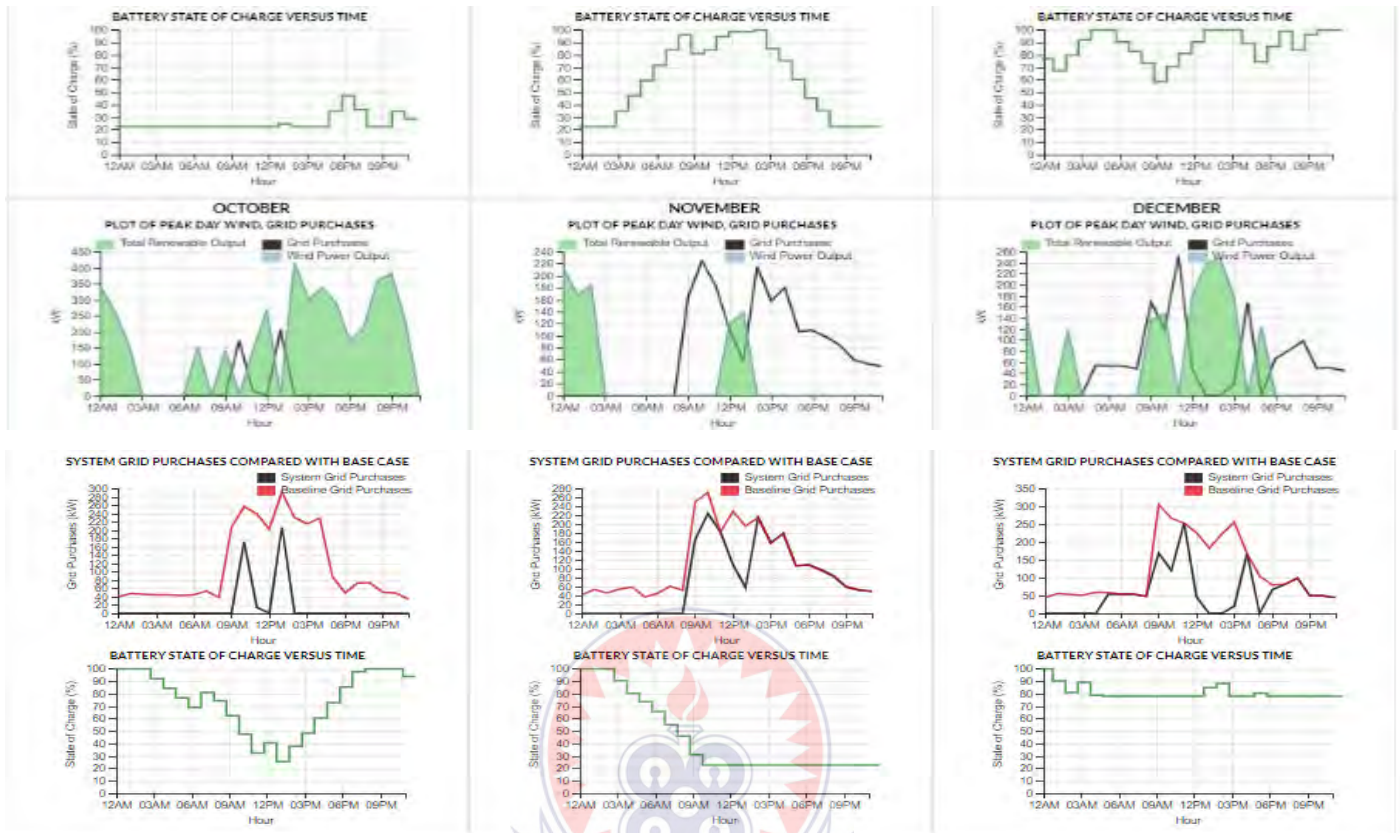
Case 4 monthly carbon dioxide emissions

	Jan	Feb	Mar	Apr	May	June	July	Aug	Sep	Oct	Nov	Dec
Monthly Total (metric tons)	17 t	14 t	17 t	16 t	17 t	19 t	18 t	20 t	20 t	17 t	18 t	17 t
Annual Total (metric tons)	210 t/yr.											

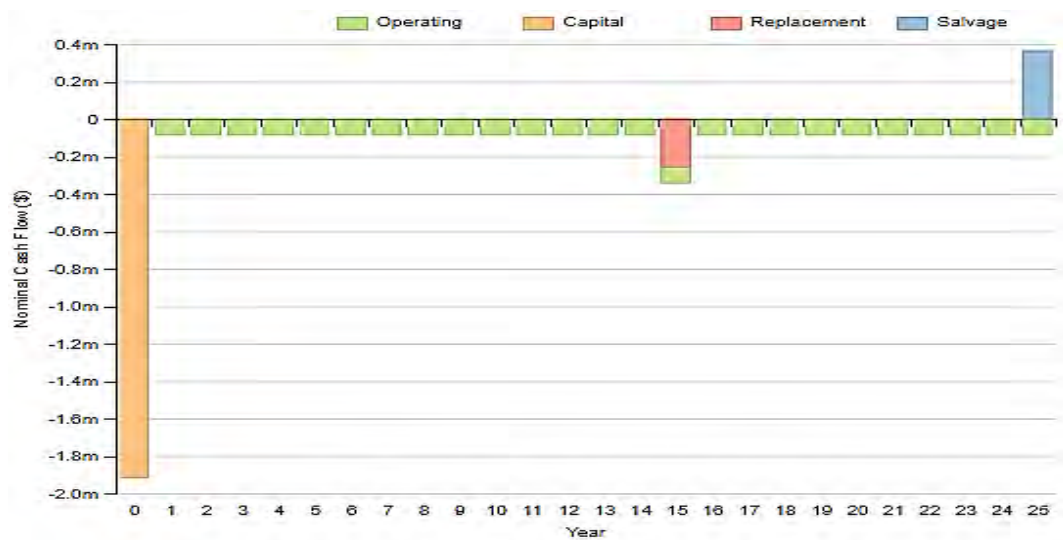
Appendix K: Case 5 system performance summary



Appendix L: Case5 system performance summary (continuation)

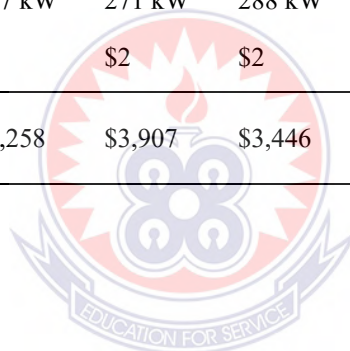


Cash flow summary for Case 5



Appendix L. Case 5 monthly bills (Predicted)

	Jan	Feb	Mar	Apr	May	June	July	Aug	Sep	Oct	Nov	Dec
Energy Charges	\$6,325	\$3,251	\$3,870	\$3,163	\$3,811	\$3,346	\$3,020	\$3,483	\$3,269	\$5,096	\$7,809	\$9,246
Cosumption	32,289 kWh	23,219 kWh	27,644 kWh	22,591 kWh	25,790 kWh	23,901 kWh	21,571 kWh	24,876 kWh	23,348 kWh	30,067 kWh	38,116 kWh	43,009 kWh
Sales	14,247 kWh	23,530 kWh	29,593 kWh	24,400 kWh	23,789 kWh	28,352 kWh	34,650 kWh	35,710 kWh	30,065 kWh	21,198 kWh	13,394 kWh	10,762 kWh
Demand Charges	\$94	\$94	\$95	\$93	\$94	\$98	\$104	\$96	\$100	\$93	\$90	\$100
Peak Demand	274 kW	272 kW	277 kW	267 kW	271 kW	288 kW	314 kW	283 kW	300 kW	267 kW	257 kW	299 kW
Fixed charges (\$)	\$2	\$2	\$2	\$2	\$2	\$2	\$2	\$2	\$2	\$2	\$2	\$2
Monthly Total	\$6,421	\$3,347	\$3,967	\$3,258	\$3,907	\$3,446	\$3,126	\$3,581	\$3,371	\$5,191	\$7,901	\$9,348
Annual Total	\$56,864											



Case 5 monthly carbon dioxide emissions

	Jan	Feb	Mar	Apr	May	June	July	Aug	Sep	Oct	Nov	Dec
Monthly Total (metric tons)	20 t	15 t	17 t	14 t	16 t	15 t	14 t	16 t	15 t	19 t	24 t	27 t
Annual Total (metric tons)	213 t/yr.											